

18 DEC. 1967

**CALORIMETRIC STUDY OF NIOBIUM IN  
THE SUPERCONDUCTING,  
MIXED AND NORMAL STATES**

**INSTITUUT-LORENTZ**  
voor theoretische natuurkunde  
Nieuwsteeg 16-Leiden-Nederland

**J. FERREIRA DA SILVA**

Universiteit Leiden



2 056 418 8

Bibliotheek  
Gorlaeus Laboratoria  
Universiteit Leiden  
Postbus 9502  
NL-2300 RA LEIDEN

CALORIMETRIC STUDY OF NIOBIUM IN  
THE SUPERCONDUCTING,  
MIXED AND NORMAL STATES

PROEFSCHRIFT

TER VERKRIJGING VAN DE GRAAD VAN TEGEN  
IN DE WISSENSCHAPPELIJKE AFD. FYSICA EN  
DE WISKUNDE AAN DE UNIVERSITEIT TE LEIDEN IN OORLOG VAN  
DE FAKULTEIT DER WISSENSCHAPPELIJKE  
VERLENEN IN DE FACULTEIT DER WISSENSCHAPPELIJKE  
TEGEN OVERNEMING VAN EEN EXAMENATIE OEFENING  
OP DAT DE VERLENEN OF  
VERLENEN IN DE WISSENSCHAPPELIJKE AFD. FYSICA EN

JOSE FERREIRA DA SILVA

gedrukt te Leiden, bij de Drukkerij "De Pers" in 1951

INSTITUUT-LORENTZ  
voor theoretische natuurkunde  
Nieuwsteeg 18-Leiden-Nederland

DRUKKERIJ J. H. W. VAN DER WOUDE  
kast dissertaties

PHYSICAL REVIEW

CALCULATED STUDY OF WIGNON IN  
THE SUPERCONDUCTING  
MIXED AND NORMAL STATES

Author's name and affiliation  
Address

**CALORIMETRIC STUDY OF NIOBIUM IN  
THE SUPERCONDUCTING,  
MIXED AND NORMAL STATES**

**PROEFSCHRIFT**

TER VERKRIJGING VAN DE GRAAD VAN DOCTOR  
IN DE WISKUNDE EN NATUURWETENSCHAPPEN AAN  
DE RIJSUNIVERSITEIT TE LEIDEN, OP GEZAG VAN  
DE RECTOR MAGNIFICUS DR P. MUNTENDAM, HOOG-  
LERAAR IN DE FACULTEIT DER GENEESKUNDE,  
TEN OVERSTAAN VAN EEN COMMISSIE UIT DE  
SENAAT TE VERDEDIGEN OP  
WOENSDAG 20 DECEMBER 1967 TE 14.00 UUR

door

**JOSÉ FERREIRA DA SILVA**

geboren te Junqueira, Vila do Conde (Portugal) in 1931

1967

DRUKKERIJ J. H. PASMANS - 'S-GRAVENHAGE

CALORIMETRIC STUDY OF NIOBIUM IN  
THE SUPERCONDUCTING  
MIXED AND NORMAL STATES

PROEFSCHRIFT

Promotor: PROF. DR. C.J. GORTER

Dit proefschrift is bewerkt mede onder toezicht van Dr. Z. Dokoupil

ROSE FERRERA DA SILVA

Ph.D. Thesis, University of Groningen, 1971

1971

ROSE FERRERA DA SILVA

## CONTENTS

CHAPTER I		
INTRODUCTION		
1.1	Subject and aim of the thesis	1
1.2	Facilities and advantages of electronic measurements in the study of the properties of type II superconductors	7
1.3	Choice of subject as a suitable topic	21
CHAPTER II		
BRIEF SURVEY OF THEORY		
2.1	Introduction	24
2.2	The two types of superconductors	24
2.3	The Shubnikov-Landau-Misener-Gorkov theory	19
2.4	The characteristics of superconductivity	25
2.4.1	Type I superconductors	25
2.4.2	Type II superconductors	27
	References	31
CHAPTER III		
EXPERIMENTAL METHOD		
3.1	Introduction	33
3.2	Devices	34
3.3	Apparatus and circuit	37
3.3.1	Apparatus and circuit (A)	37
3.3.2	Apparatus and circuit (B)	38
3.4	Measuring and control circuits	40
3.5	Calibration	41
3.6	The calibration set	44
3.7	This research was supported by the Conselho Nacional de Desenvolvimento Científico e Tecnológico (CNPq), Conselho Nacional de Desenvolvimento Científico e Tecnológico, Brasília, D.F., Brazil	47
3.8	References	48

AOS MEUS PAIS  
À MINHA MULHER

This research was supported by the  
*Fundação Calouste Gulbenkian, Lisboa.*



## CONTENTS

### CHAPTER I

#### INTRODUCTION

1.1 Subject and plan of the thesis	11
1.2 Possibilities and advantages of calorimetric measurements in the study of the properties of type II superconductors	11
1.3 Choice of niobium as a suitable sample	13

### CHAPTER II

#### BRIEF SURVEY OF THEORY

2.1 Introduction	14
2.2 The two types of superconductors	14
2.3 The Ginzburg-Landau-Abrikosov-Gor'kov theory	18
2.4 The thermodynamics of superconductivity	25
2.4.1 Type I superconductors	25
2.4.2 Type II superconductors	27
References	31

### CHAPTER III

#### EXPERIMENTAL METHOD

3.1 Introduction	33
3.2 Samples	34
3.3 Apparatus and cooling procedure	35
3.3.1 Apparatus using exchange gas (A)	36
3.3.2 Apparatus using a thermomechanical switch (B)	38
3.4 Heater and thermometer circuits	40
3.5 Thermometry	41
3.6 The calculation of $\Delta T$	44
3.7 The magnetic field	47
3.8 Errors	47
References	49

CHAPTER IV  
EXPERIMENTAL RESULTS. DISCUSSION

4.1	Introduction	50
4.2	Experimental results and discussion	50
4.2.1	The specific heat in the normal state	50
4.2.2	The specific heat for $H = 0$	54
4.2.3	The thermodynamic critical field $H_c$	58
4.2.4	The energy gap $2\Delta(0)$ at the absolute zero	62
4.2.5	The specific heat in fields $H < H_{c1}(0)$	63
4.2.5.1	Nb-1	63
4.2.5.2	Nb-2 and Nb-3	65
4.2.5.3	The phase transition at $H_{c1}(T)$	66
4.2.5.4	The enthalpy balance	70
4.2.5.5	The entropy balance	75
4.2.5.6	The temperature dependence of $H_{c1}$	78
4.2.6	The specific heat in fields $H_{c1}(0) < H < H_{c2}(0)$	80
4.2.6.1	Irreversible behaviour of Nb-1	80
4.2.6.2	Reversible behaviour of Nb-2 and Nb-3	81
4.2.6.3	The linear term in the specific heat	81
4.2.7	The phase transition from the mixed to the normal state	85
4.2.7.1	The temperature dependence of the specific heat jump at $H_{c2}$	86
4.2.7.2	The temperature dependence of $H_{c2}$	87
4.2.7.3	The temperature dependence of the penetration depth	93
4.2.7.4	The mixed state differential magnetic susceptibility near $H_{c2}$	94
4.2.8	The calculation of $\kappa_o$ , $\lambda_L(0)$ , $\xi_o$ and $v_F$ for pure Nb	96
	References	97

CHAPTER V  
THE MAGNETOCALORIC EFFECT IN TYPE II  
SUPERCONDUCTORS

5.1	Introduction	101
5.2	Analysis of the magnetocaloric effect near $H_{c2}$	103
5.3	Experimental procedure	103
5.4	Results and discussion	104
	References	110

CHAPTER VI		
CONCLUDING REMARKS	Chapter I	111
SAMENVATTING	INTRODUCTION	114
SUMÁRIO		116
CURRICULUM VITAE		118

This thesis deals with the thermodynamic properties of the so-called type II superconductors starting by the superconducting, normal and mixed states. Specific heats of three specimens of this type of material with different degrees of purity were measured in the presence of magnetic fields ranging from 0 to 3.4 MG in the temperature interval 1.5 - 7.5 °K, with the stress purpose being to study the magnetic specific properties of type II superconductivity. The case of the samples has a technological effect (related with the field dependence of the mixed state) will also be studied, together with the determination of the specific heat as a function of the field, in a given temperature.

The specific constants of 3 elements. After a short introduction, the type II superconductivity is characterized and a total survey of theory presented, starting with the thermodynamic properties with the application of the data (fully in Chapter II) to the experimental method is described. In Chapter IV the experimental results are presented, discussed and compared with theory. In Chapter V a comparison is made between the field dependencies of the superconducting effect, specific heat and induced magnetization, in the same temperature. The thesis ends with a small chapter (VII) with concluding remarks, followed by a summary in Dutch and in Portuguese and particular notes.

### 1.3 Possibilities and advantages of calorimetric measurements in the study of the properties of type II superconductors

Specific heat measurements, although a classical method, have remained a useful research tool. For superconductivity, the pioneer calorimetric measurements date to Ladden in the thirties (Ladden, Van der Grinte, Kees, Van Leeu, 1934) and have been followed by the understanding of the thermodynamic properties of different superconducting type I superconductors. Type II superconductors brought into research a new superconductive phase — the mixed state, which possibilities can be worked calorimetrically. In this thesis it will be shown that new calorimetric results obtained with type II superconductors it is possible to extract quite an amount of information about mixed state properties relevant to type II superconductors. Thus, starting the study of super-

CHAPTER IV

EXPERIMENTAL RESULTS. DISCUSSION

4.1	Introduction	15
4.2	Experimental results and discussion	15
4.2.1	The specific heat in the normal state	15
4.2.2	The specific heat for $H < H_c$	16
4.2.3	The characteristic critical field $H_c$	16
4.2.4	The energy gap $2\Delta(T)$ of the absolute zero	16
4.2.5	The specific heat in fields $H < H_{c1}(T)$	17
4.2.5.1	Model	17
4.2.5.2	$H_{c1}$ and $H_{c2}$	18
4.2.5.3	The charge transition at $H_{c1}(T)$	18
4.2.5.4	The charge balance	17
4.2.5.5	The energy balance	17
4.2.5.6	The temperature dependence of $H_{c1}$	17
4.2.6	The specific heat in fields $H_c < H < H_{c2}(T)$	18
4.2.6.1	Inevitable behavior of $H_{c2}$	18
4.2.6.2	Reversible behavior of $H_{c2}$ and $H_{c1}$	18
4.2.6.3	The linear term in the specific heat	18
4.2.7	The phase transition from the normal to the superconducting state	19
4.2.7.1	The temperature dependence of the specific heat	19
4.2.7.2	The temperature dependence of $H_{c2}$	19
4.2.7.3	The temperature dependence of the penetration depth	19
4.2.7.4	The mixed state diffusion magnetic susceptibility	19
4.2.8	The calculation of $\chi_{\parallel}$ , $\chi_{\perp}$ , $T_c$ and $\gamma_{\parallel}$ for pure $YBaCuO$	19
	References	20

CHAPTER V

THE MAGNETOCALORIC EFFECT IN TYPE II SUPERCONDUCTORS

5.1	Introduction	21
5.2	Analysis of the magnetocaloric effect near $H_{c2}$	21
5.3	Experimental procedure	22
5.4	Results and discussion	24
	References	25

## Chapter I

### INTRODUCTION

#### 1.1 Subject and plan of the thesis

This thesis deals with the thermodynamic properties of the intrinsic type II superconductor niobium in the superconducting, mixed and normal states. Specific heats of three specimens of this transition metal with different degrees of purity have been measured in the presence of magnetic fields ranging from 0 to 9.4 kOe in the temperature interval  $1 \lesssim T \lesssim 10^\circ\text{K}$ , with the aim of gaining insight into the characteristic features of type II superconductivity. For one of the samples the magnetocaloric effect (connected with the field dependence of the mixed state entropy) was also studied, together with the measurement of the specific heat as a function of the field, at a given temperature.

The thesis consists of 6 chapters. After a short introduction (I), type II superconductivity is characterized and a brief survey of theory presented together with the thermodynamic relations used in the analysis of the data (II). In Chapter III the experimental method is described. In Chapter IV the experimental results are presented, discussed and compared with theory. In Chapter V a comparison is made between the field dependence of the magnetocaloric effect, specific heat and isothermal magnetization, at the same temperature. The thesis ends with a small chapter (VI) with concluding remarks, followed by summaries in Dutch and in Portuguese and curriculum vitae.

#### 1.2 Possibilities and advantages of calorimetric measurements in the study of the properties of type II superconductors

Specific heat measurements, although a classical method, have remained a useful research tool. For superconductivity, the pioneer calorimetric measurements done in Leiden in the thirties (Keesom, Van den Ende, Kok, Van Laer) laid down basic information for the understanding of the thermodynamic properties of what are now known as type I superconductors. Type II superconductors brought into research a new superconductive phase - the mixed state, whose properties can be studied calorimetrically. In this thesis it will be shown that from specific heat results obtained with type II superconductors it is possible to extract quite an amount of information about several questions relevant to type II superconductivity. Thus, besides the usual determin-

ation of the parameters  $\gamma$  (the Sommerfeld constant) and  $\Theta$  (the Debye temperature), characteristic of the normal state, one can obtain information on: 1) the energy gap at 0°K which exists in the energy spectrum of the superconducting electrons of a superconductor in zero magnetic field; 2) the nature of the transitions that take place when the phase lines  $H_{c1}(T)$  and  $H_{c2}(T)$  are crossed; 3) the thermodynamic critical field  $H_c(T)$ ; 4) the phase diagram of the superconductor; 5) the reversible magnetization  $M(H)$  near  $H_{c2}$  even in the case of hysteretic magnetic behaviour; 6) the Ginzburg-Landau parameter  $\kappa$  and the temperature dependence of the parameters  $\kappa_1$  and  $\kappa_2$  and, last but not least, one can prove 7) that the energy gap, in the presence of a field  $H > H_{c1}(0)$ , is ineffective in determining the behaviour of the specific heat ("gapless" superconductivity).

Calorimetric and magnetic results are correlated so that, in principle, a comparison between them can be established or, alternatively, one set of results can yield the other (case 5) mentioned above). Thus, the two sorts of measurements appear to be equally suitable for studying the thermodynamic properties of superconductors of both types. However, for type II superconductors, in practice (when there is not completely reversible magnetic behaviour), results obtained with magnetic measurements can be considerably disturbed while, as shall be shown, calorimetric results can even in such a case yield the thermodynamic parameters of interest. Of course, for irreversible behaviour, even calorimetric results obtained with measurements performed in the presence of a magnetic field will be disturbed but, in favourable cases (annealed samples), the effect is only apparent in a restricted temperature region in the mixed state (near the phase transition line  $H_{c1}(T)$ ).

Close to the transition from the mixed to the normal state (in fact, for  $H \gtrsim H_c(T)$  for the annealed samples Nb-2 and Nb-3) specific heat results are hysteresis-free so that (with the help of thermodynamic relations), magnetic results can be predicted in this region. As the reciprocal appears to be, in general, not true, results derived from calorimetric measurements are more reliable than the usual magnetic data. The most striking difference between the possibilities of the two sorts of measurements lies in the determination of the thermodynamic critical field  $H_c$  of a type II superconductor not displaying completely reversible behaviour (unfortunately, the usual situation). The determination of  $H_c$  can be accomplished with reasonably accurate calorimetric results obtained in zero magnetic field and in the normal state being thus free of hysteresis disturbances. In contrast, magnetic measurements in such a case will be unable to yield this thermodynamic parameter within acceptable accuracy. The parameter  $\kappa$  and its analogues  $\kappa_1$  and  $\kappa_2$  defined in Chapter II, Section 2.3 are obtained

from calorimetric results in the region where reversible behaviour is obtained (or approached in the worst case) so that they correspond to thermodynamic equilibrium situations and are therefore reliable for comparison with the theoretical predictions. In the restricted region near the  $H_{c1}(T)$  phase transition line, where the effects of irreversibility are most apparent in calorimetric measurements, no definite conclusion can be drawn about the nature of the transition unless the sample is of extremely high purity and free of physical defects, which, unfortunately, was not the case.

The cooling produced by adiabatic magnetization of a type II superconductor in the mixed state (magnetocaloric effect) can be used for measuring the specific heat as a function of the applied field at a given temperature, kept constant within narrow limits. As the behaviour of the specific heat and the magnetocaloric effect is very sensitive to the shape of the magnetization curve, in the absence of a theoretical treatment of the thermal properties derived from first principles, calorimetric results provide a means for testing the theories that predict explicitly the magnetization.

### 1.3 Choice of niobium as a suitable sample

Niobium was chosen since it was the only known intrinsic type II superconductor (even in a state of high purity this transition metal displays type II superconductivity). Later, vanadium was also found to be in this class. Niobium also offers the advantage of having a relatively high Sommerfeld constant  $\gamma$  and high Debye temperature  $\Theta$ , thus favouring an accurate separation of the electronic contribution (the only one of interest in superconductivity) from the measured specific heat. Moreover, the high transition temperature  $T_c$  of this superconductor makes it possible to reach low enough reduced temperatures  $t = T/T_c$  using a  $^4\text{He}$  cryostat. Impure, non-annealed niobium offers a wider range of the mixed state and therefore seems to be, in principle, a desirable sample for studying this phase. However, it turned out that the enhanced effects of hysteresis associated with inhomogeneities were very disturbing in some cases (high fields), complicating the results and their discussion. For this reason, the greatest amount of information was obtained with one of the high-purity annealed samples, Nb-3. The sample characteristics will be described in Chapter III, Section 3.2.

## Chapter II

## BRIEF SURVEY OF THEORY

## 2.1 Introduction

In this chapter the two types of superconductors are characterized and a brief description is given of some fundamental aspects of theory as far as it is pertinent to the experimental results. Simple presentation rather than exhaustive derivation will be given, emphasis being placed on the relations used in the analysis of the data.

The thermodynamic description of superconductors requires the knowledge of the magnetization. For type I a set of useful thermodynamic relations follow directly from perfect diamagnetism which occurs in the whole range of superconductivity from zero field up to  $H_c$  in the case of zero demagnetizing coefficient. For type II some of these relations are also valid while others can be established on basis of Abrikosov's vortex model describing the magnetic behaviour in the mixed state. In particular, an expression was derived for the specific heat in the mixed state near  $H_{c2}$ , the region where the magnetization is explicitly given by theory.

## 2.2 The two types of superconductors

It was known from early work that impure metals, compounds and alloys can exhibit superconductivity up to much higher values of the magnetic field than those usually quenching the superconductive properties of pure metals (de Haas and Voogd<sup>1</sup>) in Leiden, Mendelssohn and his Oxford group<sup>2</sup>, Shubnikov's group in Kharkov<sup>3</sup>). The peculiarity of such materials is that the transition from the region of complete Meissner effect (zero magnetic induction  $B$  inside the superconductor) to the normal state ( $B = H$ ,  $H$  being the applied field) does not take place abruptly at a well defined field  $H_c$  as happens in "soft" superconductors, e.g. tin, lead or aluminium, but extends instead, over quite a range of high fields ("hard" or "high-field" superconductors). Abrikosov has shown many years later that in the Ginzburg-Landau (GL) theory<sup>4</sup> is implicit the existence of two types of superconductors<sup>5</sup>. After this, "soft" superconductors became generally known as type I and "hard"- or "high-field" superconductors as type II. The persistence of superconductivity in high fields had at first been ascribed by Mendelssohn<sup>2</sup> to inhomogeneities of the material resulting in a mesh-like superconductive structure of thin filaments embedded in the bulk normal body (sponge model).



This simple view could not resist the impact of experimental evidence. For instance, the results of specific heat measurements on the "high-field" superconductor  $V_3Ga$ <sup>6)</sup> could be explained by the sponge model only by assuming that the density of filaments was so great that they fill most of the volume<sup>7)</sup>. Thus, contrarily to the former expectation, high-field superconductivity behaves as a bulk property. Further, some high-field superconductive alloys display nearly reversible magnetic behaviour<sup>3,8)</sup>, this being inconsistent with the irreversibility that one expects from a multiply connected filamentary structure.

In principle, a microstructure of alternating superconducting and normal regions (layer model) can also account for the behaviour of "high-field" superconductors<sup>9,10,11,12,12a,13)</sup> on the basis of a "negative" surface energy  $\alpha_{ns}$  at the boundary of the two phases. As will be shown in Section 2.3, there are in superconductivity two characteristic lengths - the coherence length  $\xi$  and the penetration depth  $\lambda$  - the relative magnitude of which determines the type of behaviour. The coherence length measures the range of order or correlation between the electrons responsible for superconductivity and the penetration depth measures the distance at which the applied magnetic field extends into the superconductor. The existence of a non-zero range of coherence prevents the abrupt variation of the degree of superconductive order at a normal-superconducting phase boundary. The resulting gradient of the order parameter is accompanied by an extra positive term to the free energy of the condensed (superconductive) phase. The penetration of the external field results, on the contrary, in a decrease of the magnetic energy of the diamagnetic sample. The resulting interphase surface energy  $\alpha_{ns}$  is given approximately<sup>14)</sup> by:  $(\xi - \lambda)H_c^2/8\pi$ .  $\alpha_{ns}$  can be either positive or negative according the relative magnitude of  $\xi$  and  $\lambda$ , the general behaviour of the superconductor depending critically upon the sign of  $\alpha_{ns}$ . A positive  $\alpha_{ns}$  will prevent a superconductive sample submitted to an increasing external field  $H$  from splitting into normal and superconducting regions unless at part of its surface the local field is higher than the external field  $H$  (then this local field prematurely reaches  $H_c$  which leads to the formation of the intermediate state). Such a superconductor with  $\alpha_{ns} > 0$  is called type I. A type I superconductor, in the absence of demagnetizing effects, resists the penetration of the external field (Meissner effect) up to a value  $H_c(T)$  such that the magnetic work done by  $H$  on the superconductive body per unit volume equals the condensation energy density

$$-\int_0^{H_c(T)} MdH = \frac{H_c^2(T)}{8\pi} = G_n(T, H_c) - G_s(T, 0) . \quad (2-1)$$

Here  $M = -H/4\pi$  is the magnetic moment per unit volume of the superconductor (magnetization) and  $G$  the Gibbs free energy density (the indices  $n$  and  $s$  stand for normal and superconducting respectively). On the contrary, when  $\alpha_{ns}$  is negative, it will, at a given value  $H_{c1}(T)$  of the external field, be energetically more favourable for the superconductor to have a mixed composition of alternating thin normal and superconducting regions, the normal regions being much thinner than the superconducting ones. Upon increasing the external field  $H$  above  $H_{c1}(T)$  the superconductive regions also become thinner and thinner, so that the magnetic field penetrates more and more into the superconductor. The magnetic moment of the sample (its absolute value) thus decreases from  $H_{c1}(T)/4\pi$  at  $H_{c1}(T)$  to zero<sup>13)</sup> at such a field  $H_{c2}(T)$  that

$$-\int_0^{H_{c2}(T)} MdH = G_n(T, H_{c2}) - G_s(T, 0) = \frac{H_c^2(T)}{8\pi} \quad (2-2)$$

This kind of behaviour is characteristic of type II superconductors for which the thermodynamic critical field  $H_c(T)$  does not indicate anymore a first order phase transition but is a simple parameter measuring the condensation energy. For  $H_{c1}(T) < H < H_{c2}(T)$  the superconductor is said to be in the mixed state. The lower critical field,  $H_{c1}$ , represents the limit of complete Meissner effect for an increasing field, while the higher critical field,  $H_{c2}$ , represents the limit of stability of the normal state for a decreasing field. There are materials with  $H_{c2}$  of the order of a few hundred kOe. The two types of reversible magnetic behaviour are depicted in Fig. II.1 where the isothermal magnetization -  $4\pi M$  is plotted against the applied field  $H$  ( $H_c$  was taken as the common unit).

Accordingly, the phase diagram of a type II superconductor includes (for bulk properties) two transitions lines  $H_{c1}(T)$  and  $H_{c2}(T)$  and three phases while for type I superconductors there is only one line  $H_c(T)$  and two phases, as shown in Fig. II.2, where the symbols  $s$ ,  $m$  and  $n$  stand for superconducting (or Meissner), mixed (or Shubnikov) and normal states, respectively. The nature of the transitions at  $H_{c1}(T)$  and  $H_{c2}(T)$  can be either studied by calorimetric or magnetic measurements. Usually, calorimetric measurements are performed at constant magnetic field, increasing the temperature (line 1) while magnetic measurements are performed isothermally (line 2). The layer model of Van Beelen and Gorter<sup>13)</sup> yields a first order transition at  $H_{c1}(T)$  and a second order one at  $H_{c2}(T)$ .

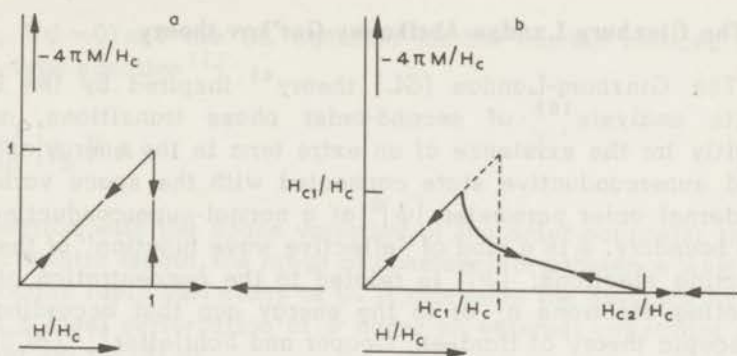


Fig. II.1 The two types of reversible magnetic behaviour of superconductors.

a. type I

b. type II

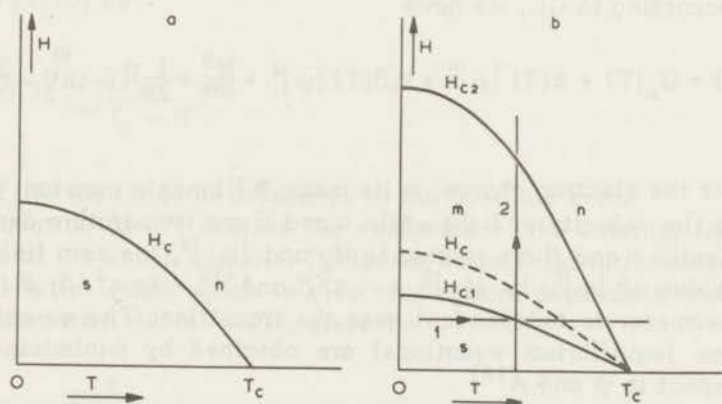


Fig. II.2 Phase diagram of a type I (a) and a type II (b) superconductor.

Despite giving not so good an agreement with some experimental results as compared with the more sophisticated Abrikosov's model of the mixed state involving flux quantization<sup>15</sup>), layer models have the merit of showing very simply that superconductors with negative interphase surface energy have a reversible magnetic behaviour different to those with positive  $\alpha_{ns}$ .

### 2.3 The Ginzburg-Landau-Abrikosov-Gor'kov theory

The Ginzburg-Landau (GL) theory<sup>4)</sup> inspired by the Landau-Lifshitz analysis<sup>16)</sup> of second-order phase transitions, accounts explicitly for the existence of an extra term in the energy of the condensed superconductive state connected with the space variation of the internal order parameter  $|\psi|^2$  at a normal-superconducting interphase boundary.  $\psi$  is a kind of "effective wave function" of the superconducting electrons;  $|\psi|^2$  is related to the concentration of superconducting electrons  $n_s$  or to the energy gap that according to the microscopic theory of Bardeen, Cooper and Schrieffer<sup>17)</sup> (BCS) exists in the energy spectrum of the superconducting electrons. Near a second-order phase transition the order parameter becomes very small so that the difference between the Gibbs free energy of the superconductive phase and the normal state can be expanded in powers of  $|\psi|^2$  plus the extra term connected with the existence of a gradient of  $\psi$ . In the presence of a magnetic field  $H$  derived from a vector potential  $A$ , taking  $2e$  as the effective charge of a superconducting carrier (Cooper pair), according to GL, we have

$$G_s(H, T) = G_n(T) + \alpha(T) |\psi|^2 + \frac{1}{2} \beta(T) |\psi|^4 + \frac{H^2}{8\pi} + \frac{1}{2m} [(-i\hbar\nabla - \frac{2eA}{c})\psi]^2. \quad (2-3)$$

Here  $e$  is the electron charge,  $m$  its mass,  $\hbar$  Planck's constant divided by  $2\pi$ ,  $c$  the velocity of light while  $\alpha$  and  $\beta$  are temperature dependent coefficients.  $\alpha$  and  $\beta$  are related to  $H_c$  and  $|\psi_0|^2$ , the zero field equilibrium value of  $|\psi|^2$ , by  $|\psi_0|^2 = -\alpha/\beta$  and  $H_c^2 = 4\pi\alpha^2/\beta$ ;  $\beta$  is practically temperature independent near the transition. The so-called GL equations (equilibrium equations) are obtained by minimizing (2-3) with respect to  $\psi$  and  $A$ <sup>18)</sup>

$$\alpha(T)\psi + \beta(T)|\psi|^2\psi + \frac{1}{2m} (-i\hbar\nabla - \frac{2eA}{c})^2\psi = 0 \quad (2-4)$$

$$j = \frac{e\hbar}{im} (\psi^*\nabla\psi - \psi\nabla\psi^*) - \frac{4e^2}{mc} \psi^*\psi A. \quad (2-5)$$

(2-4) gives the equilibrium value of the order parameter in the presence of an external field and (2-5) gives the density of shielding currents with which the superconductor reacts to the applied field. If the applied field is weak (weak field limit) the "effective wave function" does not deviate much from the zero field equilibrium value

( $\psi = \psi_0$ ,  $\nabla\psi = 0$ ) and the GL equation for the current reduces to the London-type equation<sup>11)</sup>

$$j = -\frac{4e^2}{mc} |\psi_0|^2 A. \quad (2-5')$$

In connection with the space variation of the order parameter there is a characteristic length, the range of coherence or coherence length  $\xi(T)$  that prevents rapid variations of  $\psi$ . It measures the distance to which extends a local perturbation of  $\psi$  under an external constraint and is given (ref.18) p.178) by

$$\xi^2(T) = \frac{\hbar^2}{2m|\alpha|}. \quad (2-6)$$

For a pure material, near the temperature  $T_c$  of the transition to the normal state in zero field the temperature dependence of  $\xi$  is given (ref.18) p.178) by

$$\xi(T) \approx 0.74 \xi_0 \left( \frac{T_c}{T_c - T} \right)^{1/2} \quad (2-7)$$

where  $\xi_0$  is the range of coherence at the absolute zero.

Equation (2-5') implies the exclusion of the external field from the bulk of the superconductor (Meissner effect) and introduces another characteristic length which is also temperature dependent, the "weak field penetration depth"  $\lambda(T)$ , given by

$$\lambda^2(T) = \frac{mc^2}{16\pi e^2 |\psi_0|^2} \quad (2-8)$$

as can be seen treating equation (2-5) in one dimension. For a pure metal in the free electron approximation, according to BCS  $\lambda(T)$ , near  $T_c$ , is given (ref.18, p.180) by

$$\lambda(T) \approx \frac{1}{\sqrt{2}} \lambda_L(0) \left( \frac{T_c}{T_c - T} \right)^{1/2} \quad (2-9)$$

where  $\lambda_L(0)$  is the London penetration depth at absolute zero, given by

$$\lambda_L^2(0) = \frac{mc^2}{4\pi ne^2} \quad (2-10)$$

where  $n$  is the number of free electrons per  $\text{cm}^3$ .

Near  $T_c$ ,  $\lambda(T)$  and  $\xi(T)$  both diverge ( $\psi_0 \rightarrow 0$ ) but their ratio  $\kappa = \lambda(T)/\xi(T)$  remains finite

$$\lim_{T \rightarrow T_c} \frac{\lambda(T)}{\xi(T)} = \kappa = \frac{mc}{2e\hbar} \left(\frac{\beta}{2\pi}\right)^{1/2}. \quad (2-11)$$

$\kappa$  is called the GL parameter of the superconductor.

For a pure metal, from (2-7) and (2-9) one gets, approximately

$$\kappa_0 = 0.96 \frac{\lambda_L(0)}{\xi_0}. \quad (2-12)$$

Consequently,  $\kappa$  is approximately temperature independent near  $T_c$ .  $\kappa$  measures the relative magnitude of  $\lambda$  in terms of  $\xi$  and thus determines the value and the sign of the surface energy  $\alpha_{ns}$ , at a normal-superconducting boundary. Within the approximation  $\alpha_{ns} = (\xi - \lambda)H_c^2/8\pi$  one may say that at a critical value in the order of  $\kappa \approx 1$  lies the division between the two groups of superconductors.

From the relations  $|\psi_0|^2 = -\alpha/\beta$ ,  $H_c^2 = 4\pi\alpha^2/\beta$ , (2-6) and (2-8), follows

$$H_c(T) = \frac{\phi_0}{2\pi\sqrt{2} \lambda(T) \xi(T)}, \quad (2-13)$$

where  $\phi_0 = ch/2e = 2.067 \times 10^{-7} \text{ G}\cdot\text{cm}^2$  is the flux quantum. Near  $T_c$ , from (2-11) and (2-13) we have

$$\kappa = 2\sqrt{2}\pi H_c(T) \lambda^2(T)/\phi_0. \quad (2-13')$$

When superconductivity has been quenched by sufficiently high field, upon decreasing the field, superconducting regions may begin to nucleate in the bulk of the material at the value of the applied field<sup>15)</sup>

$$H_{c2} = \kappa\sqrt{2} H_c. \quad (2-14)$$

$H_{c2}$  represents the highest value of the applied field for which the

GL equation for the order parameter has non zero solutions ( $\psi \neq 0$ ) in the whole volume of the superconductive body. For superconductors with  $\kappa < 1/\sqrt{2}$  (type I),  $H_{c2} < H_c$  is a supercooling field. For superconductors with  $\kappa > 1/\sqrt{2}$  (type II),  $H_{c2}$  is higher than  $H_c$  and the persistence of superconductivity above  $H_c$  implies the disappearance of the Meissner state at a field  $H_{c1} < H_c$ .<sup>15)</sup>

According to Abrikosov<sup>15)</sup>, in the mixed state ( $H_{c1} < H < H_{c2}$ ), the partial penetration of the magnetic flux through the superconductor occurs in the form of a vortex structure of quantized flux threads (fluxoids), parallel to the applied field. The fluxoid consists of an inner core (radius  $\sim \xi$ ) surrounded by a vortex of supercurrent (radius  $\sim \lambda$ ). Each fluxoid carries a single quantum of magnetic flux  $\phi_0$ .

In the cores of the fluxoids the energy spectrum of the electrons is quite different from the superconducting ground state. While in the Meissner region there is a forbidden energy gap, from which results the exponential BCS<sup>17)</sup> behaviour of the specific heat, in the mixed state according Caroli et al.<sup>19)</sup> low energy excitations are permitted in the cores of the fluxoids. From these normal-like excitations results a quite different kind of behaviour for the specific heat in the mixed state.

The lower boundary of the mixed state  $H_{c1}$  was calculated by Abrikosov<sup>15)</sup> for the case  $\kappa \gg 1$  to be

$$\sqrt{2} \kappa H_{c1}/H_c \approx \ln \kappa + 0.08 \quad (2-15)$$

and numerical solutions for all  $\kappa$  were obtained by Harden and Arp.<sup>20)</sup>

Ideally, one may imagine that flux first enters the specimen at  $H_{c1}$  in a rather abrupt way until the uniform density of fluxoids corresponds to a spacing between next neighbours of a few  $\lambda$ , at which distance they begin to interact. Thus, their mutual repulsion sets a limit to the initial penetration. Upon increasing the external field the density of fluxoids increases until the point when the interfluxoid distance becomes of the order of  $\xi$ . Then the cores begin to overlap. The penetration of the superconductor by the magnetic flux of the external field is complete at  $H_{c2}$ . From (2-13), (2-13') and (2-14) we have

$$H_{c2}(T) = \frac{\phi_0}{2\pi\xi^2(T)} \quad (2-16)$$

Thus, a "high-field" superconductor has a small range of coherence.

Upon alloying a pure superconductor its range of coherence

decreases and the penetration depth  $\lambda$  increases (Pippard<sup>21</sup>), the dependence of  $\lambda$  on the mean free path of the electrons implying a non-local relation between current density and the vector potential (Pippard<sup>21</sup>). The combined effects on  $\xi$  and  $\lambda$  due to reduction of the mean free path of the electrons lead to the enhancement of  $\kappa$ , this explaining why type II superconductors are mainly concentrated alloys and dirty metals. However, since, according to the BCS theory<sup>17)</sup>

$$\xi_0 = 0.18 \frac{\hbar v_F}{k T_c} \quad (2-17)$$

(where  $v_F$  is the Fermi velocity and  $k$  the Boltzmann constant), one may expect that even a pure superconductor with low  $v_F$  and high  $T_c$  might be (intrinsic) type II. So far as is known, these requirements are fulfilled only by the two transition metals Nb and V<sup>22)</sup> which, in fact, were found to display type II behaviour in a state of high purity.

From (2-13') and (2-14) we have

$$H_{c2}(T) = \frac{4\pi\lambda^2(T) H_c^2(T)}{\phi_0} \quad (2-18)$$

This relation provides a means for testing the validity of the GL theory when experimental values of  $H_{c2}$ ,  $\lambda$  and  $H_c$  are known. According to the original two-fluid model of Gorter-Casimir<sup>23)</sup>,  $\lambda(t) = \lambda(0)(1-t^4)^{-1/2}$  and  $H_c(t) = H_c(0)(1-t^2)$  where  $t = T/T_c$ . Thus, on phenomenological grounds, the following temperature dependence is expected for  $H_{c2}$

$$H_{c2} = H_{c2}(0) \frac{1-t^2}{1+t^2} \quad (2-19)$$

where  $H_{c2}(0) = 4\pi H_c^2(0) \lambda^2(0) / \phi_0$ . Although this relation was first explicitly used by Tinkham<sup>24)</sup> it is called after Ginzburg<sup>25)</sup> who first suggested the validity of relation (2-13') at temperatures  $T \ll T_c$  in the case  $\lambda > \xi$  (London limit), using for  $\lambda(t)$  and  $H_c(t)$  the expressions of the two-fluid model.

Near the transition to the normal state the Abrikosov vortex model<sup>15)</sup> yields explicitly the magnetic moment  $M$  of the specimen as proportional to the first power of  $H_{c2} - H$ ,  $H$  being the applied field

$$-4\pi M = \frac{H_{c2} - H}{\beta(2\kappa^2 - 1)} \quad (2-20)$$



The coefficient  $\beta$  depends on the symmetry of the vortex structure ( $\beta = 1.18$  for a square lattice,  $\beta = 1.16$  for a triangular lattice, the latter being more stable in the whole mixed state<sup>26,27</sup>). According to eq. (2-20) the transition at  $H_{c2}$  is of second order.

Attempts were made to extend the validity of the GL theory to all temperatures. In the limit  $T \rightarrow T_c$  Gor'kov<sup>28</sup> succeeded to derive equations formally identical<sup>29</sup> to those of GL with a Green's function reformulation of the BCS theory, using a position-dependent pair wave function  $\Delta(r)$  in an applied magnetic field. Since  $\Delta(r)$  goes continuously to zero at a second order transition, by linearizing the Gor'kov equations for small  $\Delta(r)$ , it became possible to obtain solutions  $H_{c2}(T)$  for  $T \ll T_c$ . In this way he calculated  $H_{c2}(0)$  in the pure, clean limit (infinite mean free path  $l$  of the electrons) arriving at the following interpolation polynomial for  $H_{c2}(T)$ <sup>30</sup>

$$H_{c2}(t) = \kappa H_c(t) [1.77 - 0.43 t^2 + 0.07 t^4]. \quad (2-21)$$

The Gor'kov expression (2-21) gives a much weaker temperature dependence for  $H_{c2}(t)$  than Ginzburg's (2-19).

Maki<sup>31</sup> extended the Gor'kov treatment to account for impurity scattering, in the limit of small  $l$ . He showed that the Abrikosov vortex structure in the neighbourhood of  $H_{c2}$ , at arbitrary temperature, is characterized by eqs. (2-14) and (2-20) with different temperature dependent parameters,  $\kappa_1(t)$  in

$$H_{c2}(t) = \sqrt{2} \kappa_1(t) H_c(t) \quad (2-22)$$

and  $\kappa_2(t)$  in

$$-4 \pi M = \frac{H_{c2} - H}{\beta [2\kappa_2^2(t) - 1]}, \quad (2-23)$$

both converging to the GL  $\kappa$  for  $t = 1$ . In the dirty limit ( $l = 0$ )  $\kappa_1(t)/\kappa$  is predicted to increase 20% from  $t = 1$  to  $t = 0$ , compared to 25% according to Gor'kov's calculation (2-21) for  $l = \infty$ .

For  $\kappa_2(t)/\kappa$  Maki predicted a decrease of 30% from  $t = 1$  to  $t = 0$  and from such a behaviour he derived the thermodynamic properties of hypothetical type III superconductors. Experimentally  $\kappa_2$  was always found to increase upon decrease of temperature.  $\kappa_2(t)$  was recalculated by Caroli et al.<sup>32</sup> in the dirty limit with the result  $\kappa_2(t) = \kappa_1(t)$  for all  $t$ , within 2%. For the clean limit, Maki and Tsuzuki<sup>33</sup> derived

relations identical to (2-22) and (2-23) with results for  $\kappa_1(t)$  rather similar to those of Gor'kov. For  $\kappa_2(t)$  they predicted a more rapid increase upon decreasing temperature than for  $\kappa_1(t)$ , with a logarithmic singularity at  $t = 0$ . Recently Eilenberger<sup>34)</sup> has calculated  $\kappa_1(t)$  and  $\kappa_2(t)$  for arbitrary impurity concentration. He showed in particular that the singularity in  $\kappa_2(t)$  at  $t = 0$  disappears when a slight impurity is present.

The BCS - Gor'kov model on which the calculations of  $\kappa_1(t)$  are based assume weak electron-phonon interaction and a spherical Fermi surface.

For comparison of experimental and theoretical results for  $H_{c2}(t)$  Helfand and Werthamer<sup>35)</sup> introduced the reduced quantity

$$h^*(t) = \frac{H_{c2}(t)}{-(dH_{c2}/dt)_{t=1}} \quad (2-24)$$

Theoretically,  $h^*(t)$  as  $\kappa_1(t)/\kappa$  is not very sensitive to impurity. At the clean limit  $h^*(0) = 0.727$ , this corresponding to  $\kappa_1(0)/\kappa = 1.263$  while at the dirty limit  $h^*(0) = 0.693$  (or  $\kappa_1(0)/\kappa = 1.203$ ). In the case of pure Nb the strength of the electron-phonon coupling has no apparent effect on  $h^*(t)$ <sup>36)</sup>. It then follows that the discrepancies between experiment and theory regarding  $H_{c2}$  are likely to be due only to Fermi surface anisotropy. In fact, Hohenberg and Werthamer<sup>37)</sup> showed that when such an effect is taken into account  $h^*(0)$  is enhanced with respect to the value obtained on basis of a spherical Fermi surface, although they have not yet been able to compute the new value.

In attaining the derivation of the GL theory from first principles, Gor'kov has expressed the phenomenological constants of this theory in terms of microscopic characteristics of the metal, such as the electron mean free path,  $l$ , the Fermi velocity,  $v_F$ , and the density of states (for one direction of spin) at the Fermi surface,  $N(0)$ . For the GL parameter  $\kappa$  Gor'kov<sup>29)</sup> derived the general expression  $\kappa = \kappa_0/\chi(\rho)$ , where  $\kappa_0 = 0.96 \lambda_L(0)/\xi_0$  corresponds to the pure metal and  $\chi(\rho)$  is a function of the parameter  $\rho = 0.884 \xi_0/l$ . In terms of measurable quantities, Goodman<sup>12)</sup> has approximated Gor'kov's expression for  $\kappa$  as

$$\kappa = \kappa_0 + 7.5 \times 10^3 \rho_0 \gamma^{1/2} \quad (2-25)$$

where  $\rho_0$  is the normal state residual resistivity in  $\Omega \cdot \text{cm}$  and  $\gamma$  the Sommerfeld constant in  $\text{erg} \cdot \text{cm}^{-3} \cdot \text{K}^{-2}$ .

## 2.4 The thermodynamics of superconductivity

### 2.4.1 Type I superconductors

The thermodynamic description of the reversible behaviour of superconductors is based on the magnetic Gibbs free energy

$$G(T,H) = U - TS - MH \quad (2-26)$$

where  $U$  is the internal energy,  $T$  the absolute temperature,  $S$  the entropy,  $M$  the magnetic moment of the specimen and  $H$  the applied magnetic field. Assuming that the specimen is a very long ellipsoid parallel to the magnetic field, the demagnetizing factor of which may be neglected, the magnetization is uniform and the Gibbs free energy density is everywhere the same for a given  $T$  and  $H$  all over the volume of the superconductive body. For the sake of simplicity the specimen volume is taken equal to unity so that  $M$  is the magnetization and  $G$  the Gibbs free energy density.

Since  $dU = TdS + HdM$  we have

$$dG = -SdT - MdH, \quad (2-27)$$

and

$$S = - \left( \frac{\partial G}{\partial T} \right)_H, \quad (2-28)$$

and

$$M = - \left( \frac{\partial G}{\partial H} \right)_T. \quad (2-29)$$

The specific heat (at constant field) will then be

$$C = T \left( \frac{\partial S}{\partial T} \right)_H = - T \left( \frac{\partial^2 G}{\partial T^2} \right)_H. \quad (2-30)$$

Upon isothermal magnetization the Gibbs free energy of the superconductor increases with the applied field  $H$

$$G_s(T,H) = G_s(T,0) - \int_0^H MdH. \quad (2-31)$$

For a type I superconductor  $M = -H/4\pi$  and therefore

$$G_s(T, H) = G_s(T, 0) + \frac{H^2}{8\pi} . \quad (2-32)$$

At the transition to the normal state  $G_s(T, H_c) = G_n(T, H_c)$ .  $H_c$  is the thermodynamic critical field at the temperature  $T$ , related to the condensation energy density  $G_n(T, H_c) - G_s(T, 0)$  by eq. (2-1). Experimentally,  $H_c$  was found to have, approximately, a parabolic temperature dependence  $H_c(t) \approx H_c(0) (1-t^2)$  (see Fig. IV.16). Neglecting the small normal state magnetic susceptibility,  $G_n$ ,  $S_n$  and  $C_n$  are field independent quantities.

From (2-28) and (2-32) one gets

$$S_s(T, H) = S_s(T, 0) , \quad (2-33)$$

and from (2-30) and (2-33) we have

$$C_s(T, H) = C_s(T, 0) . \quad (2-34)$$

Therefore, complete diamagnetism implies field independent specific heat and entropy.

From (2-1) and (2-28) the entropy difference between the superconducting and the normal state is obtained as

$$\Delta S(T) = S_n(T) - S_s(T, 0) = -\frac{H_c}{4\pi} \frac{dH_c}{dT} . \quad (2-35)$$

At  $T = T_c$  the transition to the normal state is second order in Ehrenfest's sense<sup>38)</sup> since  $H_c(T_c) = 0$  and therefore  $\Delta S(T_c) = 0$ . At  $T = 0$  the third law of thermodynamics implies  $dH_c/dT = 0$ . For  $T \neq 0$  and  $T_c$ , the transition is first order with a latent heat  $T \Delta S$ .

From (2-30) and (2-35) the difference between the specific heat in the superconducting and normal state is derived as

$$\Delta C(T) = C_s(T, 0) - C_n(T) = \frac{T}{4\pi} \left[ \left( \frac{dH_c}{dT} \right)^2 + H_c \frac{d^2 H_c}{dT^2} \right] . \quad (2-36)$$

At  $T = T_c$  we have the Rutgers' relation

$$\frac{\Delta C(T_c)}{T_c} = \frac{1}{4\pi} \left( \frac{dH_c}{dT} \right)^2_{T_c} , \quad (2-37)$$

relating the magnitude of the specific heat jump at the transition to

the normal state in zero field to the slope of the thermodynamic critical field at  $T = T_c$ .

The quantities  $\Delta C(T)$  and  $\Delta S(T)$  can be calculated from the temperature dependence of  $H_c$  (derived from magnetization measurements). Reciprocally the thermodynamic critical field can be obtained from calorimetric results by two integrations, as follows

$$\int_0^T \left[ \frac{C_n}{T} - \frac{C_s}{T} \right] dT = \Delta S(T) \quad (2-38)$$

and

$$\int_{T_c}^T \Delta S dT = G_n(T) - G_s(T,0) = \frac{H_c^2(T)}{8\pi} . \quad (2-39)$$

#### 2.4.2 Type II superconductors

Adopting for type II superconductors the concept of thermodynamic critical field  $H_c$  as given by relation (2-2), eqs. (2-35), (2-36) and (2-37) hold independently of the type of the superconductor. Obviously, relation (2-33) and (2-34) are also valid for type II superconductors but restricted to fields  $H < H_{c1}$ .

However, since in the mixed state the entropy is a function of the applied field, as shall be discussed in Chapter V, relation (2-35) says nothing about the nature of the transition to the normal state except in the cases  $H = 0$  and  $T = 0$ . On basis of Maki's extension of Abrikosov's prediction for the magnetization near  $H_{c2}$  (eq. (2-23)), the transition to the normal state should be second order for all  $T$ , which is confirmed by experiment, down to the lowest attained temperature.

The area under the isothermal reversible magnetization curve yields  $H_c$  (eq. (2-2)). In practice, such a calculation is inevitably affected by hysteresis and is therefore not free from error. Calorimetrically,  $H_c$  can be calculated freely of disturbances by hysteresis even in the case of the most irreversible magnetic behaviour. By using relations (2-38) and (2-39),  $H_c$  is derived from zero field and normal state specific heat results which are independent of the degree of reversibility of the magnetic behaviour.

It remains yet to be established on microscopic grounds the

analytical treatment of the behaviour of the specific heat of intrinsic, low  $\kappa$ , type II superconductors in the mixed state. However, on basis of Abrikosov's vortex model that yields explicitly linear magnetization  $M \propto (H - H_{c2})$  (eq. (2-23)) near the transition to the normal state, it is possible to derive expressions for the entropy and therefore the specific heat in that region. These expressions provide a means for a rather severe test of Abrikosov's prediction for  $M(H)$  near  $H_{c2}$  since the calorimetric quantities are very sensitive to the exact shape of the magnetization curve.

Assuming that  $H_{c2}(t)$  is a second (or higher) order phase transition line, the electronic Gibbs free energy density in the mixed state at temperature  $T$  and applied field  $H$  is given by

$$G_m(H, T) = G_n(T) - \int_{H_{c2}}^H M dH, \quad (2-40)$$

$$\text{where } G_n(T) = -\frac{1}{2} \gamma T^2 \quad (2-41)$$

is the normal state, field independent, electronic Gibbs free energy density ( $\gamma$  being the Sommerfeld constant).

In the immediate neighbourhood of the transition to the normal state, according to Abrikosov - Maki (eq. (2-23)) we have, for all  $T$  in the mixed state

$$M = \chi_m (H - H_{c2}) \quad (2-42)$$

$$\text{where } \chi_m = (\partial M / \partial H)_T = 1/4\pi\beta [2\kappa_2^2(T) - 1] \quad (2-43)$$

is the field independent differential magnetic susceptibility in the mixed state, for  $H_{c2} - H \ll H_{c2}$ .  $H_{c2}$ ,  $M$  and  $\chi_m$  are temperature dependent quantities.

From (2-40), (2-41) and (2-42) we have

$$G_m(H, T) = -\frac{1}{2} \gamma T^2 - \frac{1}{2} \chi_m (H_{c2} - H)^2. \quad (2-44)$$

The entropy in the mixed state near  $H_{c2}$  per unit volume is then given by

$$S_m(H, T) = \gamma T + \frac{1}{2} \frac{d\chi_m}{dT} (H_{c2} - H)^2 + \chi_m (H_{c2} - H) \frac{dH_{c2}}{dT}. \quad (2-45)$$

This expression yields in fact a transition of second or higher order when the applied field  $H$  reaches the upper threshold field  $H_{c2}$ . Thus,

for  $T = T_s$ ,  $H = H_{c2}(T_s)$  we have  $S_m(H_{c2}, T_s) = \gamma T_s = S_n(T_s)$ . At  $T=0$  the third law of thermodynamics implies:  $dH_{c2}/dT = d\chi_m/dT = 0$  and consequently from (2-22) and (2-43),  $d\kappa_2/dT = d\kappa_1/dT = 0$ , for  $T = 0$ .

The specific heat in the mixed state in the immediate vicinity of  $H_{c2}$  is given (per unit volume) by

$$C_m(H, T) = T \left[ \gamma + \frac{1}{2} \frac{d^2 \chi_m}{dT^2} (H_{c2} - H)^2 + 2 \frac{d\chi_m}{dT} (H_{c2} - H) \frac{dH_{c2}}{dT} + \chi_m \left( \frac{dH_{c2}}{dT} \right)^2 + \chi_m (H_{c2} - H) \frac{d^2 H_{c2}}{dT^2} \right]. \quad (2-46)$$

At the transition to the normal state we have the Ehrenfest<sup>12a,39)</sup> type relation

$$\frac{C_m(T_s) - \gamma T_s}{T_s} = \chi_m \left( \frac{dH_{c2}}{dT} \right)^2, \quad (2-47)$$

relating the discontinuity in the specific heat  $\Delta C(T_s) = C_m(T_s) - C_n(T_s)$  to the temperature of the transition  $T_s$ , the differential magnetic susceptibility in the mixed state at  $H_{c2}$  and the slope of the phase transition line. This relation makes it possible to derive from specific heat results the values of  $\chi_m = (\partial M / \partial H)_T$  for  $H = H_{c2}$  and, therefore, the parameter  $\kappa_2(t)$  through relation (2-23). Expression (2-46) holds for all  $T$  and in the limit  $T \rightarrow 0$  it yields an interesting result. Defining  $\gamma'(H) = \lim_{T \rightarrow 0} (C_m(H, T)/T)$ , one has

$$\frac{\gamma'(H)}{\gamma} = 1 + \frac{1}{2\gamma} \left( \frac{d^2 \chi_m}{dT^2} \right)_{T=0} [H_{c2}(0) - H]^2 + \frac{\chi_m(0)}{\gamma} [H_{c2}(0) - H] \left( \frac{d^2 H_{c2}}{dT^2} \right)_{T=0}. \quad (2-48)$$

Experimentally it was found (Section 4.2.7.4) that  $\chi_m(T)$  is at the lowest temperatures a non vanishing, slow decreasing function upon decreasing temperature so that the term in  $d^2 \chi_m/dT^2$  for  $T = 0$  is negligible, at least for  $H_{c2}(0) - H \ll H_{c2}(0)$ .  $d^2 \chi_m/dT^2$  at  $T = 0$  will be even zero if, as a first approximation (which experiment appears to confirm<sup>40)</sup>), we take near the absolute zero

$$H_{c2}(t) = H_{c2}(0) (1 - at^2). \quad (2-49)$$

$$\text{Then we have} \quad \frac{dH_{c2}}{dT} = pT \quad (2-50)$$

$$\text{and} \quad \frac{d^2 H_{c2}}{dT^2} = p \quad (2-51)$$

$$\text{where} \quad p = -2aH_{c2}(0)/T_c^2. \quad (2-52)$$

Experimentally it was found (Section 4.2.7.1) that, for  $T$  not too close to  $T_c$ , the magnitude of the specific heat jump at the transition to the normal state varies as

$$\frac{\Delta C(T)}{T} = \epsilon T^2, \quad (2-53)$$

where  $\epsilon$  is a numerical coefficient.

From (2-47), (2-51) and (2-52) it is therefore concluded that near the absolute zero,  $\chi_m$  is temperature independent and non zero

$$\chi_m(0) = \frac{\epsilon}{p^2}. \quad (2-54)$$

If the expression for the temperature dependence of  $H_{c2}$  includes terms of power greater than the second then  $(d^2 \chi_m / dT^2)_{T=0} \neq 0$  but remains small. Neglecting in (2-48) the term in  $(d^2 \chi_m / dT^2)_{T=0}$  we have

$$\frac{\gamma'(H)}{\gamma} = 1 + \frac{\chi_m(0)}{\gamma} [H_{c2}(0) - H] \left( \frac{d^2 H_{c2}}{dT^2} \right)_{T=0}. \quad (2-55)$$

By means of relations (2-51), (2-52) and (2-54) expression (2-55) becomes

$$\frac{\gamma'(H)}{\gamma} = 1 - a + a \frac{H}{H_{c2}(0)}, \quad (2-56)$$

$$\text{where} \quad a = \frac{\epsilon T_c^2}{2a\gamma}. \quad (2-57)$$

The behaviour of the mixed state specific heat in the neighbourhood of the absolute zero and at high fields ( $H_{c2}(0) - H \ll H_{c2}(0)$ ) is therefore expected to be quite different from the zero field specific heat which vanishes exponentially at absolute zero due to the existence of a forbidden gap in the excitation spectrum of the superconducting electrons (BCS<sup>17</sup>). On basis of the sole assumption that near  $H_{c2}$  the magnetization is given by eq. (2-42) with  $\chi_m$  field independent, the specific heat for  $T = 0$  and  $H \approx H_{c2}(0)$  is expected to contain a term linear both in the temperature and the applied field.



This linear term was first predicted by Gorter et al.<sup>41,42</sup> on thermodynamic grounds. Assuming that the transition at  $H_{c2}(T)$  is always of second order and that  $dH_{c2}/dT$  vanishes at the absolute zero, the entropy at all temperatures and the specific heat divided by the absolute temperature,  $C/T$ , in the limit  $H \rightarrow H_{c2}(0)$ , cannot vary discontinuously. Thus,  $\lim_{T \rightarrow 0} [C_m(H,T)/T]$  is of the order of  $\gamma$  for  $H \approx H_{c2}(0)$ .

The linear term owes its origin to the low energy excitations which the energy spectrum of the superconducting electrons contains in the cores of the Abrikosov vortices (Caroli et al.<sup>19</sup>).

## References

1. De Haas, W.J. and Voogd, J., Commun. Kamerlingh Onnes Lab., Leiden, No. 208b (1930).
2. Keely, T.C., Mendelssohn, K. and Moore, J.R., Nature **134** (1934) 773; Mendelssohn, K. and Moore, J.R., Nature **135** (1935) 826; Mendelssohn, K., Proc.Roy.Soc. (London) A **152** (1935) 34.
3. Shubnikov, L.V., Khotkevich, V.I., Shepelev, J.D. and Riabinin, J.N., J.exptl.theoret.Phys. (U.S.S.R.) **7** (1937) 221.
4. Ginzburg, V.L. and Landau, L.D., J.exptl.theoret.Phys., (U.S.S.R.) **20** (1950) 1064; Phys.Abh.Sow.Un., Folge **1** (1958) 7.
5. Abrikosov, A.A., Dokl. Akad.Nauk.SSSR **86** (1952) 489.
6. Morin, F.J., Maita, J.P., Williams, H.J., Sherwood, R.C., Wernick, J.H. and Kunzler, J.E., Phys.Rev.Letters **8** (1962) 275.
7. Hauser, J.J. and Helfand, E., Phys.Rev. **127** (1962) 386.
8. Calverley, A. and Rose-Innes, A.C., Proc.Roy.Soc. (London) A **255** (1960) 267.
9. London, H., Proc.Roy.Soc. (London) A **152** (1935) 650.
10. Gorter, C.J., Physica **2** (1935) 449.
11. London, F., Superfluids, vol. I, (John Wiley Sons, Inc., New York, 1950) pp. 125-130.
12. Goodman, B.B., Phys.Rev.Letters **6** (1961) 597.
- 12a. Goodman, B.B., I.B.M. J.Res.Develop. **6** (1962) 63.
13. Van Beelen, H. and Gorter, C.J., Comm.Leiden, Suppl.No. **121a**; Physica **29** (1963) 896.
14. See, for instance, Lynton, E.A., Superconductivity, ed. B.L. Worsnop (Methuen, London, 1962) p. 55.
15. Abrikosov, A.A., J.exptl.theoret.Phys. (U.S.S.R.) **32** (1957) 1442; Soviet Phys. JETP **5** (1957) 1174.
16. Landau, L.D. and Lifshitz, E.M., Statistical Physics (Pergamon Press, London 1958) p. 434.
17. Bardeen, J., Cooper, L.N. and Schrieffer, J.R., Phys.Rev. **108** (1957) 1175.

18. See, for instance, De Gennes, P.G., *Superconductivity of Metals and Alloys*, ed. D.Pines (W.A. Benjamin, Inc., New York, 1966) p. 176.
19. Caroli, C., De Gennes, P.G. and Matricon, J., *Phys.Letters* **9** (1964) 307.
20. Harden, V.L. and Arp., V., *Cryogenics* **3** (1963) 105.
21. Pippard, A.B., *Proc.Roy.Soc. A* **203** (1950) 210; idem *A* **216** (1953) 547.
22. Keesom, P.H., and Radebaugh, R., *Phys.Rev.Letters* **13** (1964) 685.
23. Gorter, C.J. and Casimir, H.B.G., *Phys.Z.* **35** (1934) 963; *Z.techn. Phys.* **15** (1934) 539.
24. Tinkham, M., *Phys.Rev.* **129** (1963) 2413.
25. Ginzburg, V.L., *J.exptl.theoret.Phys. (U.S.S.R.)* **30** (1956) 593; *Soviet Phys. JETP* **3** (1956) 621.
26. Kleiner, W.H., Roth, L.M. and Autler, S.H., *Phys.Rev.* **133** (1964) A 1226.
27. Matricon, J., *Phys.Letters* **9** (1964) 289; *Proc. IX Int.Conf. on Low Temp.Phys. Columbus, Ohio*, eds. J.G. Daunt et al. (New York, Plenum Press) p. 544.
28. Gor'kov, L.P., *J.exptl.theoret.Phys. (U.S.S.R.)* **36** (1959) 1918; *Soviet Phys. JETP* **9** (1959) 1364.
29. Gor'kov, L.P., *J.exptl.theoret.Phys. (U.S.S.R.)* **37** (1959) 1407; *Soviet Phys. JETP* **10** (1960) 998.
30. Gor'kov, L.P., *J.exptl.theoret.Phys. (U.S.S.R.)* **37** (1959) 833; *Soviet Phys. JETP* **10** (1960) 593.
31. Maki, K., *Physics* **1** (1964) 21.
32. Caroli, C., Cyrot, M. and De Gennes, P.G., *Solid State Commun.* **4** (1966) 17.
33. Maki, K. and Tsuzuki, T., *Phys.Rev.* **139** (1965) A 868.
34. Eilenberger, G., *Phys.Rev.* **153** (1967) 584.
35. Helfand, E. and Werthamer, N.R., *Phys.Rev.* **147** (1966) 288.
36. Werthamer, N.R. and McMillan, W.L., *Phys.Rev.* **158** (1967) 415.
37. Hohenberg, P.C. and Werthamer, N.R., *Phys.Rev.* **153** (1967) 493.
38. Ehrenfest, P., *Leiden Comm.Suppl.75b*; *Proc. Kon.Nederl.Akad. Wet., Amsterdam* **35** (1932) 736.
39. Ehrenfest, P., *Proc.Kon.Nederl.Akad.Wet., Amsterdam* **36** (1933) 153.
40. Ohtsuka, T. and Takano, N., preprint to be published in *J.Phys. Soc.Japan*.
41. Gorter, C.J., *Proc.Int.Conf. on the Science of Superconductivity, Colgate University, Hamilton, New York, 1963*; *Rev.mod.Phys.* **36** (1964) 49.
42. Gorter, C.J., van Beelen, H. and De Bruyn Ouboter, R., *Phys. Letters* **8** (1964) 13.

## Chapter III

## EXPERIMENTAL METHOD

## 3.1 Introduction

In this chapter a description is given of the method and apparatus used for the measurements of the specific heat of niobium. The specific heat  $C$  of a specimen is defined as

$$C(T) = \lim_{\Delta T \rightarrow 0} \frac{\Delta Q}{\Delta T} \quad (3-1)$$

and thus can be obtained directly by determining the increase  $\Delta T$  in the temperature  $T$  of the sample to which a known quantity of heat  $\Delta Q$  has been supplied.

In general, the same  $\Delta Q$  produces different  $\Delta T$ 's on the same sample at the same temperature, according to the conditions under which the energy is supplied. Throughout this thesis the condition is that of constant applied magnetic field. In terms of the magnetic Gibbs function,  $G$ ,  $C_H$  is given by  $C_H = -T(\partial^2 G / \partial T^2)_H$  (Section 2.4.1). Defining a magnetic enthalpy  $E$  as

$$E = U - HM \quad (3-2)$$

where  $U$  is the internal energy,  $H$  the applied magnetic field and  $M$  the magnetic moment of the sample, it can also be shown that

$$C_H = \left(\frac{\partial E}{\partial T}\right)_H \quad (3-3)$$

Although the index  $H$  in  $C_H$  has been dropped everywhere, the meaning of  $C$  in the text is that of  $C_H$ .

The heat capacity,  $C_t$ , of the calorimeter plus sample plus addenda (heater and thermometer) is directly measured. The (molar) specific heat of the sample is calculated by subtracting from  $C_t$  the heat capacity of the calorimeter plus addenda as measured in separate runs.

Basic to accurate low temperature calorimetry are the following requirements: 1) good thermal insulation of the calorimeter from the surroundings, achieved by means of high vacuum and by minimizing

the thermal conductance of the suspension threads and electrical leads; 2) heater and thermometer in good thermal contact with the sample and mounted in such a way that heat flows from the heater to the thermometer mainly through the bulk of the sample; 3) low thermal relaxation time  $\tau$  ( $\tau$  measures the rate at which the sample approaches a homogeneous temperature distribution after heat has been supplied locally). In particular,  $\tau$  should be kept smaller than the response time of the apparatus with which temperature variations of the sample are recorded. Otherwise the interpretation of the heating curves is not straightforward.

The order of magnitude of  $\tau$  is given<sup>1)</sup> by  $\tau \approx C/\kappa L$  where  $C$  is the heat capacity of the sample,  $\kappa$  its thermal conductivity and  $L$  a linear dimension of the sample. For superconductors,  $\tau$  may vary considerably with the magnetic field and temperature through  $C$  and  $\kappa$ . For a type II superconductor near  $H_{c1}(T)$  both  $C$  and  $\kappa$  display anomalies in the direction of increasing  $\tau$ . In the extreme case of Nb-3, near  $H_{c1}(T)$   $\tau$  was calculated to increase by a factor in the order of 100 with respect to the normal state values. In the normal state, at 4.2°K,  $\tau$  was in the order  $10^{-5}$  seconds. Even so, the calculated value of  $\tau$  did not reach the response time of the recording apparatus (in the order of a few seconds) although relaxation effects were apparent at  $H_{c1}(T)$ .

For reducing the error produced by the heat leak to the surroundings during the heating time it is required that the heat lost during the time  $\tau$  be much less than the energy  $\Delta Q$  supplied to the sample:  $\tau \dot{Q} \ll \Delta Q$  ( $\dot{Q}$  is the heat leak per second). This condition was certainly fulfilled since typical values of  $\tau \dot{Q}/\Delta Q$  were in the order of  $10^{-4}$  for a temperature difference between sample and bath of one degree.

### 3.2 Samples

Nb-1 was a bundle of 2200 impure unannealed thin niobium wires with a total mass of 0.0745 gram-moles closely packed in a calorimeter (1 gram-mole = 92.91). Each wire has a diameter of 0.1 mm and a length of 44.1 mm. Since hysteretic behaviour was expected, thin wires were chosen in order to reduce the effects of irreversibility. The wires were cut from a coil supplied by Fansteel Metallurgical Corporation.

The annealed samples each consisted of 8 wires of diameter 0.76 mm and length 42.5 mm (Nb-2) and 45 mm (Nb-3). The masses were 0.0138 (Nb-2) and 0.0145 (Nb-3) gram-moles. The wires making up samples Nb-2 and Nb-3 were cut from two refined annealed niobium wires received from the General Electric Research Laboratory,

Schenectady, New York, through the kindness of Dr. W. de Sorbo who carried out the heat treatment. The origin of this material is the same as that mentioned in ref.2), where it was referred to as Stauffer Temescal - an electron-beam melted (one-pass) ingot of Nb. The two wires have been heated separately by passing an electrical current of about 24 A through each of them in a vacuum of approximately  $5 \times 10^{-7}$  mm Hg. Total heating time was 8¼ hours for Nb-2 and 7¼ hours for Nb-3. The annealing temperature, measured with optical pyrometer was 1830 °C for Nb-2 and 1800 °C for Nb-3.

The result of annealing and outgassing appears to depend critically on the annealing temperature, time and vacuum. Notwithstanding the similarity of the thermal treatment undergone by the two samples, the slightly different annealing times and temperatures may account for the different characteristics of the two specimens. In an attempt to remove strains introduced by the cutting procedure, each end of the wire segments constituting samples Nb-2 and Nb-3 was etched by dipping it for a few seconds in a 50-50 volume mixture of concentrated  $\text{HNO}_3$  and 48% solution of HF. The resistance ratio  $R(273^\circ\text{K})/R(4.2^\circ\text{K})$  of the three samples measured potentiometrically after the measurements were performed, were 7, 47 and 145 respectively for Nb-1, Nb-2 and Nb-3.

The chemical analysis of the samples gave the results shown in Table I.

Table I  
Results of the chemical analysis of the three Nb samples

element sample	O	N	C	Si	Ta	Fe	Cr	Mg	Ni	Al	Ag	Mo	Sn
Nb-1 (wt %)	0.16	<0.005	0.05	0.01	0.12	0.008	0.02	0.001	0.01	0.003	0.001	0.03	<0.002
Nb-2 and Nb-3 (p.p.m.)	≤ 30	~ 30		~ 300	~ 60	< 10	< 5	10	< 10	< 5		< 50	< 5

Ag was not found in Nb-2 and Nb-3 and the C concentration could not be calculated because the mass available for analysis was too small. All samples were polycrystalline.

### 3.3 Apparatus and cooling procedure

For many years it was usual in Leiden to cool the calorimeter by using gaseous helium to establish thermal contact with the surrounding bath of the cryogenic liquid (exchange gas method). The measurements on the first sample (Nb-1) were performed in this way. It was,

however, soon learned that when the cooling was brought into the neighbourhood of  $1^{\circ}\text{K}$  it was not possible to remove the residual traces of the contact gas no matter what the pumping time. Thus, satisfactory thermal insulation of the calorimeter from the surroundings could not be achieved at the lowest temperatures. Moreover, the desorption of the exchange gas in the course of the run affected the results.

Although the difficulties associated with the use of contact gas were reasonably well overcome by pumping it out at a somewhat higher temperature and by removing its residual traces from the calorimeter surface, suspension threads and electrical leads by a cryopump effect, an alternative means of establishing and breaking thermal contact between sample and bath (a thermomechanical switch) was devised for the measurements with samples Nb-2 and Nb-3. This last cooling procedure introduces no disturbances and allows the immediate starting of the measurements after the cooling to the lowest temperature.

For both cooling procedures, before each measurements, the vacuum jacket surrounding the calorimeter was pumped at room temperature with a "Speedivac" oil vapour diffusion pump model 203B. The highest vacuum that could be reached with this pump was in the order of  $10^{-7}$  mm Hg, measured with a Philips Special Ionization Vacuum Gauge type PW 7902. When exchange gas ( $^4\text{He}$ ) was used it was introduced into the vacuum system at room temperature and at a pressure low enough to prevent condensation at the lowest temperature to be reached.

The temperature of the bath was reduced by pumping its vapour with the central pump of the laboratory to  $1.4^{\circ}\text{K}$  and below that by means of a "Speedivac" vapour booster pump model 9B3 with which a temperature of about  $0.9^{\circ}\text{K}$  could be reached.

Next, a description is given of the apparatus used with each cooling procedure, reference being made only to the parts that vary between one method and the other.

### 3.3.1 Apparatus using exchange gas (A)

Apparatus A is shown in Fig.III.1 at the level of sample location. The thin niobium wires constituting sample Nb-1 were packed in a calorimeter *c* having the heater *h* at one end and the thermometer *th* at the other end. The calorimeter was suspended by means of four silk threads *s* from four stainless steel vertical rods *p* attached to the top of the vacuum jacket *j*. These silk threads were maintained under tension by means of two phosphor-bronze springs *sp*. The electrical leads of the thermometer (constantan) and those of the heater (Nb-20% Zr)

passed through the Pt-glass seal *g* on the top of the vacuum jacket.  $^4\text{He}$  exchange gas could be introduced or high vacuum established inside the jacket through the pumping line *pl* made of German silver, in which some copper radiation shields *r* were placed. Through the small Pt-glass seal *f* a small amount of helium contact gas was introduced into the calorimeter in an attempt to improve the thermal contact between the wires.

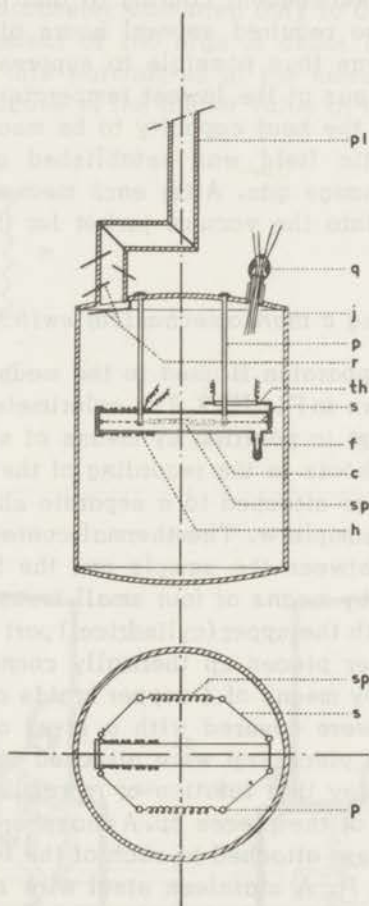


Fig. III.1 Apparatus *A* using the exchange gas method.

The heater was a constantan wire wound anti-inductively with a room temperature resistance of  $120\Omega$ . The parts of the calorimeter in connection with the heater and the thermometer were made from electrolytic copper while the middle part was made from stainless steel. In that way the flow of heat through the calorimeter wall was

decreased so that overshoots in the recording of the temperature of the sample were avoided.

In spite of the conventional design of apparatus *A* the disturbances caused by the use of contact gas were removed by the following cooling procedure: as soon as the calorimeter was cooled to about 1.6°K by the  $^4\text{He}$  exchange gas, the jacket *j* was evacuated and the temperature of the liquid helium bath was reduced to about 0.9°K in order to restrict the subsequent cooling to that due to parasitic heat leaks. This procedure required several hours of waiting in order to reach 1.3°K but it was thus possible to suppress desorption effects of the  $^4\text{He}$  exchange gas at the lowest temperatures. Such effects can be very disturbing if the heat capacity to be measured is very small. The required magnetic field was established at 1.6°K just before pumping out the exchange gas. After each measuring run contact gas was again admitted into the vacuum jacket for the calibration of the thermometer.

### 3.3.2 Apparatus using a thermomechanical switch (*B*)

The modified apparatus *B* used in the measurements on samples Nb-2 and Nb-3 is shown in Fig. III.2. The calorimeter *c*, made of electrolytic copper, was kept in position by means of six silk threads *s*. In order to avoid over-shoots in the recording of the sample temperature, the thermometer *th* was attached to a separate sheet of copper placed near one end of the sample *w*. The thermal contact between the wires of the sample and between the sample and the heater *h* and thermometer was regulated by means of four small brass screws *b*. Surrounding and concentric with the upper (cylindrical) part *t* of the calorimeter, there were two copper pieces *cp* thermally connected to the wall of the vacuum jacket *j* by means of 4 copper braids *cb*. The inner surfaces of these pieces *cp* were covered with a layer of indium to improve thermal contact. The pieces *cp* were attached to rotatory teflon segments *rp* in such a way that rotation of *rp* resulted in horizontal linear pincer movement of the pieces *cp*. A phosphor-bronze spring *sp* and a tungsten wire *tw* were attached to each of the two rotatory segments *rp* at the same point *P*. A stainless steel wire *l* was passed through the pumping line *pl* and attached at the cryostat cap to a bellows *m*, the other end being connected with the movable segments *rp*, via the wire *tw*. Radiation shields are indicated by *r*; *g* is a platinum-glass seal through which pass the electrical leads to the thermometer and heater.

Pulling on the bellows brings the pieces *cp* into strong contact with the upper part of the calorimeter, thus thermally connecting it



with the bath. Upon releasing the pulling force on the bellows, (which is then pressed down by the atmospheric pressure) the springs  $sp$ , being under tension recall the contacts  $cp$ , thus insulating the calorimeter from the surroundings. Because of friction, the temperature of the sample rose somewhat when opening the contacts, this effect being most apparent in zero magnetic field at the lowest temperatures where the heat capacity of the sample is the smallest. Even so, the warming up of the calorimeter amounted only to  $0.36^{\circ}\text{K}$ , corresponding to an energy development of 280 ergs at about  $1^{\circ}\text{K}$ . With the sample in the normal state, this warming-up at the same temperature did not even reach  $0.1^{\circ}\text{K}$  because of the higher value of the heat capacity.

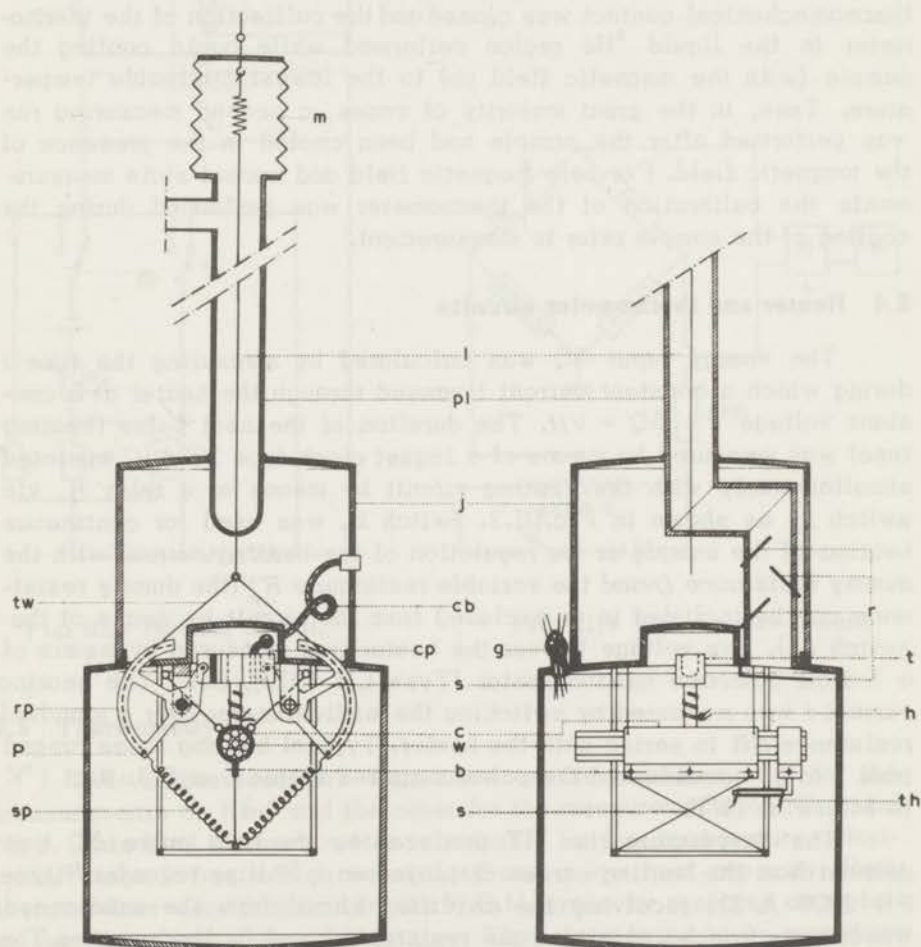


Fig. III.2 Apparatus B using a thermomechanical switch.

With the thermal switch closed, the temperature of the calorimeter was reduced to about  $0.9^{\circ}\text{K}$  by pumping on the vapour of the helium bath and then the required magnetic field was established. Upon opening the thermomechanical contact the sample became thermally insulated from the surroundings and the measurement could thus be immediately started. In the course of each measuring run the temperature of the bath was periodically adjusted (up to  $4.2^{\circ}\text{K}$ ) in order to minimize the parasitic heat exchange between sample and environment. The whole temperature range of interest (maximum  $1^{\circ}\text{K}$  to about  $10^{\circ}\text{K}$ ) was thus passed at constant magnetic field in a single run, the temperature being increased by the very process of measuring. Once the normal state was reached (for fields crossing the mixed state) the thermomechanical contact was closed and the calibration of the thermometer in the liquid  $^4\text{He}$  region performed while again cooling the sample (with the magnetic field on) to the lowest attainable temperature. Then, in the great majority of cases, a second measuring run was performed after the sample had been cooled in the presence of the magnetic field. For zero magnetic field and normal state measurements the calibration of the thermometer was performed during the cooling of the sample prior to measurement.

### 3.4 Heater and thermometer circuits

The energy input  $\Delta Q$  was calculated by measuring the time  $t$  during which a constant current  $i$  passed through the heater at a constant voltage  $V$ :  $\Delta Q = Vit$ . The duration of the heat pulse (heating time) was measured by means of a Jaquet clock type 309d, C, operated simultaneously with the heating circuit by means of a relay  $R$ , via switch  $k$ , as shown in Fig.III.3. Switch  $k_1$  was used for continuous heating of the sample or for regulation of the heating current with the dummy resistance  $D$  and the variable resistance  $R_v$  (the dummy resistance can be included in or excluded from the circuit by means of the switch  $k_2$ ). The voltage  $V$  over the heater was measured by means of a 5-digit Solartron millivoltmeter (Type LM 1010), D.V. The heating current  $i$  was measured by switching the millivoltmeter over a standard resistance  $NR$  in series with the heater. Typical heating times ranged from 5 to 25 seconds and the power supplied varies from  $0.3\mu\text{W}$  at  $1^{\circ}\text{K}$  to  $140\mu\text{W}$  at  $10^{\circ}\text{K}$ .

The temperature rise  $\Delta T$  produced by the heat pulse  $\Delta Q$  was derived from the heating curves displayed on a Philips recorder  $R$  (type PR 2200 A/21) receiving the amplified signal from the unbalanced Wheatstone bridge containing the resistor  $th$  used as thermometer. The thermometer circuit is presented in Fig.III.4. During the calibration

of the thermometer the amplifier A (Leeds and Northrup stabilized d-c microvolt amplifier No. 9835-B) was used as a null-detector.  $\Delta T$  values ranged from a few millidegrees at 1°K up to few tenths of a degree at 10°K. The voltage input to the bridge remained constant within 1% from 1°K to 10°K with the result that the power dissipated in the thermometer was smallest at the lowest temperature, where the resistance was largest. This power dissipation amounted to 3.8 nW at 1°K and was four times larger at 10°K.

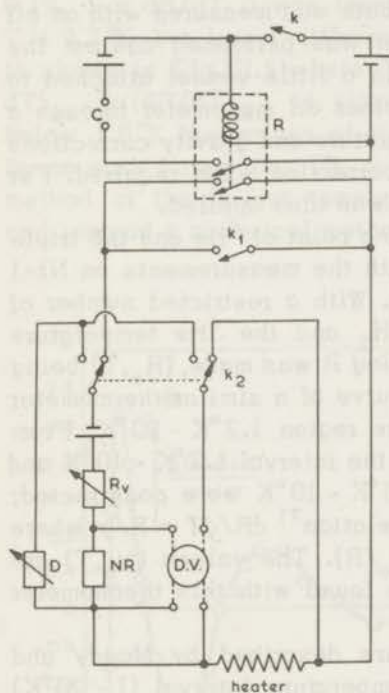


Fig. III.3 Heating circuit.

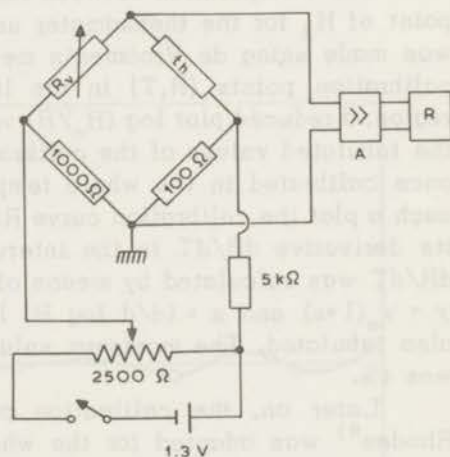


Fig. III.4 Thermometer circuit.

### 3.5 Thermometry

Two carbon resistors were used as thermometers, one for the measurements on Nb-1 and the other for the measurements on Nb-2 and Nb-3. This kind of thermometer is suitable for low temperature calorimetry since it has a high sensitivity and a low heat capacity. Both thermometers were prepared by the F.O.M. group for research on metals at the Kamerlingh Onnes Laboratory. They were found to be reproducible while kept at low temperatures but the reproducibility was lost

once they had been warmed up to room temperature. Magnetoresistance effects were also observed. Thus, calibration of the thermometer was required for each measurement. The secondary standards used for calibration of the carbon thermometers were the vapour pressure of liquid hydrogen (using the L-60 scale of temperatures<sup>3</sup>) helium-4 (using the 1958 <sup>4</sup>He scale of temperatures<sup>4</sup>) and helium-3 (using the 1962 <sup>3</sup>He scale of temperatures<sup>5</sup>). The pressure of the bath vapour was read on a Hg manometer by means of a cathetometer. For  $1.4 < T < 2.2^\circ\text{K}$  the vapour pressure of the <sup>4</sup>He bath was measured with an oil manometer. Below  $1.4^\circ\text{K}$  the calibration was performed against the vapour pressure of the <sup>3</sup>He condensed in a little vessel attached to the vacuum jacket and connected to another oil manometer through a stainless steel capillary. Standard temperature and gravity corrections were applied as well as a hydrostatic correction when required. For  $T < 1^\circ\text{K}$ , a thermomolecular correction<sup>6</sup> was also applied.

The interpolation between the boiling point of <sup>4</sup>He and the triple point of H<sub>2</sub> for the thermometer used with the measurements on Nb-1 was made using de Vroomen's method<sup>7</sup>. With a restricted number of calibration points (R,T) in the liquid H<sub>2</sub> and the <sup>4</sup>He temperature region, a reduced plot  $\log(R_0/R)$  versus  $\log R$  was made, (R<sub>0</sub>,T) being the tabulated values of the calibration curve of a similar thermometer once calibrated in the whole temperature region  $1.2^\circ\text{K} - 30^\circ\text{K}$ . From such a plot the calibration curve R(T) in the interval  $1.3^\circ\text{K} - 10^\circ\text{K}$  and its derivative dR/dT in the interval  $1.6^\circ\text{K} - 10^\circ\text{K}$  were constructed; dR/dT was calculated by means of the relation<sup>7</sup>  $dR/dT = R/\gamma$  where  $\gamma = \gamma_0(1+s)$  and  $s = (d/d \log R) \log(R_0/R)$ . The values ( $\gamma_0, T$ ) are also tabulated. The maximum value of s found with this thermometer was 4%.

Later on, the calibration procedure described by Moody and Rhodes<sup>8</sup> was adapted for the whole temperature interval (1 - 20°K) using an Electrologica X-1 electronic computer. With five experimental calibration points in the liquid H<sub>2</sub> temperature region and twelve in the liquid <sup>4</sup>He region an interpolation was made by fitting the calibration data to a polynomial of the form<sup>8</sup>

$$\frac{1}{T} = \sum_{\nu=0}^n a_\nu (\ln R)^\nu, \quad (3-4)$$

where the  $a_\nu$  are constants and  $\nu$  is an integer. The method of least squares was used, the minimized quantity being  $\sum_{i=1}^N [(1/T_i - 1/T_f)T_i^2]^2$ , where  $T_f$  is the value given by relation (3-4) for the experimentally

found  $R(T_1)$  while  $N$  is the number of experimental calibration points. The calibration programme included an adjustable rejection criterion so that every experimental point deviating more than 3 mdeg in the liquid  $^4\text{He}$  region and more than 10 mdeg in the liquid  $\text{H}_2$  region from the value given for  $T$  by relation (3-4) is excluded from the minimization process. In general, a value of  $n = 3$  in relation (3-4) was sufficient to include all deviations within this criterion.

For the temperature, the two calibration procedures agreed within 0.1%. For  $dR/dT$  it was found that they agreed within 0.2% for  $3.6 < T < 9.3^\circ\text{K}$  but larger differences appeared at lower temperatures, as is shown in Fig. III.5 where  $\Delta(dR/dT)/(dR/dT) = [(dR/dT)_{\text{MR}} - (dR/dT)_{\text{deV}}]/(dR/dT)_{\text{MR}}$  is plotted versus  $T$ . As it is well known that below  $1.6^\circ\text{K}$  the values of  $\gamma_0$  in the de Vroomen tables are affected by an error larger than 1%, the calculation of  $dR/dT$  by means of this method at the lowest temperatures was avoided from the beginning and instead a numerical method was used.

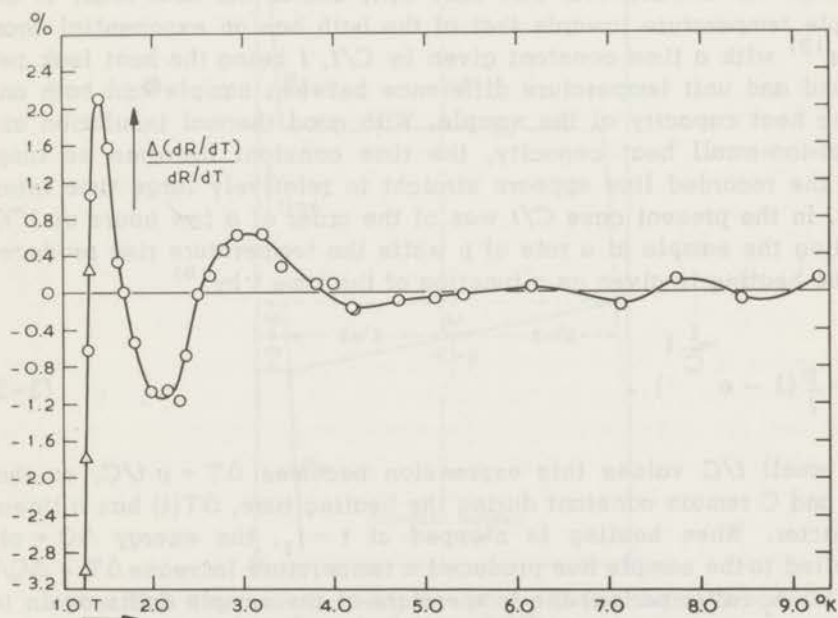


Fig. III.5 Difference between the values of  $dR/dT$  calculated by means of Moody-Rhodes' (MR) and de Vroomen's (de V) methods in % of  $(dR/dT)_{\text{MR}}$ , plotted versus  $T$ .

The two types of points refer to calibrations of the thermometer used with the measurements on Nb-1 in two different runs.

For the thermometer used with the measurements on Nb-2 and Nb-3 the experimental calibration data were also fitted by a third degree polynomial of the form (3-4) using a minimization procedure and computer programme similar to that described above and with equally satisfactory results. Recently, the calibration data of similar carbon thermometers in the whole temperature region 1.2 - 77.5 °K have been fitted by a different polynomial<sup>9)</sup>  $\ln T = \sum_{j=0}^m a_j (\ln R)^j$ , the  $a_j$  being constants and  $j$  an integer. In the range  $0.9 < T < 20^\circ\text{K}$  such a relation does not yield values for  $T$  and  $dR/dT$  much different from those obtained with the Moody-Rhodes polynomial. With  $m = 6$  and  $n = 3$  the maximum difference found in  $T$  was 0.2% (for  $7.5 < T < 10^\circ\text{K}$ ), while the maximum difference in  $dR/dT$  was 0.5% (for  $6 < T < 8^\circ\text{K}$ ).

### 3.6 The calculation of $\Delta T$

The sample temperature was recorded by means of the apparatus described in Section 3.4. The drift  $T(t)$ , due to the heat leak, of the sample temperature towards that of the bath has an exponential character<sup>10)</sup> with a time constant given by  $C/l$ ,  $l$  being the heat leak per second and unit temperature difference between sample and bath and  $C$  the heat capacity of the sample. With good thermal insulation and a not-too-small heat capacity, the time constant becomes so large that the recorded line appears straight in relatively large time intervals. In the present case  $C/l$  was of the order of a few hours at  $1^\circ\text{K}$ . Heating the sample at a rate of  $p$  watts the temperature rise produced by the heating is given as a function of the time  $t$  by<sup>10)</sup>

$$\Delta T = \frac{p}{l} \left( 1 - e^{-\frac{l}{C} t} \right). \quad (3-5)$$

For small  $l/C$  values this expression becomes  $\Delta T = p t/C$ , so that if  $p$  and  $C$  remain constant during the heating time,  $\Delta T(t)$  has a linear character. When heating is stopped at  $t = t_1$ , the energy  $\Delta Q = p t_1$  supplied to the sample has produced a temperature increase  $\Delta T = \Delta Q/C$ . For  $t > t_1$  (after-period) the temperature of the sample drifts again towards that of the bath with about the same value of the time constant (for not-too-large  $\Delta T$ ) as in the fore-period ( $t < 0$ ). In the present case, with the exception of the regions where the specific heat displayed anomalies, the recorded lines  $T(t)$  were straight and their extrapolations in the fore- and after-period parallel to within a few tenths of a percent over the heating interval. The use of the Keesom and Kok

method<sup>10)</sup> for the calculation of  $\Delta T$  was thus reduced to a simple and accurate procedure - the determination of the distance  $\Delta u$  between the fore- and after-period straight lines, at the middle of the heating period and perpendicular to the time axis.

The increase  $\Delta T$  in the temperature of the sample due to the supplied heat  $\Delta Q$  produces a decrease  $\Delta R = (dR/dT)\Delta T$  in the resistance  $R$  of the thermometer; this decrease appears as a shift  $\Delta u$  in the output of the recorder.  $\Delta u$  is related to  $\Delta R$  through the sensitivity  $s$  of the system Wheatstone bridge-amplifier-recorder, defined as  $s = \Delta u / \Delta R$ . For a given bridge nearly in balance  $s$  depends upon the thermometer resistance  $R$  and the amplification factor of the system amplifier-recorder. The relation  $s(R)$  (actually  $s^{-1}(R)$ ) normalized to a given range of amplification was determined from data taken in the course of the measuring run. In the interval  $5 < R(k\Omega) < 21$  corresponding to the temperature region  $1 - 10^\circ K$ , it was always found that  $s^{-1} = cR$ ,  $c$  being a constant.

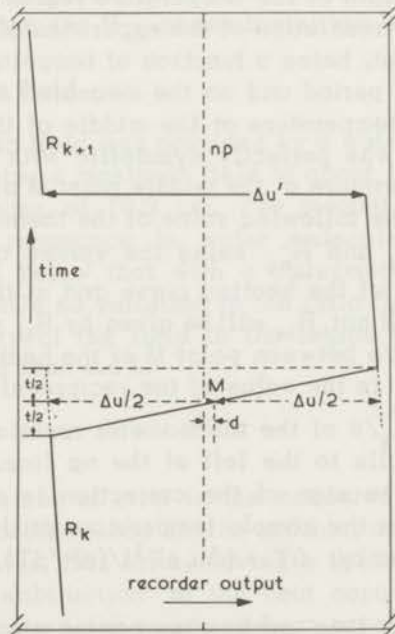


Fig. III.6 The recorder output and the extrapolation procedure used in the calculation of  $\Delta T$ .

The recorder output and the interpretation of the heating curves are shown in Fig. III.6. The measuring sequence was as follows: Firstly, the null-point line  $np$  corresponding to balance of the Wheatstone

bridge was recorded for a short time (by switching off the voltage over the bridge). Secondly, the variable branch  $R_v$  of the bridge was adjusted to a value  $R_k$  somewhat less than that corresponding to balance and the fore-period line was recorded for a few seconds. A heat pulse of known power was then fired during a measured time  $t$ , the thermometer responding to the heating without notable relaxation. When the after-period line was recorded during a time interval allowing an accurate extrapolation to the middle of the heating period,  $R_v$  was decreased to a value  $R_{k+1}$ , thus reversing the out-of-balance situation,  $\Delta u'$  being the shift produced in the recorder output. The value of  $R_v$  that brings the bridge into balance is  $(R_k + R_{k+1})/2$  for heating curves symmetrical with respect to the  $np$  line, so that the value  $(R_k - R_{k+1})/n\Delta u'$  of  $s^{-1}$  corresponds to the thermometer resistance  $R = (R_k + R_{k+1})/2n$  ( $n = 10$  is the bridge factor). The whole cycle fore-heating- and after-period and decrease of  $R_v$  is repeated thereafter a number of times depending upon the width of the temperature region to be covered and the required degree of resolution of the experimental curve.

The specific heat, being a function of temperature, varies in the course of the heating period and so the measured mean value corresponds to the sample temperature at the middle of the heating period. If the heating curve was perfectly symmetric with respect to the  $np$  line, the sample temperature at the middle point  $M$  of the heating curve would correspond to the following value of the thermometer resistance:  $R_M = R_{np} = R_k/n$ ,  $R_M$  and  $R_{np}$  being the values of the thermometer resistance at point  $M$  of the heating curve and at the crossing of the  $np$  line, respectively. If not,  $R_M$  will be given by  $R_M = R_{np} \pm d(s^{-1})_{R_{np}}$ , where  $d$  is the distance between point  $M$  of the heating curve and the  $np$  line, and  $(s^{-1})_{R_{np}}$  is the value of the reciprocal of the sensitivity for the value  $R_{np} = R_k/n$  of the thermometer resistance. The positive sign holds when  $M$  falls to the left of the  $np$  line. If  $M$  falls to the right of the  $np$  line the sign of the correction is negative. Summing up, the increase  $\Delta T$  in the sample temperature produced by supplying heat  $\Delta Q = Vit$ , is given by:  $\Delta T = (\Delta u \cdot s^{-1}) / (dR/dT)$ , so that  $C = Vit(dR/dT) / \Delta u \cdot s^{-1}$ .

The tedious and time consuming computations of the specific heat were performed on a desk calculator for sample Nb-1, the temperature being read as a function of  $R$  and  $dR/dT$  as a function of  $T$  in large scale graphs constructed on the basis of the described calibration methods. For speeding up the work a computer programme yielding directly the molar specific heat was used with the samples Nb-2 and Nb-3. The input to the computer included:

1. the coefficients of Moody and Rhodes' polynomial (3-4) previously



obtained by means of the calibration programme; 2. the sample mass (in moles); 3. the temperature dependence of the heat capacity of the calorimeter plus addenda; 4. a rejection criterion for the calculation of the line  $s^{-1}(R)$  on basis of experimental data ( $\Delta u', R_k - R_{k+1}$ ); 5. the power supplied to the sample for each point; 6. the ranges of amplification that have been used; 7. the sequence: the number of the point,  $\Delta u$ , the distance from the beginning of the ideal heating period to point M (see Fig.III.6),  $\Delta u', R_k, t$ .

The use of the described method introduces a considerable error in the calculation of the specific heat whenever this quantity varies discontinuously during the heating period, the jump in the specific heat appearing as a sudden change in the slope of the heating curve. This happens at the transition at  $H_{c2}$  and was also observed for Nb-2 and Nb-3 in the mixed state region near  $H_{c1}$ , whenever  $T_{\text{sample}} > T_{\text{bath}}$ . A method was especially devised for calculating the specific heat in these cases. This method is described in Section 4.2.5.4, together with the interpretation of the anomalous shape of the heating curves observed near the  $H_{c1}$  phase transition line.

### 3.7 The magnetic field

The magnetic field was provided by a water cooled electromagnet capable of producing a maximum field of about 10 kOe with a distance between pole pieces of 10.8 cm. The magnet was calibrated using proton magnetic resonance in water molecules for field strengths above 1 kOe and below that with a gaussmeter using a Hall effect probe. Below 5.1 kOe no variation in the ratio field-current was detected. The uniformity of the field in the region where the sample was located was better than 0.1%.

### 3.8 Errors

The main source of error in the measured specific heat was the interpolation procedure used in the calibration of the thermometers, via  $dR/dT$ . However, this error, having a systematic character, partially cancels by subtraction of the heat capacity of the calorimeter and addenda from the total measured heat capacity. The random error, calculated on the basis of the instruments' characteristics and the accuracy of the procedure used in the determination of  $\Delta T$ , was in the order of 1%. The scattering of the experimental results was in this order in the absence of perturbations (vibrations and, mainly, hysteresis). The scattering is best illustrated by the results of the heat capacity of the calorimeter and addenda used in the measurements on

Nb-2 and Nb-3, as shown in Fig.III.7. The minimum measured heat capacity amounted to  $62 \mu\text{J}\cdot\text{K}^{-1}$  at  $T = 1.046 \text{K}$ . Irreversible effects were responsible for a greater scattering of the results in the mixed state, these effects being largest for Nb-1. For sample Nb-3, the thermal relaxation effects and other disturbances observed near the phase transition line  $H_{c1}(T)$  introduced further uncertainties, quite apparent in the results obtained at the location of the peaks in the specific heat at the transition from the Meissner to the mixed state.

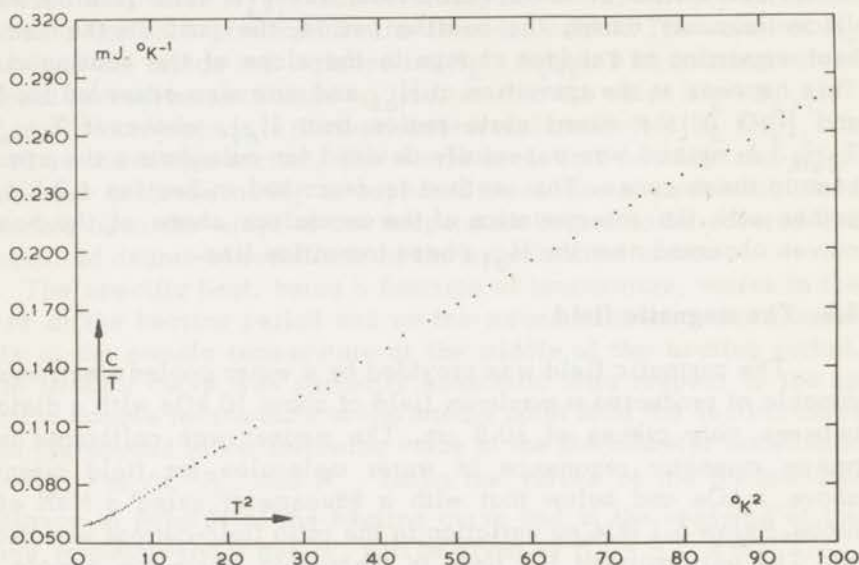


Fig. III.7 Heat capacity of the calorimeter and addenda used with the measurements on Nb-2 and Nb-3.

Due to the small mass of the samples, the subtraction of the heat capacity of the calorimeter and addenda increases the relative error in the specific heat of the sample. This effect is strongest in zero-field and for  $H < H_{c1}(0)$  at the lowest temperatures, the calorimeter then making the main contribution to the total measured heat capacity. For that reason the specific heat  $C_s$  in zero field below  $2 \text{K}$  was determined with an error of about 5%. This error decreases rapidly upon increasing the temperature, being 3% at  $3 \text{K}$  and 2% at  $3.5 \text{K}$ . With the exclusion of  $C_s$  below  $3.5 \text{K}$  and the anomalies (peaks) at the entrance into the mixed state, for fields  $H \approx H_{c1}(0)$ , the systematic errors in the absolute values of the specific heat due to inaccuracies in

the calibration of the thermometer, extrapolation of heating curves, voltmeter and clock readings, and to calorimeter and addenda corrections, should not exceed 2%.

The error in the magnetic field is expected not to exceed 0.5%. The error limits explicitly given in Chapter IV refer to the standard deviation for the quantity concerned as calculated by the computer in the analysis of the data with the least square method.

## References

1. Keesom, P.H. and Pearlman, N., *Handbuch der Physik*, Vol. XIV, ed. S. Flügge (Springer, Berlin 1956) p. 295.
2. De Sorbo, W., *Phys.Rev.* **132** (1963) 107.
3. Durieux, M. and Van Dijk, H., *Travaux du Comité Consultatif de Thermométrie*, 6e Session-1962 (Sèvres, France), Annexe 26, p.166.
4. Brickwedde, F.G., Van Dijk, H., Durieux, M., Clement, J.R. and Logan, J.K., *The 1958 He<sup>4</sup> scale of Temperatures*, *J.Res.Nat. Bur.Stand.* **64A** No 1 (1960) 1.
5. Sherman, R.H., Sydoriak, S.G. and Roberts, T.R., *J.Res.Nat.Bur. Stand.* **68A** No. 6 (1964) 579.
6. Roberts, T.R. and Sydoriak, S.G., *Phys.Rev.* **102** (1956) 304.
7. De Vroomen, A.R., Thesis, Leiden (1959).
8. Moody, D.E. and Rhodes, P., *Cryogenics* **3** (1963) 77.
9. Star, W.M., Van Dam, J.E. and Van Baarle, C., to be published.
10. Keesom, W.H. and Kok, J.A., *Proc.Kon.Nederl.Akad.Wet., Amsterdam* **35** (1932) 294; Suppl. No. 219c, *Comm.Kamerlingh Onnes Lab, Leiden*; Kok, J.A., Thesis, Leiden, (1935).

## Chapter IV

## EXPERIMENTAL RESULTS. DISCUSSION

## 4.1 Introduction

In this chapter the results obtained in the measurements of the specific heat of three samples of niobium: Nb-1 ( $\kappa = 2.36$ ), Nb-2 ( $\kappa = 0.992$ ), Nb-3 ( $\kappa = 0.893$ ) are described and discussed. The behaviour of Nb-1 is the one characteristic of an inhomogeneous sample. Although similar, the behaviour of the two annealed high-purity samples Nb-2 and Nb-3 is not identical. Since Nb-3 appeared to be the best one (higher resistance ratio,  $\Gamma$ , lower  $\kappa$ , sharper anomalies in the specific heat at  $H_{c1}(T)$ ), more measurements were performed with this sample than with Nb-2. When not stated otherwise, for results obtained in the presence of a magnetic field  $H < H_{c2}(0)$ , the field was established after the sample had been cooled down to the lowest attainable temperature.

## 4.2 Experimental results and discussion

The specific heat results obtained in several longitudinal magnetic fields covering the three states of superconductive niobium in the temperature range from about 1°K to about 10°K are displayed in Fig.IV.1 for Nb-1 and Fig.IV.2 for Nb-3, where the specific heat  $C$  divided by the temperature  $T$  is plotted versus  $T^2$ . The results for Nb-2, partially shown in Fig.IV.3, are very similar to those obtained with Nb-3 but have less sharp peaks.

## 4.2.1 The specific heat in the normal state

The normal state specific heat  $C_n$  was measured in a magnetic field  $H = 9.4$  kOe (Nb-1) and  $H = 7.05_n$  kOe (Nb-2 and Nb-3) and for each sample the results agree, within experimental accuracy, with those obtained in the other measured magnetic fields in the temperature region beyond the bulk superconductive phase.

For the separation of the electronic ( $C_{en}$ ) and lattice ( $C_{ln}$ ) contributions the results were analysed in the usual way by means of the Sommerfeld-Debye expression<sup>1)</sup>

$$C_n = C_{en} + C_{ln} = \gamma T + 1944 \times 10^3 \left(\frac{T}{\Theta}\right)^3 \text{ mJ.mole}^{-1} \cdot \text{K}^{-1}, \quad (4-1)$$

where  $\gamma$  is the Sommerfeld constant and  $\Theta$  is the Debye character-

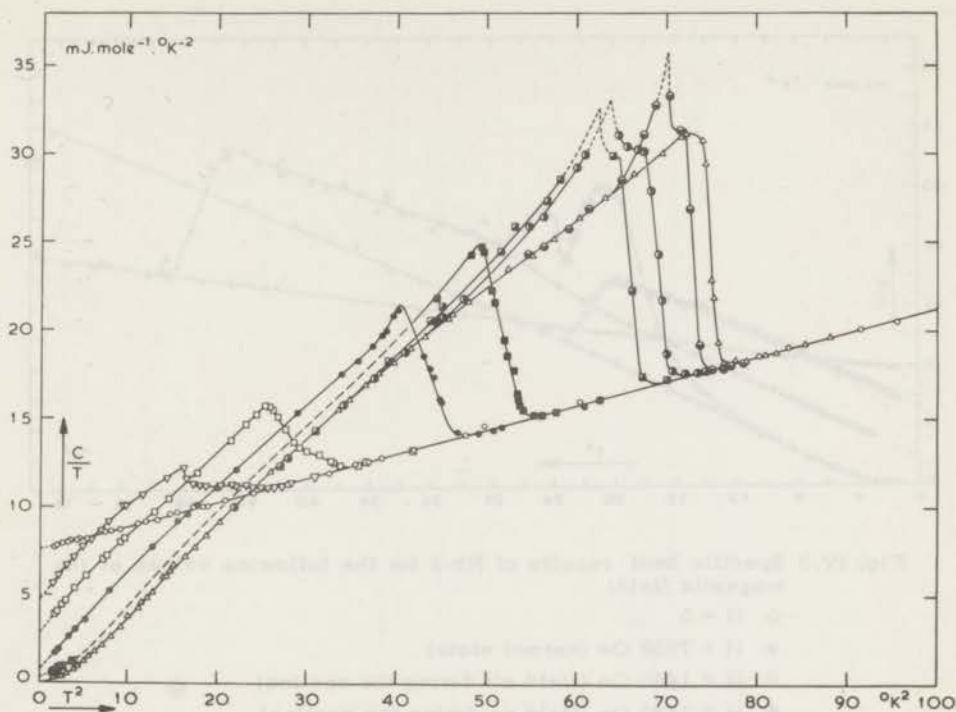


Fig. IV.1 Specific heat results of Nb-1 for the following values of the magnetic field:

- |                      |                            |                                     |
|----------------------|----------------------------|-------------------------------------|
| $\Delta$ H = 0       | $\blacksquare$ H = 734 Oe  | $\square$ H = 4337 Oe               |
| $\ominus$ H = 194 Oe | $\blacksquare$ H = 2000 Oe | $\nabla$ H = 5760 Oe                |
| $\odot$ H = 519 Oe   | $\bullet$ H = 2848 Oe      | $\circ$ H = 9400 Oe (normal state). |

The field was off during the cooling prior to each measurement.

istic temperature. It was found for each of the three samples that in a plot of  $C_n/T$  versus  $T^2$  one single straight line did not fit all experimental points in the measured temperature region as one would expect for constant  $\gamma$  and  $\Theta$ . The points below about 3°K lay on a straight line with a slope smaller than defined by points obtained at higher temperatures, the difference being greater than the experimental accuracy, as is shown in Fig.IV.4 for Nb-3. A similar result has been found for different samples of Nb by other investigators<sup>2,3,4</sup>). The inclusion of terms higher than third power in the usual  $T^3$  lattice contribution would account for the results but gives too low a value for  $\Theta$  in comparison with the values determined from ultrasonic measurements. A possible solution can be found by assuming  $\Theta$  to be temperature de-

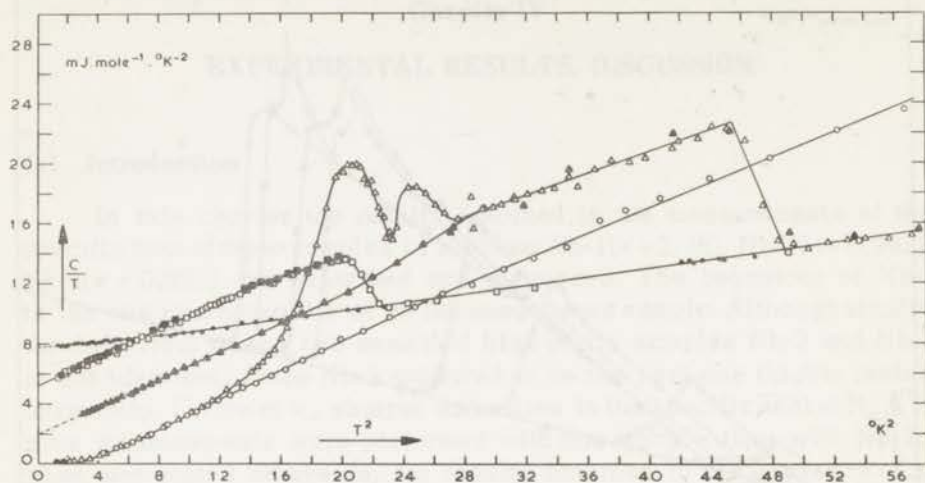


Fig. IV.3 Specific heat results of Nb-2 for the following values of the magnetic field:

- $H = 0$
- $H = 7050$  Oe (normal state)
- △  $H = 1480$  Oe (field off during the cooling)
- ▲  $H = 1480$  Oe (field on during the cooling)
- $H = 2895$  Oe (field off during the cooling)
- $H = 2895$  Oe (field on during the cooling) .

pendent above the temperature at which the straight line  $C_n/T$  versus  $T^2$  changes slope. This assumption is supported by further experimental evidence that shall be presented below.

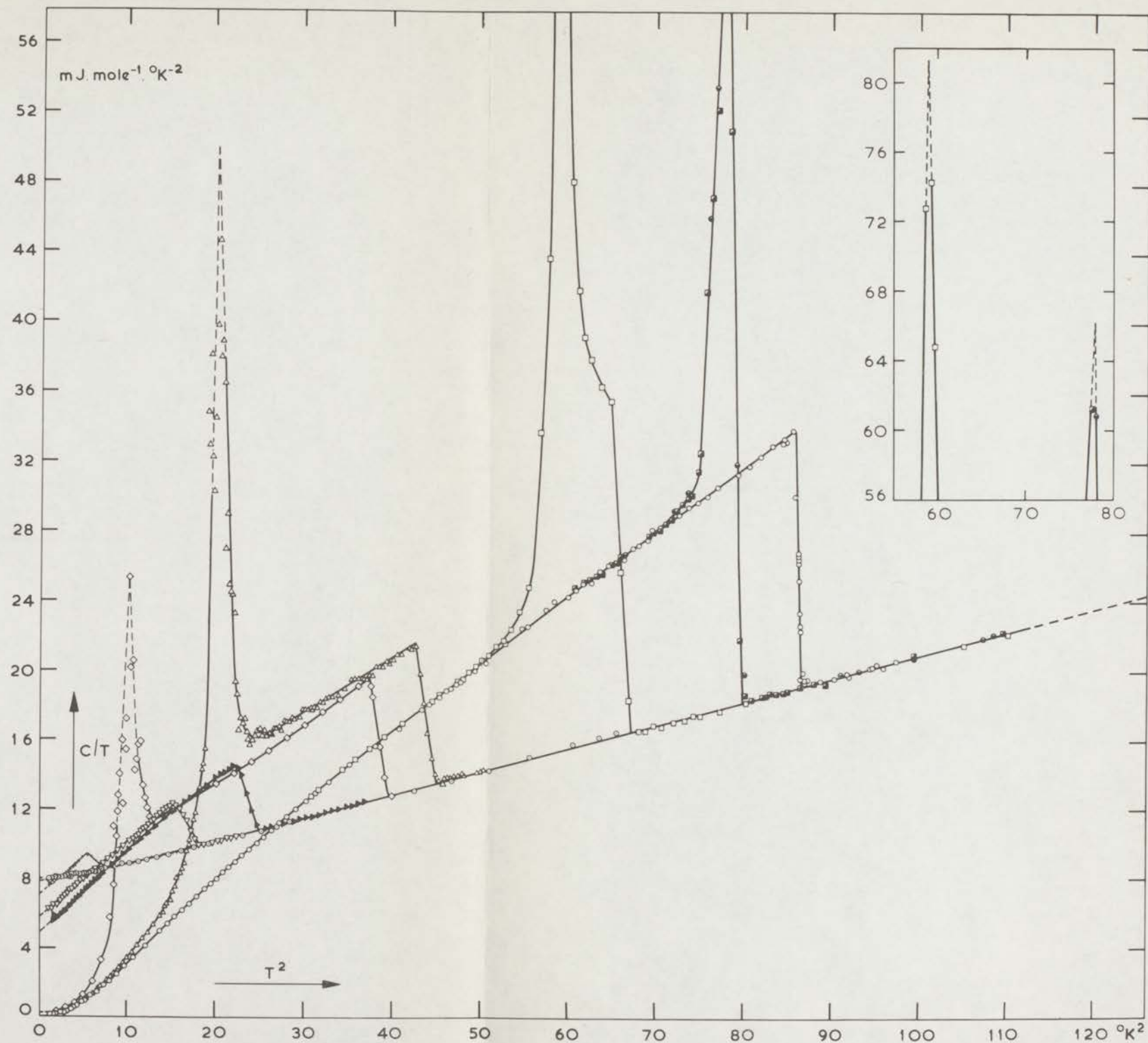
A least-squares-fit of the normal state data below about  $3^\circ\text{K}$  with the expression  $C_n/T = \gamma + AT^2$  with  $A = 1944 \times 10^3/\Theta^3$  will then yield  $\gamma$  and  $\Theta$  for  $T \lesssim 3^\circ\text{K}$ . In Table I are shown the values of  $\gamma$ ,  $\Theta$  and  $T_c$ , the transition temperature in zero magnetic field, corresponding to the three Nb samples. For comparison, other recent calorimetric results for Nb are also given.

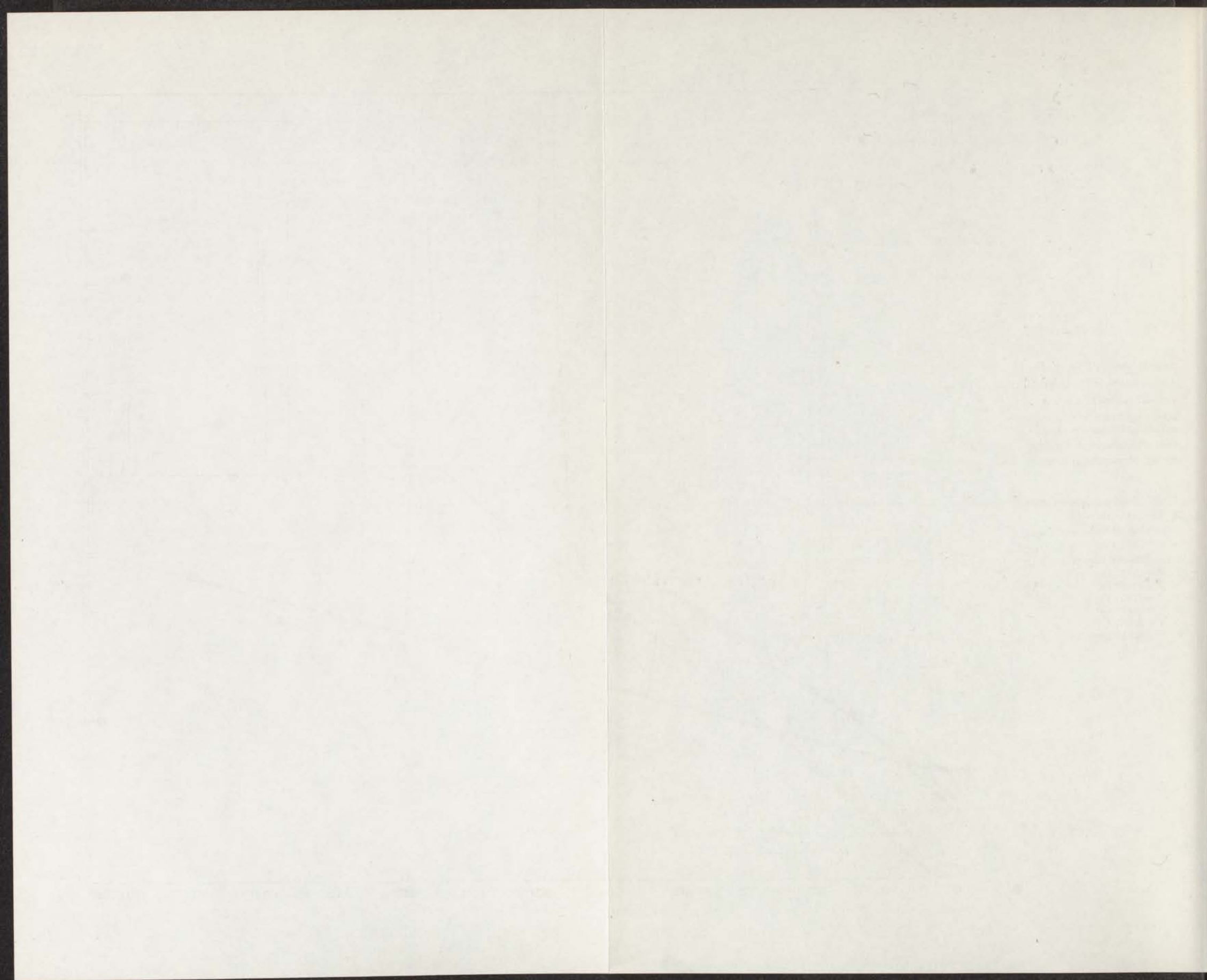
For Nb-2 and Nb-3 the higher values of  $\Theta$  at the lower temperatures are in agreement with the results obtained from the low temperature ( $T = 4.2^\circ\text{K}$ ) elastic constants of niobium of similar quality:  $\Theta = 277^\circ\text{K}^{(7)}$ ,  $\Theta = 271 \pm 5^\circ\text{K}^{(8)}$  and  $\Theta = 272^\circ\text{K}^{(9)}$ . Taking  $\gamma = \text{constant}$  (as determined at the lower temperatures),  $\Theta(T)$  can be found with the aid of eq. (4-1).  $\Theta(T)$  is depicted in Fig. IV.5 for Nb-3.

Fig. IV.2 (Nb-3)

Specific heat  $C$ , divided by the absolute temperature  $T$ , plotted versus  $T^2$  for the following values of the magnetic field (when not stated otherwise the magnetic field was off during the cooling).

- $H = 0$
- ⊙  $H = 7050$  Oe (normal state)
- $H = 194$  Oe  
(field off during the cooling)
- $H = 194$  Oe  
(field on during the cooling)
- $H = 597$  Oe
- △  $H = 1480$  Oe
- ◇  $H = 1732$  Oe
- ▴  $H = 2488$  Oe
- ▽  $H = 2895$  Oe
- $H = 3610$  Oe







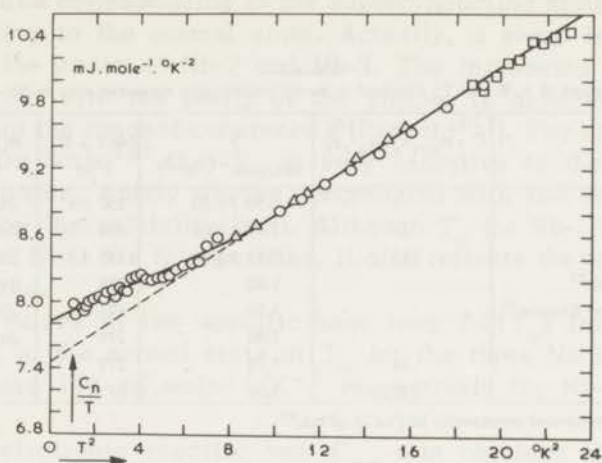


Fig. IV.4 Plot of  $C_n/T$  versus  $T^2$  for Nb-3 at the lowest temperatures, showing the change in the slope of the normal state specific heat line at about  $T^2 \approx 9 \text{ } ^\circ\text{K}^2$ . The experimental points refer to values of  $C_n$  obtained in the following values of the field:

○  $H = 7050 \text{ Oe}$      $\Delta H = 3610 \text{ Oe}$      $\square H = 2895 \text{ Oe}$ .

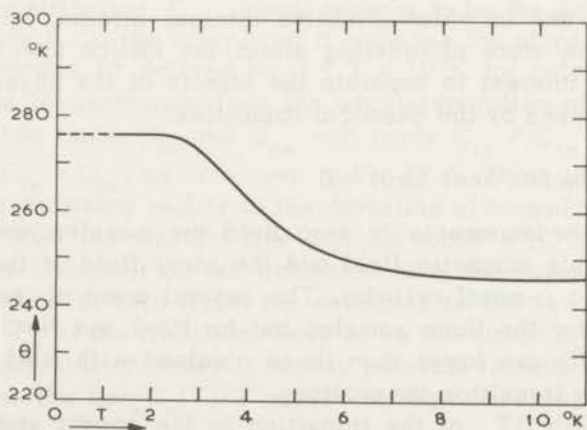


Fig. IV.5 The calculated temperature dependence of  $\theta$  for Nb-3.

Table I  
 Values of  $\gamma$ ,  $\Theta$  and  $T_c$  obtained in recent calorimetric measurements on Nb

	$\Gamma = R_{273^\circ\text{K}}/R_{4.2^\circ\text{K}}$	$\gamma$ (mJ.mole <sup>-1</sup> .°K <sup>-2</sup> )	$\Theta(T = 0)$ (°K)	$\Theta(T = 10)$ (°K)	$T_c$ (°K)
This thesis Nb-1	7	7.59 ± 0.03	250 ± 4	241 ± 1	8.68
This thesis Nb-2	47	7.78 ± 0.01	274 ± 3	243 ± 1	9.23
This thesis Nb-3	145	7.82 ± 0.01	276 ± 3	246 ± 1	9.28
Leupold and Boorse <sup>2)</sup>		7.80	275	241	9.20
Van der Hoeven and Keesom <sup>3)</sup>		7.79	275	238	
Heiniger <sup>5)</sup>		7.80	278	244*	9.33
Shen et al. <sup>6)</sup>	24	7.79	277		9.13
Shen et al. <sup>6)</sup>	110	7.85	277		9.26

\*) This value was estimated graphically in Fig.11 of ref.<sup>4)</sup>

Examining the results presented in Table I, it can be concluded that the state of purity and the degree of internal defects of the Nb sample affect the values of both the parameters  $\gamma$  and  $\Theta$ . This is clearly seen in the case of the two extreme cases of Nb-1 and Nb-3. Comparing the values of  $\gamma$  and  $\Theta$  for these two samples one concludes that both parameters increase with the refinement of the quality of the sample. A similar result was found with vanadium<sup>10)</sup>. According to Heiniger et al.<sup>4)</sup> the  $\Theta$  value of a pure element is in general lowered by the addition of a small amount of impurity. Yet it remains to be seen how far and in which direction internal strains, lattice dislocations and the state of ordering affect the lattice specific heat. It should be of interest to separate the effects of the physical defects from those caused by the chemical impurities.

#### 4.2.2 The specific heat for $H = 0$

In the measurements in zero field the samples were screened from the earth's magnetic field and the stray field of the laboratory by means of a  $\mu$ -metal cylinder. The general trend of the line  $C_s(T)$  is the same for the three samples but for Nb-2 and Nb-3 the corresponding results are lower than those obtained with Nb-1 on account of their higher transition temperature.

The width  $\Delta T_c$  of the transition to the normal state is highly dependent upon the quality of the sample (46 mdeg for Nb-1 in contrast with about 1 mdeg for Nb-2 and Nb-3). In the heating curves which include the transition, this can be seen as a change in the slope

from the value corresponding to the superconducting state to the value corresponding to the normal state. Actually, a sharp break was observed in the cases of Nb-2 and Nb-3. The increasing sharpness of the transition with the purity of the sample is associated with the increasing of the range of coherence  $\xi$  (Pippard<sup>11</sup>). For niobium it was found by De Sorbo<sup>12</sup> that  $T_c$  is very sensitive to the presence of dissolved gases, mainly oxygen, decreasing with the solute concentration below the solubility limit. Although  $T_c$  for Nb-1 is lower than for Nb-2 and Nb-3 due to impurities, it also reflects the opposite effect due to strains.

The values of the specific heat jump  $\Delta C(T_c)$  from the superconducting to the normal state at  $T_c$  for the three Nb samples were 124, 137 and 139 mJ.mole<sup>-1</sup>.°K<sup>-1</sup> respectively for Nb-1, Nb-2 and Nb-3.

The electronic specific heat  $C_{es}$  was obtained by subtracting the lattice contribution  $C_{ls}$  (taken to be the same as in the normal state,  $C_{ln}$ ) from the specific heat measured in zero field,  $C_s$ .

The procedure described for the analysis of the normal state data implying a temperature dependent  $\Theta$  above about 3°K yields a lattice contribution  $C_{ln}$  to the specific heat  $C_n$  such that  $C_s$  approaches  $C_{ln}$  when the temperature is sufficiently reduced, as shown in Fig.IV.6 for Nb-3.  $C_{es}$ , being an increasing exponential function of temperature<sup>13</sup>, becomes negligible at the lowest temperatures, so that  $C_s \approx C_{ls}$ . Thus, when the temperature is rather low ( $T \approx 1^\circ\text{K}$ ), the specific heat measured in zero field,  $C_s$ , is not much different from the lattice contribution,  $C_{ls}$ , which appears to be the same as  $C_{ln}$  as seen in Fig.IV.6. On the other hand if one uses the slope of the straight line  $C_n/T$  versus  $T^2$  defined for  $3 < T < 10^\circ\text{K}$  for calculating  $C_{ln}$  at all measured temperatures, then the usual separation of the specific heat  $C_s$  in two terms  $C_{ls}$  and  $C_{es}$  will imply  $C_{ls} \neq C_{ln}$  or  $C_{es} < 0$  if we assume  $C_{ls} = C_{ln}$ , as also seen in Fig.IV.6. There is still another argument for ascribing reality to the deviation of normal state specific heat points from the straight line defined above 3°K. In view of the second order character of the transition from the superconducting to the normal state in zero field, the entropies in the two states at the temperature  $T_c$  of the transition have to be the same:  $S_s(T_c) = S_n(T_c)$ . Within experimental accuracy it is only possible to have this condition fulfilled when the line  $C_n(T)/T$  passes through the experimental points obtained below 3°K.

In Fig.IV.7 is shown a semilogarithmic plot of  $C_{es}$  for Nb-3 versus the reciprocal of the reduced temperature  $1/t = T_c/T$ . For  $1.9 < 1/t < 6.1$ ,  $C_{es}$  follows the BCS exponential law<sup>13</sup>

$$C_{es} = \gamma T_c a e^{-\frac{b}{T}} \quad (4-2)$$

with  $a = 8.0$  and  $b = 1.53$  to be compared with the BCS values  $a = 8.5$  and  $b = 1.44$ . Nb-2 gave the same results and for Nb-1 the values  $a=9.7$  and  $b = 1.62$  were found. For the three samples, for  $T = T_c$  the electronic specific heat is larger than the BCS prediction. Thus, while according to BCS theory  $C_{es}(T_c)/\gamma T_c = 2.43$ , the value 2.91 was found for all three Nb samples. The original two-fluid model of Gorter-Casimir<sup>14)</sup> predicts for this ratio the value 3. According to the available data<sup>15)</sup> the values of  $C_{es}(T_c)/\gamma T_c$  for known superconductors range from below the BCS prediction up to above the value given by the original two-fluid model in apparent correlation with  $T_c/\Theta$  that

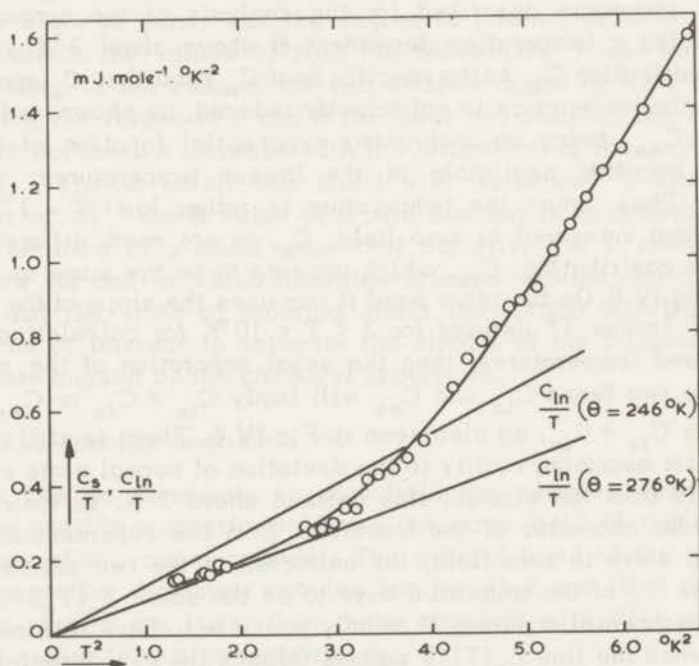


Fig. IV.6 The low temperature specific heat of Nb-3 in the Meissner region,  $C_s$ , compared with the lattice contribution to the normal state specific heat  $C_{ln}$ , calculated for two different values of  $\Theta$ .

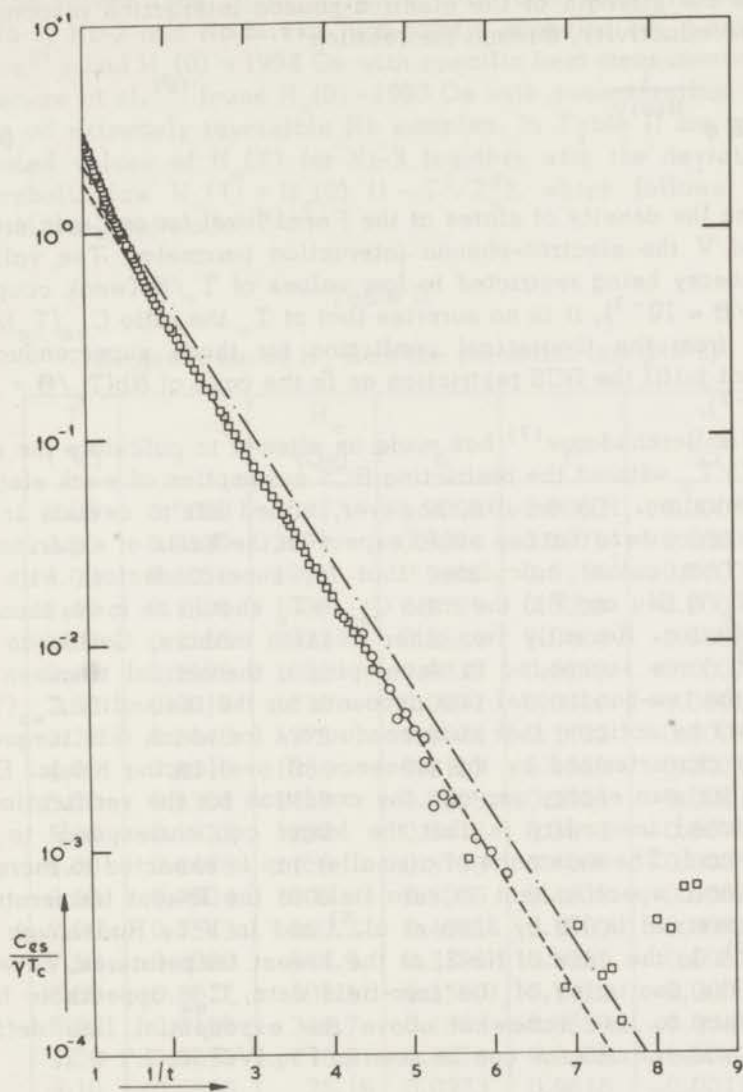


Fig. IV.7 Semilogarithmic plot of the electronic specific heat  $C_{es}$ , of Nb-3 in zero field ( $\square$ ) and in the field  $H = 1480$  Oe ( $\circ$ ), divided by the normal state electronic specific heat at  $T_c$ ,  $\gamma T_c$ , versus  $1/t = T_c/T$ .  
 --- according to the BCS theory<sup>13)</sup>.

measures the strength of the electron-phonon interaction responsible for superconductivity, through the relation<sup>13,16)</sup>

$$\frac{T_c}{\Theta} = 0.85 e^{-\frac{1}{N(0)V}}, \quad (4-3)$$

$N(0)$  being the density of states at the Fermi level for one spin orientation and  $V$  the electron-phonon interaction parameter. The validity of BCS theory being restricted to low values of  $T_c/\Theta$  (weak coupling limit,  $T_c/\Theta \approx 10^{-3}$ ), it is no surprise that at  $T_c$  the ratio  $C_{es}(T_c)/\gamma T_c$  deviates from the theoretical prediction for those superconductors that do not fulfil the BCS restriction as is the case of Nb ( $T_c/\Theta = 3.4 - 3.8 \times 10^{-2}$ ).

Melik-Barkhudarov<sup>17)</sup> has made an attempt to calculate the ratio  $C_{es}(T_c)/\gamma T_c$  without the restricting BCS assumption of weak electron-phonon coupling. His results, however, turned out to deviate in the direction opposite to that one would expect on the basis of experimental results. That author calculates that for superconductors with the highest  $T_c/\Theta$  (Hg and Pb) the ratio  $C_{es}/\gamma T_c$  should be lower than the BCS prediction. Recently two other Russian authors, Geilikman and Kresin<sup>18)</sup>, have succeeded in developing a theoretical treatment on basis of the two-band model that accounts for the inequality  $C_{es}(T_c)/\gamma T_c > 2.43$  by noticing that superconductors for which this inequality holds are characterized by the presence of overlapping bands. Each band has its own energy gap and the condition for the verification of the mentioned inequality is that the larger gap corresponds to the narrower band. The existence of a smaller gap is expected to increase the electronic specific heat in zero field at the lowest temperatures as was observed in Nb by Shen et al.<sup>6)</sup> and in V by Radebaugh and Keesom<sup>10)</sup>. In the case of Nb-3, at the lowest temperatures, notwithstanding the scattering of the zero-field data,  $C_{es}$  appears to have the tendency to rise somewhat above the exponential line defined at higher temperatures, as can be seen in Fig.IV.7 for  $1/t > 7$ .

#### 4.2.3 The thermodynamic critical field $H_c$

As already stated in the general introduction, calorimetric results make it possible to calculate the thermodynamic critical field  $H_c(T)$  free from the effects of irreversibility even in the case of superconductors with hysteretic behaviour. Following the procedure described in Section 2.4.1 (eq. (2-38) and (2-39)),  $H_c$  was obtained by double integration of specific heat results in zero field and normal state. At

0°K the values 1864, 2004, 2014 Oe were found for  $H_c$ , respectively for Nb-1, Nb-2 and Nb-3. For high-purity, annealed Nb, Leupold and Boorse<sup>2)</sup> found  $H_c(0) = 1994$  Oe with specific heat measurements while Finnemore et al.<sup>19)</sup> found  $H_c(0) = 1993$  Oe with magnetization measurements on extremely reversible Nb samples. In Table II are given the computed values of  $H_c(T)$  for Nb-3 together with the deviation from a parabolic law  $H_c(T) = H_c(0) (1 - T^2/T_c^2)$ , which follows from the original two-fluid model<sup>14)</sup>.

Table II

The deviation of  $H_c$  from the parabolic law (Nb-3)

T (°K)	t	$H_c$ (Oe)	h	$t^2$	$\Delta h$
0.00	0.0000	2014	1.0000	0.0000	0.0000
0.50	0.0539	2009	0.9974	0.0029	+0.0003
1.00	0.1078	1991	0.9886	0.0116	+0.0002
1.40	0.1509	1969	0.9779	0.0228	+0.0007
2.00	0.2155	1922	0.9544	0.0464	+0.0008
2.40	0.2586	1881	0.9338	0.0669	+0.0007
2.80	0.3017	1831	0.9091	0.0910	+0.0001
3.20	0.3448	1773	0.8804	0.1189	-0.0007
4.00	0.4310	1634	0.8113	0.1858	-0.0029
5.00	0.5388	1417	0.7036	0.2903	-0.0061
5.50	0.5927	1292	0.6413	0.3513	-0.0074
6.00	0.6466	1155	0.5736	0.4180	-0.0084
6.50	0.7004	1008	0.5005	0.4906	-0.0089
7.00	0.7543	850.2	0.4221	0.5690	-0.0089
7.50	0.8082	681.9	0.3386	0.6532	-0.0082
8.00	0.8621	503.5	0.2500	0.7432	-0.0068
8.50	0.9159	314.7	0.1563	0.8389	-0.0048
9.00	0.9698	116.4	0.0578	0.9405	-0.0017
9.10	0.9806	75.19	0.0373	0.9616	-0.0011
9.20	0.9914	33.91	0.0168	0.9829	-0.0003
9.28	1.0000	0.00	0.0000	1.0000	0.0000

The deviation  $\Delta h(t) = H_c(t)/H_c(0) - (1 - t^2) = h - (1 - t^2)$  is plotted versus  $t^2$  in Fig. IV.8 for Nb-1, Nb-2 and Nb-3, where for comparison the deviation curves for Pb<sup>20)</sup>, Al<sup>21)</sup> and that according to the BCS theory<sup>13)</sup> are also presented. The deviation curves for the three samp-

les are rather similar. The main features of the function  $\Delta h(t^2)$  for the three Nb samples are that  $\Delta h$  is positive for  $t^2 < 0.095$  and the observed maximum negative deviation is only about 1/3 of the BCS prediction for Nb-1 and 1/4 for Nb-2 and Nb-3. According to the BCS theory, valid in the weak coupling limit, the departure of  $H_c(T)$  from the parabolic law should always be negative. Superconductors with rather low values of  $T_c/\Theta$  as e.g. Al ( $2.7 \times 10^{-3}$ )<sup>21)</sup> follow very well the BCS prediction for  $H_c(T)$ <sup>21)</sup>. Hg and Pb, with the highest known values of  $T_c/\Theta$  ( $5.9 \times 10^{-2}$  and  $7.5 \times 10^{-2}$  respectively) have a positive deviation  $\Delta h$  in the whole temperature range<sup>20,21)</sup>. This constitutes a second example of an empirical correlation between a superconductive property and the strength of the electron-phonon coupling. Niobium, having an electron-phonon interaction of intermediate strength is thus in agreement with such a correlation scheme.

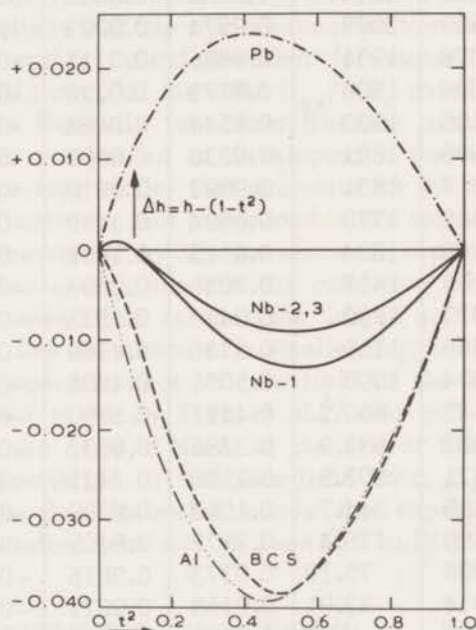


Fig. IV.8 The deviation of  $H_c(T)$  from a parabolic law  $H_c(T) = H_c(0)(1 - t^2)$ , plotted as  $\Delta h = h - (1 - t^2)$  versus  $t^2$  for the three niobium samples. The deviations of Pb<sup>20)</sup>, Al<sup>21)</sup> and according to the BCS theory<sup>13)</sup> are given for comparison.



As a check of the correctness of the computed values of  $H_c$  near  $T_c$  use was made of the Rutgers' relation (2-37) established in Section 2.4.2 and relating the specific heat jump at  $T_c$  to the slope of the thermodynamic critical field at the same temperature. The results are shown in Table III where a comparison is made between the values of  $(dH_c/dT)_T$  calculated from a) the computed  $H_c(T)$  and b) the measured jump<sup>c</sup>  $\Delta C(T_c)$  in the specific heat at  $T_c$ , by means of eq. (2-37). For each of the three samples the agreement between the two values is within experimental accuracy.

Table III

The values of  $(dH_c/dT)_T$  calculated from  
a)  $H_c(T)$   
b)  $\Delta C(T_c)/T_c$ , by means of eq. (2-37).

sample	$-(dH_c/dT)_{T_c}$ (Oe. °K <sup>-1</sup> )	
	a)	b)
Nb-1	411	408
Nb-2	419	416
Nb-3	420	417

If the formalism of Kok<sup>22)</sup> and Gorter-Casimir<sup>14)</sup> is accepted it can be shown that

$$\gamma = \frac{V}{8\pi} \left( \frac{dH_c}{dT} \right)_{T_c}^2, \quad (4-4)$$

where  $V$  is the molar volume and  $\gamma$  the Sommerfeld constant. The experimental results confirm the dependence of  $(dH_c/dT)_T$  on  $\gamma$  according eq. (4-4) inasmuch as the former was found to vary as the square root of the latter. Thus, in the so-called law of corresponding states, relating  $T_c$ ,  $\gamma$  and  $H_c(0)$ :

$$\begin{aligned} \gamma T_c^2 / H_c^2(0) &= 0.17 \quad \text{according to the BCS theory}^{13)} \\ &= 0.159 \quad \text{according to the formalism of Kok}^{22)} \text{ and} \\ &\quad \text{Gorter-Casimir}^{14)}, \end{aligned}$$

all the three parameters are found to vary with the degree of purity of the sample. This conclusion does not quite confirm the results of

De Sorbo<sup>12)</sup> who found from resistivity measurements on niobium with different amounts of dissolved gases (O and N) that  $(dH_c/dT)_{T_c}$  (and therefore  $\gamma$ ) was independent of impurity content. In the present case, the C values for  $\gamma T_c^2/H_c^2(0)$  are 0.152, 0.153, 0.154 respectively for Nb-1, Nb-2 and Nb-3.

#### 4.2.4 The energy gap $2\Delta(0)$ at the absolute zero

From the BCS expression for the difference in free energy at 0°K between the normal and superconducting states, Goodman<sup>23)</sup> has derived the relation

$$\frac{2\Delta(0)}{kT_c} = \frac{4}{\sqrt{3}} \pi \left( \frac{H_c^2(0)V}{8\pi\gamma T_c^2} \right)^{1/4}, \quad (4-5)$$

where  $2\Delta(0)$  is the gap in the energy spectrum of the electrons at absolute zero (BCS<sup>13)</sup>),  $k$  the Boltzmann constant and  $V$  the molar volume. This relation brings the calculation of the energy gap at the absolute zero within the scope of specific heat measurements. The calculated values of  $2\Delta(0)/kT_c$  for the three samples are given in Table IV (using  $V = 10.8 \text{ cm}^3/\text{mole}^2$ ).

Table IV

The values of  $2\Delta(0)/kT_c$  computed from relation (4-5)

sample	$2\Delta(0)/kT_c$
Nb-1	3.71
Nb-2	3.70
Nb-3	3.69

These results confirm Anderson's prediction<sup>23a)</sup> that the energy gap is not much affected by the presence of non magnetic impurities.

Using the Goodman relation (4-5), Finnemore et al.<sup>19)</sup> from magnetization measurements on Nb calculated for  $2\Delta(0)/kT_c$  the value 3.66 while the value 3.69 was calculated from calorimetric measurements by Leupold and Boorse<sup>2)</sup>. Also for Nb, electron tunneling measurements gave the values 3.59<sup>24)</sup> and  $3.84 \pm 0.06$ <sup>25)</sup> and ultrasonic measurements the value  $3.63 \pm 0.06$ <sup>8)</sup> and  $3.75 \pm 0.05$ <sup>26)</sup>. The BCS theory predicts for  $2\Delta(0)$  the value 3.52. It is known<sup>27)</sup> that there is also a correlation between  $2\Delta(0)/kT_c$  and  $T_c/\theta$ , the BCS prediction being only verified for superconductors with the lowest values of  $T_c/\theta$ .

Introducing an effective interaction parameter  $N(0)V^*$  larger than the value of  $N(0)V$  calculated from  $T_c/\Theta$  on basis of eq. (4-3) Sheehen<sup>28)</sup> carried out a semi-empirical extension of the BCS theory to intermediate and strong-coupling superconductors. He derived relations between  $\Delta(0)$ ,  $H_c(0)$ ,  $T_c$ ,  $\Delta C(T_c)$ ,  $\gamma$  and the slope of  $H_c$  near  $T_c$  in reduced units  $(dh/dt)_{t=1}$  ( $h = H_c(t)/H_c(0)$ ,  $t = T/T_c$ ), the conclusions being

$$\frac{\Delta C(T_c)}{\gamma T_c} = 0.27 \left( \frac{\Delta(0)}{kT_c} \right)^3 = 0.27 \left( \left| \left( \frac{dh}{dt} \right)_{t=1} \right| \right)^3. \quad (4-6)$$

The last equation of (4-6) is identical with the empirical relation (Toxen<sup>29)</sup>)

$$\frac{2\Delta(0)}{kT_c} = \frac{2 T_c}{H_c(0)} \left| \left( \frac{dH_c}{dT} \right)_{T_c} \right|, \quad (4-7)$$

known to hold for nearly all superconductors.

The correlation found by Sheehen is confirmed in the present case although the values of  $\Delta(0)$  calculated from  $(dh/dt)_{t=1}$  and from  $\Delta C(T_c)$  are somewhat higher than the values obtained according Goodman's relation (4-5). For Nb-3 one gets  $2\Delta(0)/kT_c = 3.87$  from  $(dh/dt)_{t=1} = -1.93$ , and 3.84 from  $\Delta C(T_c)/\gamma T_c = 1.91$ .

We conclude this section by reminding the reader that the values of the quantities  $\Delta C(T_c)/\gamma T_c$ ,  $2\Delta(0)/kT_c$  and  $\Delta h(t) = h - (1 - t^2)$  are expected to depart in the observed direction from the BCS predictions if retardation and damping effects in the effective electron-interactions are taken into account for strong-coupling superconductors<sup>30)</sup>. In particular, agreement with experiment is found for  $2\Delta(0)/kT_c$  and  $\Delta h(t)$  in the extreme case of Pb<sup>31)</sup>.

Probably such retardation and damping effects also play a not negligible role in the zero field properties of intermediate-coupling superconductors like Nb, which properties also differ from the predictions of BCS theory.

#### 4.2.5 The specific heat in fields $H < H_{c1}(0)$

##### 4.2.5.1 Nb-1

The specific heat line for low fields was found to coincide with the zero field curve until, at a certain temperature depending upon the applied field, it began to depart smoothly upwards. This smooth vari-

ation of the specific heat extends nearly up to the temperature  $T_s$  where the jump to the normal state occurs. Although the specific heat was not reproducible just below  $T_s$  it was always possible to resolve the jump unambiguously. The results obtained with Nb-1 at the magnetic field values  $H = 194, 519$  and  $734$  Oe are included in Fig.IV.1. From the figure it can be seen that the specific heat displays an anomaly besides the one associated with the transition to the normal state.

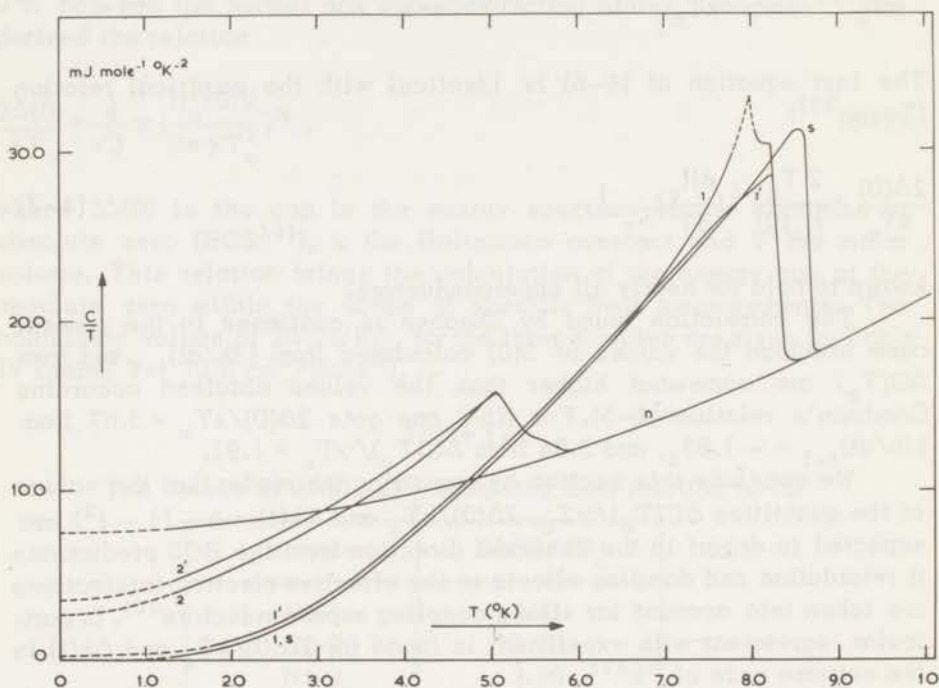


Fig. IV.9 The dependence of the specific heat upon the way in which the sample Nb-1 has been cooled down before the measurement.

n normal state

s zero field

1  $H = 519$  Oe, with the sample cooled down in the absence of the field

1'  $H = 519$  Oe, with the sample cooled down in the presence of the field

2  $H = 4337$  Oe, with cooling in the absence of the field

2'  $H = 4337$  Oe, with cooling in the presence of the field.

The cooling procedure prior to the measurement had an effect on the specific heat. When the sample had been cooled down from the normal state in the presence of the magnetic field, the specific heat is higher than that at zero field in almost the entire temperature range and no indication of a peak is ever observed. The jump to the normal state is now smaller as can be seen in Fig.IV.9, line 1', for  $H = 519$  Oe. The effect is due to incomplete flux expulsion (trapped flux) during the cooling in the presence of the field.

#### 4.2.5.2 Nb-2 and Nb-3

Just as observed with Nb-1, the specific heat for low fields was found to be the same as in zero field up to a certain temperature which is a decreasing function of the applied field. Above this temperature, it rose steeply to a rather sharp peak in the case of Nb-3, as can be seen in Fig.IV.2 for fields  $H = 194, 597, 1480$  and  $1732$  Oe. For Nb-2 the results were similar, to those of Nb-3 with somewhat lower peaks as can be seen in Fig.IV.3 for  $H = 1480$  Oe (it is presumed that the hump following the main peak is not a characteristic of the sample but rather of its topology, as discussed in Section 4.2.5.3).

Increasing the temperature above the value at which the peak was found, the specific heat  $C$  increased roughly as  $T^3$  up to a temperature  $T_s$  at which it jumped to the normal state. In the case of the lowest measured field (194 Oe) the jump to the normal state did not appear resolved from the peak, as can be seen in Fig.IV.2.

Contrary to Nb-1, for Nb-2 and Nb-3 the anomaly in the specific heat was quite reproducible for the lower fields (cf. results for  $H = 194$  Oe in Fig.IV.2) no matter in which way the sample was cooled down, whether in the presence or absence of the field. But for  $H \geq 1480$  Oe the peak was totally missing both for Nb-2 and Nb-3 when the field was on during the cooling of the sample; this is shown in Fig.IV.3 for Nb-2 and Fig.IV.10 for Nb-3. The effect of trapped flux is quite apparent at the lower temperatures, as an increase of the specific heat over the zero-field values. However, both for Nb-2 and Nb-3, for temperatures at which the applied field was greater than  $H_c$  the specific heat was independent of the way in which the sample had been previously cooled. The reproducibility of the mixed state specific heat of Nb-2 and Nb-3 in the region  $T_1 \lesssim T < T_s$  where  $T_1$  is defined by  $H_c(T_1) = H$  and  $T_s$  by  $H_{c2}(T_s) = H$ ,  $H$  being the applied field, contrasts markedly with the hysteretic magnetic behaviour of both samples in the whole range of superconductivity as will be seen in Section 4.2.5.4.

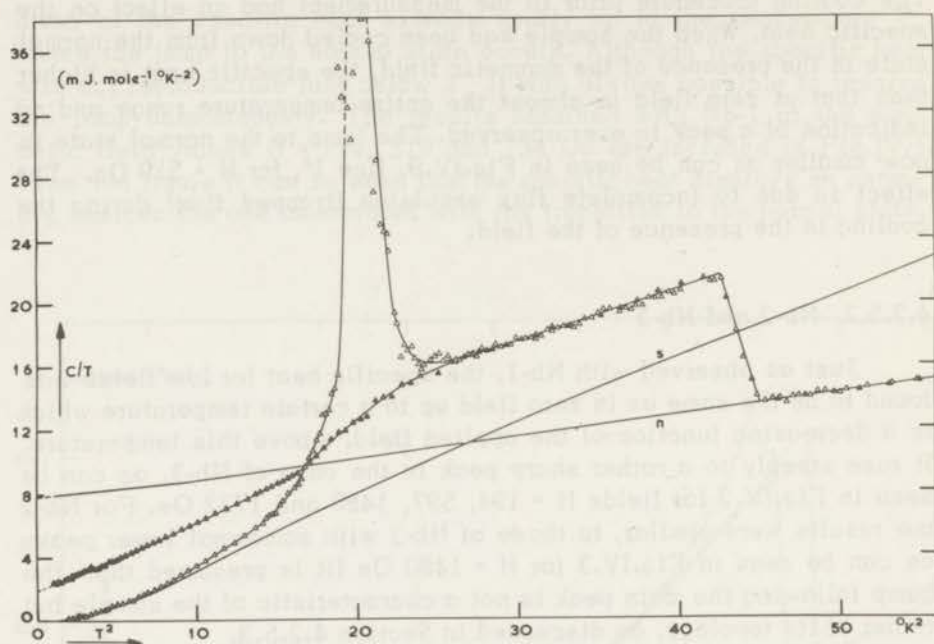


Fig. IV.10 The dependence of the specific heat upon the way in which the sample Nb-3 has been cooled down before the measurement, for  $H = 1480$  Oe.

- Δ with field off during the cooling prior to the measurement
- ▲ with field on during the cooling prior to the measurement
- s zero field specific heat curve
- n normal state specific heat curve

#### 4.2.5.3 The phase transition at $H_{c1}(T)$

Below the  $H_{c1}$  phase transition line the specific heat is expected to be field independent on account of the Meissner effect as seen in Section 2.4.1. This is confirmed, within experimental accuracy, for the three samples. Accordingly, it is tempting to identify  $H_{c1}$  with the applied field at the temperature at which the specific heat line begins to deviate from the values corresponding to zero field. This should be correct in the absence of demagnetizing effects, i.e. for a needle-shaped sample aligned along the magnetic field direction. For any real geometry other than an ellipsoid the knowledge of the demagnetizing coefficient is complicated by the fact that it is not constant along the sample. In the present case (wires in a longitudinal field) the demagnetizing effects are maximum at the ends of each wire

and minimum at its mid-point with the consequence that the transition to the mixed state at constant applied field will not take place for the whole sample at a given temperature but rather within a small range of temperatures.

The nature of the specific heat anomaly (at constant field) associated with the phase transition at  $H_{c1}(T)$  is closely related to the change undergone by the magnetic moment  $M$  of the sample at this boundary when increasing the applied field at constant temperature. This can be seen from the Ehrenfest-like relation for the phase transition line  $H_{c1}(T)$ <sup>32,33,34</sup>

$$\frac{C_m - C_s}{T} = \left(\frac{dH_{c1}}{dT}\right)^2 \left[ \left(\frac{\partial M_m}{\partial H}\right)_T - \left(\frac{\partial M_s}{\partial H}\right)_T \right], \quad (4-8)$$

where the indices  $s$  and  $m$  stand for superconducting and mixed state, respectively. If  $(\partial M_m / \partial H)_T$  at  $H = H_{c1}$  is finite but different from  $(\partial M_s / \partial H)_T$ , the transition is second order. A jump in the magnetization will imply a transition of first order, with latent heat. On the other hand, a logarithmic singularity in the mixed state differential susceptibility will imply a  $\lambda$ -type transition.

There has been much discussion about the nature of this transition. From the theoretical point of view the most recent predictions seem to be in favour a transition of  $\lambda$ -type<sup>35,36</sup> of the order  $(1 + 2K)$ <sup>37</sup> (for a definition of  $K$  see ref.37)). The Abrikosov vortex model yields a  $\lambda$ -type transition at  $H_{c1}$  (Goodman<sup>38</sup>).

Experimentally, a logarithmic singularity in the magnetic permeability  $(\partial B / \partial H)_T$  at  $H = H_{c1}$  was reported from magnetization measurements in high-purity annealed Nb<sup>39</sup> ( $\Gamma = 500$ ). But Finnemore et al.<sup>19</sup> also performing magnetization measurements in high-purity annealed Nb ( $\Gamma = 2000$ ), did not confirm that result. They reported instead a large but finite discontinuity in  $(\partial M / \partial H)_T$  at  $H = H_{c1}$ , (this implying a second order transition) shortly followed by a rapid decrease of  $(\partial M / \partial H)_T$  at a slightly higher field. It was further claimed that the field interval in which the rapid variation of the magnetization took place could not be accounted for by the demagnetizing coefficient of the sample, which was too small. However, it is not clear whether or not this might be due to smearing out of a  $\lambda$ -type or first order transition followed by a rapid variation of  $(\partial^2 G / \partial H^2)_T$  in the mixed state. Demagnetizing effects are expected to truncate a  $\lambda$ -type transition<sup>38</sup> and to change an ideal first order transition into two of second order as in the case of the intermediate state in type I superconductors<sup>40</sup>. Hysteresis and inhomogeneities further complicate the transition.

The departure of the specific heat lines from the values corresponding to zero field and the observed peaks are clearly associated with the mixed state where the entropy and therefore the specific heat are field dependent. However, the results deviate from those one should expect for a type II superconductor in thermodynamic equilibrium. In particular, the location of the peak in the phase diagram as will be seen in Section 4.2.5.6 (Fig.IV.16) for Nb-3 lies too close to  $H_c(T)$ , this indicating retardation in the penetration of magnetic flux into the bulk of the sample. This effect is most apparent in the case of Nb-1 for which the peak lies very close to the transition to the normal state.

Ideally, for any value of the applied field  $H_{c1} < H < H_{c2}$ , at a given temperature, there is an equilibrium uniform distribution of flux threads inside the type II superconductor, the flux density corresponding to the thermodynamically reversible  $M(H)$  curve at this temperature. Upon changing  $H$  or  $T$  the fluxoids must adjust themselves to a new equilibrium configuration. However, in practice, the movement of the fluxoids may be countered by local changes in the superconducting parameters produced by inhomogeneities of the sample, from which results pinning of the flux<sup>41)</sup>. For an increasing field, flux pinning increases the absolute value of the magnetization above the value corresponding to thermodynamic equilibrium, the opposite occurring in a decreasing field<sup>42)</sup>. Thermal activation counteracts flux pinning<sup>43)</sup> so that for a sample with a not-too-high defect concentration thermodynamic equilibrium might in principle, be approached or even attained. However, at  $H_{c1}$ , even for a defect-free sample there is an energy barrier<sup>44)</sup> that prevents flux from penetrating into the specimen or escaping from it. In fact, hysteresis is hardly absent at  $H_{c1}$  although surface flaws and end effects as well as thermal activation may counter the effects of the surface barrier.

Considerable magnetic hysteresis was found in a Nb sample of the same origin as Nb-1 as can be seen in Fig.IV.11 where the magnetization curve for  $T = 6.95^\circ\text{K}$  (obtained by Goedemoed et al.<sup>44a)</sup>) is presented, both for increasing and decreasing fields. The magnetic behaviour of Nb-2 and Nb-3 also showed hysteresis as can be seen in Fig.IV.12. The relative magnitude of the residual paramagnetic moment due to locked-in flux when  $H$  has been reduced to zero from above  $H_{c2}$ , compared to the maximum diamagnetic moment at  $H \approx H_{c1}$ , is minimum for Nb-3 and maximum for Nb-1.

During the measurements of the specific heat of sample Nb-3, when the temperature approached the region of the anomaly (peak), the recording of the heating curves for  $H \geq 1480$  Oe showed unusual effects. For the same power supplied to the sample as used at lower temper-



atures, the rate of variation of the temperature of the sample, with the time decreased abnormally and a sudden cooling was sometimes observed while supplying heat from outside. On other occasions the temperature of the sample stayed constant for short periods during the heating process. Also, when the temperature of the sample drifted towards the bath temperature ( $T_{\text{bath}} \gtrsim T_{\text{sample}}$ ) in the fore- and after-periods of the heating curves, a number of sudden small coolings were observed. These cooling effects might be due to the creation of a large number of vortices, this producing the sudden cooling of the

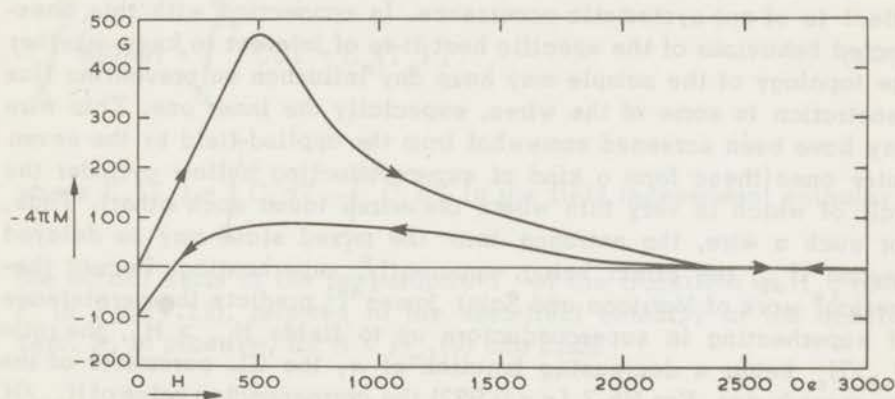


Fig. IV.11 The isothermal magnetization of Nb-1 at  $T = 6.95^{\circ}\text{K}$  plotted as  $-4\pi M$  versus the applied field  $H$  for increasing and decreasing field, measured by Goedemoed et al.<sup>44a)</sup>.

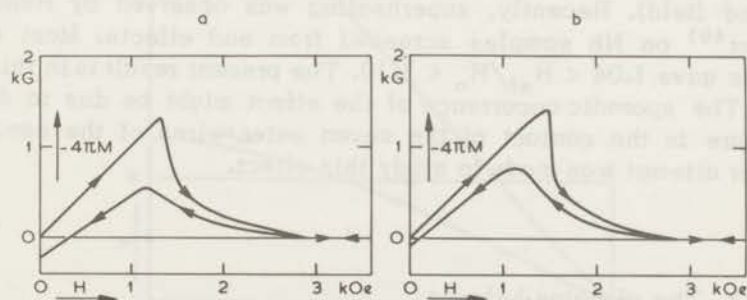


Fig. IV.12 The isothermal magnetization for increasing and decreasing field, for

a. Nb-2 at  $T = 4.20^{\circ}\text{K}$ , measured by Goedemoed<sup>44b)</sup>

b. Nb-3 at  $T = 4.22^{\circ}\text{K}$ , measured by Van Kolmeschate<sup>45)</sup>.

superconducting matrix in which they are embedded. It is likely that the observed sudden cooling effects indicate non-equilibrium states, since they occurred in a region of the phase diagram very near the line defined by the values of the thermodynamic critical field  $H_c > H_{c1}$ . Anyhow they disturb the measurement of the specific heat. The hump that follows the main peak for  $H = 1480$  Oe (Nb-2) as can be seen in Fig.IV.3 seems unlikely to be caused by a change in the structure of the magnetic lattice of fluxoids threading the superconductor in the mixed state. In fact, it appears to have definitely been shown<sup>46,47)</sup> that the triangular lattice is more stable than the square lattice over the whole range of the mixed state. On the other hand the peculiar effect is of not systematic occurrence. In connection with this unexpected behaviour of the specific heat it is of interest to know whether the topology of the sample may have any influence on preventing flux penetration in some of the wires, especially the inner one. This wire may have been screened somewhat from the applied field by the seven outer ones (these form a kind of superconducting hollow cylinder the wall of which is very thin where the wires touch each other). Thus, for such a wire, the entrance into the mixed state may be delayed beyond  $H_{c1}$ , the effect being, apparently, superheating. Recent theoretical work of Matricon and Saint James<sup>48)</sup> predicts the persistence of superheating in superconductors up to fields  $H_{sh} > H_c$ , the ratio  $H_{sh}/H_c$  being a decreasing function of  $\kappa$ , the GL parameter of the superconductor. For Nb-2, ( $\kappa = 0.992$ ) the corresponding value of  $H_{sh}/H_c$  according to Matricon and Saint James, is about 1.3. The temperature interval where the secondary peak in the specific heat is located for the case of  $H = 1480$  Oe for Nb-2 corresponds to  $1.02 < H/H_c < 1.09$  ( $H_c$  represents the values of the thermodynamic critical field at the temperatures of the beginning and the end of the hump, while  $H$  is the applied field). Recently, superheating was observed by Renard and Rocher<sup>49)</sup> on Nb samples screened from end effects. Most of their results gave  $1.04 < H_{sh}/H_c < 1.10$ . The present result is in this range.

The sporadic occurrence of the effect might be due to different pressure in the contact of the seven outer wires of the sample. No further attempt was made to study this effect.

#### 4.2.5.4 The enthalpy balance

Combining the definition of magnetic enthalpy given in Section 3.1 as  $E = U - MH$ , with the first principle of thermodynamics  $dU = dQ + HdM$ , ( $dQ$  being the heat supplied to the sample at constant field), we have

$$dE = C dT - MdH . \quad (4-9)$$

Thus, the variation of the enthalpy between two states  $(T,H)$ , one, for instance,  $(0,0)$  and the other on the  $H_{c2}$  phase transition line  $(T_s, H_{c2})$ , can be calculated as the sum of the magnetic work done isothermally at  $T = 0^\circ\text{K}$  on the sample by the external field between 0 and  $H = H_{c2}(T_s)$  and the integrated values of the specific heat,  $C$ , measured at constant field,  $H$ , between 0 and  $T_s$ . For a closed path in the phase diagram like ABCDA in Fig.IV.13 one has  $\oint dE = 0$  or, in an equivalent way

$$-\int_0^H M(0)dH + \int_0^{T_s} C dT = E_n(T_s) , \quad (4-10)$$

where  $E_n(T_s) = \int_0^{T_c} C_s dT - \int_{T_c}^{T_s} C_n dT$  is the field independent enthalpy in

the normal state at the temperature  $T_s$  of the transition at  $H_{c2}$  (point F in Fig.IV.13), referred to the zero-field enthalpy at the absolute zero. If, in practice, for  $H < H_{c1}(0)$  one finds

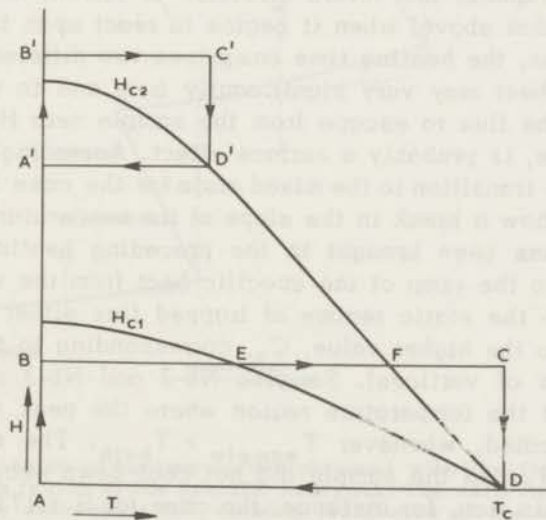


Fig. IV.13 Closed paths ABCDA and A'B'C'D'A' in the phase diagram used in the enthalpy and entropy computation.

$$\Delta E = E_n(T_s) - \left[ - \int_0^H M(0) dH + \int_0^{T_s} C dT \right] > 0, \quad (4-11)$$

since  $\int_0^H M(0)dH = H^2/8\pi$  corresponds to reversible behaviour (perfect

Meissner effect), it is evident that the enthalpy difference,  $\Delta E$ , is caused by too small values of the measured mixed state specific heat  $C_m$ . The lowering of the measured  $C_m$  results in fact, from an error introduced by the calculation of the specific heat by means of the usual Keesom and Kok's method (Section 3.6) whenever the specific heat varies largely and discontinuously during the heating time, and this might happen near the  $H_{c1}$  phase transition line, in some conditions, as described below.

Suppose that near  $H_{c1}$  the adjustment of the Abrikosov vortex structure<sup>50)</sup> to a new equilibrium configuration, corresponding to a different temperature at constant field, occurs without (or little) relaxation for increasing temperature but with a large time lag when the sample is allowed to cool down somewhat from a state  $(T_1, H)$  to a state  $(T_1 - \Delta T, H)$ . Upon warming up the sample once again from the temperature  $T_1 - \Delta T$ , when there is no (or little, short lasting) flux pinning one expects the vortex structure to remain unchanged up to  $T_1$  (or somewhat above) when it begins to react upon the temperature increase. Thus, the heating time comprises two different regimes and the specific heat may vary significantly from one to the other. The inability of the flux to escape from the sample near  $H_{c1}$ , when it is cooled a little, is probably a surface effect. Accordingly, the heating curves at the transition to the mixed state for the case that  $T_{\text{sample}} > T_{\text{bath}}$  must show a break in the slope at the temperature  $T_1$  at which the sample has been brought in the preceding heating. This break corresponds to the jump of the specific heat from the value,  $C_1$ , corresponding to the static regime of trapped flux either for cooling or warming up to the higher value,  $C_2$ , corresponding to the entrance of flux (creation of vortices). Samples Nb-2 and Nb-3 showed clearly this effect at the temperature region where the peak in the specific heat was located, whenever  $T_{\text{sample}} > T_{\text{bath}}$ . The effect was not at all present when the sample did not cool down near  $H_{c1}$  ( $T_{\text{bath}} > T_{\text{sample}}$ ). This was, for instance, the case for  $H = 1732$  Oe (Nb-3) at which field the transition at  $H_{c1}$  takes place below the boiling point of  $^4\text{He}$ .

In Fig.IV.14 is shown a succession of heating curves for  $H = 597$  Oe

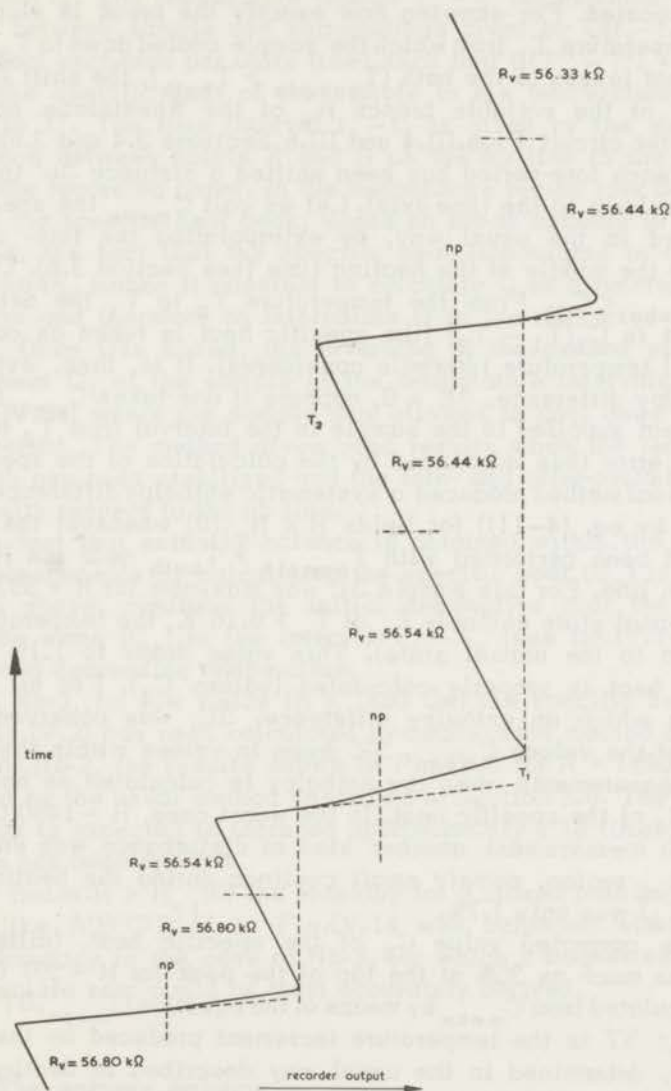


Fig. IV.14 Succession of heating curves obtained with Nb-3 for  $H=5970e$  in the region of the specific heat peak. The shift  $\Delta u'$  produced by decreasing the variable resistance of the Wheatstone bridge (see thermometer circuit, Fig.III.4 and the recorder output, Fig.III.6) has been omitted without changing the time. At the middle of the lowest curve  $T = 7.576^\circ K$  while  $T = 7.671^\circ K$  at the middle of the highest;  $T_{\text{bath}} = 4.2^\circ K$ .

(Nb-3) taken at the temperature region where the peak in the specific heat is located. For showing how exactly the break in slope occurs at the temperature  $T_1$  from which the sample cooled down to  $T_2 = T_1 - \Delta T$ , due to heat losses to the bath ( $T_{\text{sample}} > T_{\text{bath}}$ ), the shift  $\Delta u'$  due to decrease of the variable branch  $R_v$  of the Wheatstone bridge (see thermometer circuit Figs. III.4 and III.6, Sections 3.4 and 3.6) has been omitted (each fore-period has been shifted a distance  $\Delta u'$  to the right perpendicularly to the time axis). Let us call  $C_{\text{mean}}$  the specific heat determined in the usual way, by extrapolating the fore- and after-period to the middle of the heating time (see Section 3.6). Obviously,  $C_1 < C_{\text{mean}} < C_2$ . From the temperature  $T_2$  to  $T_1$  the net enthalpy increment is  $C_2(T_1 - T_2)$  (the specific heat is taken as constant in the small temperature intervals considered). It is, then, evident that an enthalpy difference,  $\Delta E > 0$ , appears if one takes  $C_{\text{mean}}(T_1 - T_2)$  as the heat supplied to the sample in the interval from  $T_2$  to  $T_1$ . For Nb-3 the error thus introduced by the calculation of the specific heat by the usual method produced a systematic enthalpy difference,  $\Delta E > 0$ , (defined by eq. (4-11)) for fields  $H < H_{c1}(0)$  whenever the measurement had been performed with  $T_{\text{sample}} > T_{\text{bath}}$  near the  $H_{c1}$  phase transition line. For this sample  $\Delta E$  was maximum for  $H = 597$  Oe (8.5% of the normal state enthalpy  $E_n$  at  $T_s = 8.16$  °K, the temperature of the transition to the normal state). This value drops to 1.1% when the specific heat is properly calculated (values  $C_2$ ). For all the other fields in which an enthalpy difference,  $\Delta E$ , was observed by integration of the values  $C_{\text{mean}}$ ,  $\Delta E$  drops to values within the accuracy of the measurements when the enthalpy is calculated on basis of the values  $C_2$  of the specific heat. In the worst case,  $H = 1480$  Oe (Nb-3), for which measurement another kind of disturbance was encountered in the  $H_{c1}$  region, namely small coolings during the heating period,  $\Delta E/E_n(T_s)$  was only 1.7%.

The corrected value  $C_2$  of the specific heat, (differing from  $C_{\text{mean}}$  as much as 35% at the top of the peak for  $H = 597$  Oe (Nb-3)) was calculated from  $C_{\text{mean}}$  by means of the equation  $C_{\text{mean}} \Delta T = C_1 \Delta T_1 + C_2 \Delta T_2$ ;  $\Delta T$  is the temperature increment produced by the supplied heat  $\Delta Q$ , determined in the usual way described in Section 3.6 and  $\Delta T_1$  is the part of  $\Delta T$  before the break in the slope of the heating curve, while  $\Delta T_2 = \Delta T - \Delta T_1$ .  $C_1$  was calculated on basis of the fore- and after-period of the heating curves (see Fig. III.6) as follows. For  $T_{\text{sample}} \neq T_{\text{bath}}$ , the intersections A and B (not shown) of the null point line  $np$ , with the extrapolations of the straight lines corresponding to an after-period and the next fore-period (after decreasing the variable resistance  $R_v$  of the Wheatstone bridge from the value  $R_k$  to  $R_{k+1}$ ) give, by means of the calibration curve  $R(T)$  of the carbon

thermometer, the temperatures  $T'$  and  $T''$  of the sample at two different times  $t_1$  and  $t_2$ . The temperature change  $T'' - T'$  corresponds to a heat exchange between sample and surroundings given by  $\dot{Q}(t_1 - t_2)$  (where  $\dot{Q}$  is the heat exchange per unity time) such that  $C(T'' - T') = \dot{Q}(t_1 - t_2)$ ,  $C$  being the specific heat of the sample in the temperature interval from  $T''$  to  $T'$ . The time interval  $t_1 - t_2$  is given by the quotient of the distance between points  $A$  and  $B$  on the  $np$  line to the constant speed of the recording paper. In the temperature region just before and just after the specific heat peak, where no break appears in the heating curves, the fact that the specific heat (calculated in the usual way) is known, makes it possible to calculate  $\dot{Q}$  as a function of the temperature and therefore to interpolate it in the restricted region of the peak. Once  $\dot{Q}$  is known, the reversing of the method yields the specific heat  $C_1$  of the sample at the temperature intervals  $T_1 - T_2$  (see Fig.IV.14) where the sample was allowed to cool down after the heating period. The method gives good results when the temperature of the bath has been stabilized and the fore- and after-period are well inclined with respect to the  $np$  line.

The fact that enthalpy balance is obtained within the accuracy of the measurements by calculating the specific heat ( $C_2$ ) in the way described above, confirms the initial assumption that the specific heat is the same ( $C_1$ ) in the interval  $T_1 - T_2$  (see fig.IV.14) for increasing and decreasing temperature.

For Nb-3, for low fields ( $H \leq 1480$  Oe) the specific heat at the peaks (Fig.IV.2) has been calculated by means of the method described above. For Nb-2, the results shown in Fig.IV.3 for  $H = 1480$  Oe were calculated by the usual method described in Section 3.6. The maximum at the peak is expected to increase approximately 1.13 times after the correction has been applied.

For fields  $H > H_{c1}(0)$  the enthalpy for a closed path in the phase diagram like  $A'B'C'D'A'$  in Fig.IV.14 was balanced within experimental accuracy in the case of Nb-3, for which a magnetization curve at the absolute zero could be most accurately derived.

#### 4.2.5.5 The entropy balance

For all paths at constant field that cross the mixed state, for Nb-1, and in the restricted range of fields  $597 \text{ Oe} < H \leq H_{c1}(0)$  for Nb-2 and Nb-3, it was found that the integrated values of  $C/T$  ( $C$  being the measured specific heat), from the absolute zero up to the temperature  $T_s$  of the transition to the normal state, were systematically lower than the corresponding rise in entropy

$$\int_0^{T_s} \frac{C}{T} dT < S_n(T_s), \quad (4-12)$$

where  $S_n(T_s)$  is the normal state entropy at  $T_s$ .

The irreversible behaviour implied by this inequality is due to the mechanism that retards the transition into the mixed state and/or prevents the Abrikosov vortex structure to adjust itself, at each temperature, to the equilibrium pattern. In the case of Nb-3 evidence for metastable states appear, at the temperature region of the peak in the specific heat, as irregularities in the heating curves (see Section 4.2.5.3). An analogous conclusion can be drawn from the fact that the peak in the specific heat lies very close to  $H_c$ , the thermodynamic critical field, as will be seen in Section 4.2.5.6. Since for Nb-2 and Nb-3, in part of the mixed state, the specific heat is independent of the way in which the previous cooling has been performed, and given the second-order character of the transition to the normal state ( $S_m(T_s) = S_n(T_s)$ ),  $S_m$  being the entropy in the mixed state), one may calculate  $S_m(T)$  in the following way: starting at  $T = T_s$  with  $S_m(T_s) = S_n(T_s)$ , the entropy  $S_m(T)$  in the mixed state was calculated by subtracting

from  $S_n(T_s)$  the values  $\int_{T_s}^T (C_m/T - C_n/T) dT$ . In this way the temper-

ature of the transition at  $H_{c1}$  was approached from above, passing through the reversible region of the specific heat curves. Starting from the low temperature side,  $S_m(T)$  was calculated by adding to  $S_s(T)$  the entropy in the pure superconducting state the values of

$$\int_{T_1}^T (C_m/T - C_s/T) dT,$$

where  $T_1$  is the temperature at which the specific heat curve begins to depart from that for zero field. In this way the entropy production

defined as  $\Delta S = S_n(T_s) - \int_0^{T_s} (C/T) dT$  was located in the neighbourhood

of  $H_{c1}(T)$ , reasonably far from the regions where the specific heat was found to be reversible. In the case of Nb-3 the irreversible entropy production was negligible for  $H = 194$  Oe and  $H = 597$  Oe ( $\Delta S/S_n(T_s) \leq 1\%$ ) and was the highest for  $H = 1809$  Oe ( $\Delta S/S_n(T_s) = 13.5\%$ ). For the same sample the electronic entropy  $S_e(H, T)$  is depicted in Fig. IV.15.



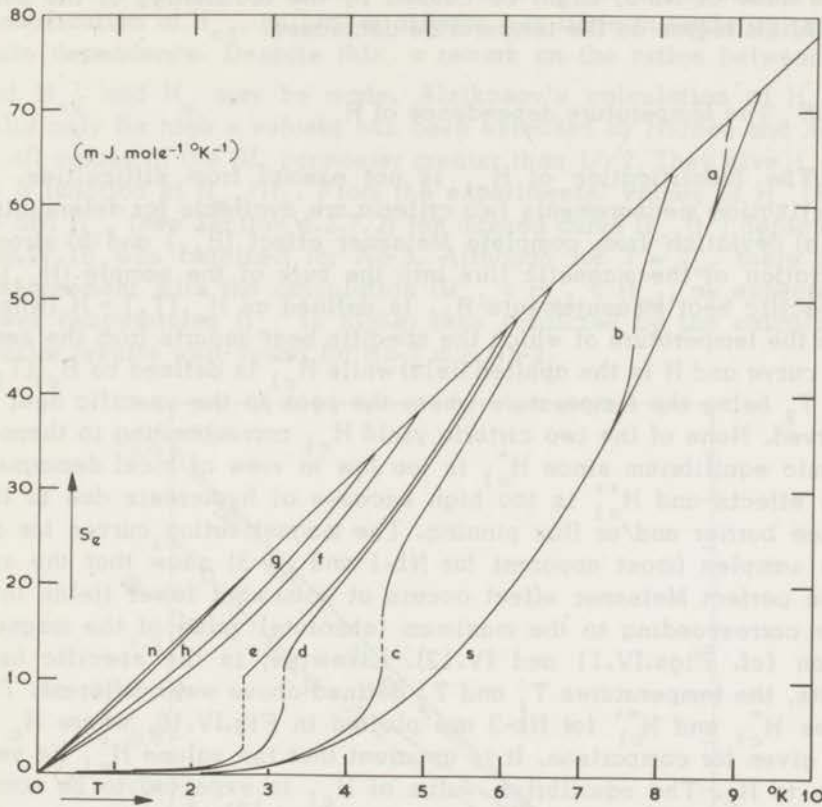


Fig. IV.15 The temperature and field dependence of the electronic entropy (Nb-3)

s	zero field and $H < H_{c1}(T)$	d	$H = 1732$ Oe
n	normal state	e	$H = 1809$ Oe
a	$H = 194$ Oe	f	$H = 2488$ Oe
b	$H = 597$ Oe	g	$H = 2895$ Oe
c	$H = 1480$ Oe	h	$H = 3610$ Oe

These results, together with the fact that for Nb-2 and Nb-3 the effect of irreversibility disappeared ( $\Delta S = 0$ ) for  $H \gg H_{c1}(0)$ , seem to rule out the idea that there might be an "intrinsic" irreversibility associated with the motion of the Abrikosov vortices. The irreversible entropy production was the largest for Nb-1, the sample which displayed the highest magnetic hysteresis and, as already mentioned, for this sample the effect of irreversibility was seen for all measured fields. The increase of  $\Delta S$  with the field up to  $H_{c1}(0)$ , clearly observed

in the case of Nb-3, might be caused by the broadening of the non-equilibrium region as the temperature decreases.

#### 4.2.5.6 The temperature dependence of $H_{c1}$

The identification of  $H_{c1}$  is not exempt from difficulties. In magnetization measurements two criteria are available for determining  $H_{c1}$ : a) deviation from complete Meissner effect ( $H_{c1}^*$ ) and b) strong penetration of the magnetic flux into the bulk of the sample ( $H_{c1}^{**}$ ). In specific heat measurements  $H_{c1}$  is defined as  $H_{c1}^*(T_1) = H$  (where  $T_1$  is the temperature at which the specific heat departs from the zero-field curve and  $H$  is the applied field) while  $H_{c1}^{**}$  is defined as  $H_{c1}^{**}(T_2) = H$ ,  $T_2$  being the temperature where the peak in the specific heat is observed. None of the two criteria yield  $H_{c1}$  corresponding to thermodynamic equilibrium since  $H_{c1}^*$  is too low in view of local demagnetizing effects and  $H_{c1}^{**}$  is too high because of hysteresis due to the surface barrier and/or flux pinning. The magnetization curves for all three samples (most apparent for Nb-1 and Nb-3) show that the end of the perfect Meissner effect occurs at somewhat lower fields than those corresponding to the maximum (absolute) value of the magnetization (cf. Figs. IV.11 and IV.12). Likewise, in the specific heat results, the temperatures  $T_1$  and  $T_2$  defined above were different. The values  $H_{c1}^*$  and  $H_{c1}^{**}$  for Nb-3 are plotted in Fig. IV.16, where  $H_c$  is also given for comparison. It is apparent that the values  $H_{c1}^{**}$  lie very close to  $H_c$ . The equilibrium value of  $H_{c1}$  is expected to be somewhere between  $H_{c1}^*$  and  $H_{c1}^{**}$ . Finnemore et al.<sup>19)</sup> found in magnetization measurements on Nb with almost reversible behaviour that  $H_{c1}^{**}(0) = 1736$  Oe. Our Nb-3, having a higher  $\kappa$  value, should be expected, if it behaved reversibly, to have a lower value of  $H_{c1}^{**}(0)$  than that found in reference 19).

The results presented in Fig. IV.16 confirm, near  $H_{c1}$ , the related behaviour of calorimetric and magnetic results: where the complete Meissner effect ends ( $H_{c1}^*$ ), the specific heat departs from the zero-field curve; where the magnetization has its most rapid variation ( $H_{c1}^{**}$ ) the specific heat has its maxima. The most pronounced anomalies in the heating curves (small coolings, intervals of constant temperature) appear at  $H_{c1}^{**}$ .

For Nb-2 the values of  $H_{c1}^*$  and  $H_{c1}^{**}$  were near the corresponding values for Nb-3 for the same reduced temperature (not shown). For Nb-1,  $H_{c1}^*$  was systematically lower than for Nb-2 and Nb-3 and, in particular,  $H_{c1}^*(0)$ , obtained by extrapolation, was found to be 1.14 kOe (also not shown). This behaviour is what one should expect for a

superconductor with a higher  $\kappa$ -value. Because of the ambiguity in the identification of  $H_{c1}$ , no further attempt was made to study its temperature dependence. Despite this, a remark on the ratios between  $H_{c1}$  and  $H_{c2}$  and  $H_c$  may be made. Abrikosov's calculation of  $H_{c1}^{(50)}$ , valid only for high  $\kappa$  values, has been extended by Harden and Arp<sup>51)</sup> to all values of the GL parameter greater than  $1/\sqrt{2}$ . They give  $H_{c1}/H_c$  as a function of  $H_{c2}/H_c$ . From the experimental values of  $H_c$  (Table II) and  $H_{c2}$  (see Section 4.2.7.2) the dashed curve  $H_{c1}(t^2)$  depicted in Fig. IV.16 was obtained for Nb-3. Although for  $T \approx T_c$ , there is no disagreement with the calculation ( $H_{c1}^* < H_{c1} < H_{c1}^{**}$ , as expected) at lower temperatures  $H_{c1}$  is higher than predicted by the calculation. Similar results were found for Nb-1 and Nb-2.

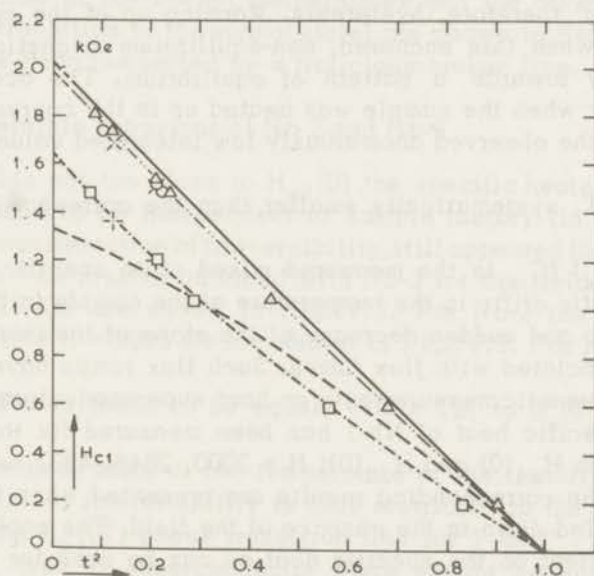


Fig. IV.16 The temperature dependence of the lower critical field for Nb-3, defined as:

- the end of the Meissner effect ( $H_{c1}^*$ , line ---) from magnetization results (points  $\times$ ) and from specific heat results (points  $\square$ );
- the locus ( $H_{c1}^{**}$ , line -.-) of the specific heat maxima (points  $\Delta$ ) or the magnetization maxima (points  $\times$ ). Points (O) locate the most pronounced irregularities observed in the heating curves.

The temperature dependence of  $H_{c1}$  according to Harden and Arp<sup>51)</sup> is represented by the dashed line. The thermodynamic critical field  $H_c$  is represented by the full line.

#### 4.2.6 The specific heat in fields $H_{c1}(0) < H < H_{c2}(0)$

##### 4.2.6.1 Irreversible behaviour of Nb-1

For Nb-1, considerable disturbances and irregularities were encountered in this region of the phase diagram. In the course of runs with applied fields  $H > H_{c1}(0)$ , erratic drifts in the direction of warming up were observed in the temperature of the sample and some of the heating curves correspond to an abnormally large temperature increment for the usual heating time, from which results too small a value for the specific heat. All these complications might be ascribed to the inhomogeneity of the metal caused, for example, by impurities, lattice dislocation, strains<sup>41</sup>). Such structural defects pin down the Abrikosov vortices, thus creating macroscopic flux gradients inside the sample<sup>52</sup>), and producing, therefore, hysteresis. Warming up of the sample is to be expected when this anchored, non-equilibrium magnetic structure, moves rapidly towards a pattern of equilibrium. The occurrence of irreversibility when the sample was heated up in the course of the run accounts for the observed anomalously low integrated values

$\int_0^T (C_m/T) dT$ , systematically smaller than the corresponding rise in entropy  $S_n(T_s)$  ( $C_m$  is the measured mixed state specific heat). The observed erratic drifts in the temperature of the sample in the direction of warming up and sudden decrease of the slope of the heating curves might be associated with flux jumps. Such flux jumps have also been observed in magnetic measurements on hard superconductors<sup>41,42,53,54</sup>).

The specific heat of Nb-1 has been measured for the following fields between  $H_{c1}(0)$  and  $H_{c2}(0)$ :  $H = 2000, 2848, 4337$  and  $5760$  Oe. In Fig.IV.1 the corresponding results are presented when the sample has been cooled down in the absence of the field. The cooling procedure has an effect on the specific heat as can be seen for the case of  $H = 4337$  Oe depicted in Fig.IV.9 (lines 2 and 2' respectively). When the cooling took place in the presence of the field the observed specific heat values were larger and less irregularities were met. The specific heat curves for the two cooling procedures converge in the neighbourhood of the transition to the normal state.

On account of the irregularities mentioned above, all points whose heating curves presented anomalous shape have been rejected. In repeating the runs only the points that appeared to be reproducible have been retained (these were the higher ones). The lines depicted in Fig.IV.1 and lines 2 and 2' in Fig.IV.9 have been defined using this criterion.

For the field  $H = 2000$  Oe the results were particularly affected by the irreversible effects. The points at the lowest temperatures lie above the line corresponding to  $H = 0$  but, as the temperature increases, they fall below this line and remain there, however scattered, until the transition temperature is approached. Here the measured points appear again above the line for zero field and they define in the usual way the transition to the normal state. Probably these observed effects were due to a rather pronounced metastable state of magnetization of the sample. In fact, such a field of 2 kOe lying relatively close to  $H_{c1}(0) = 1.14$  kOe crosses the region of the phase diagram where the magnetic moment has its highest values. In view of the anomalous behaviour for this field, only two sets of experimental points, (one set containing those at the lowest temperatures and the other one, those close to the transition to the normal state) are shown in Fig.IV.1; these two sets have been connected by a fictitious broken line.

#### 4.2.6.2 Reversible behaviour of Nb-2 and Nb-3

For fields not too close to  $H_{c1}(0)$  the specific heats of Nb-2 and Nb-3 were found to be independent of sample history (in the case of Nb-3 a slight manifestation of irreversibility, still appeared for  $H = 2488$  Oe, for  $T \leq 2^\circ\text{K}$ ). The results obtained with Nb-3 for the fields  $H = 2488$ , 2895 and 3610 Oe are shown in Fig.IV.2. For Nb-2 the results obtained in the field  $H = 2895$  Oe are shown in Fig.IV.3. For  $H \geq 2895$  Oe

$\int_0^{T_s} (C_m/T) dT$  was found to be equal, within 1%, to  $S_n(T_s)$  — the en-

tropy in the normal state at the temperature of the transition. For the annealed samples, irreversibility is thus restricted to the mixed state region near the  $H_{c1}(T)$  phase transition line for  $T \ll T_c$ . For a fairly homogeneous type II superconductor there should be not much flux pinning and thus no high flux gradients. Near  $H_{c2}$ , when the temperature increases, the almost overlapping Abrikosov vortices move slowly towards positions of thermodynamic equilibrium. Thus, as the temperature increases, the variation of magnetic flux threading the sample is a quasi-static process in the high field region of the phase diagram.

#### 4.2.6.3 The linear term in the specific heat

From Fig.IV.1, IV.2 and IV.3 one concludes that  $\gamma' = \lim_{T \rightarrow 0} C(H, T)/T \neq 0$  for  $H > H_{c1}(0)$ . For Nb-3 the quantity  $\gamma'/\gamma$

is plotted in Fig. IV.17 against  $H/H_{c2}(0)$ , both for cooling in the absence and presence of the field ( $\gamma$  is the coefficient of the normal state electronic specific heat,  $H$  is the applied field and  $H_{c2}(0)$  is the upper threshold field at the absolute zero, given in Section 4.2.7.2). From the results one concludes that when the field was applied after the previous cooling of the sample, the mixed state specific heat for fields  $H > H_{c1}(0)$  contains a linear term  $\gamma'T$ , of which the coefficient  $\gamma'$  increases with the applied field,  $H$ , more rapidly for  $H_{c1} > (0)$  than it does near  $H_{c2}(0)$ . When the sample was cooled down in the presence of the field the linear term appeared in a wider range of fields being only zero for the lowest ones. For the same value of the applied field the linear term was larger when the field was on during the cooling prior to the measurement, except for  $H > 2895$  Oe where it was independent of sample history.

It was shown in Section 2.4.2 (eq.(2-56)) that the mixed state specific heat for fields  $H$  such that  $H_{c2}(0) - H \ll H_{c2}(0)$  was expected to contain a term, linear both in  $T$  and  $H$ , under the sole assumption that at all temperatures the magnetization near  $H_{c2}$  is given by Abrikosov's results<sup>50)</sup>  $M = \chi_m(H - H_{c2})$  with temperature dependent (Maki<sup>55)</sup>, Maki and Tsuzuki<sup>55a)</sup>, but otherwise field independent  $\chi_m$ . For Nb-3,

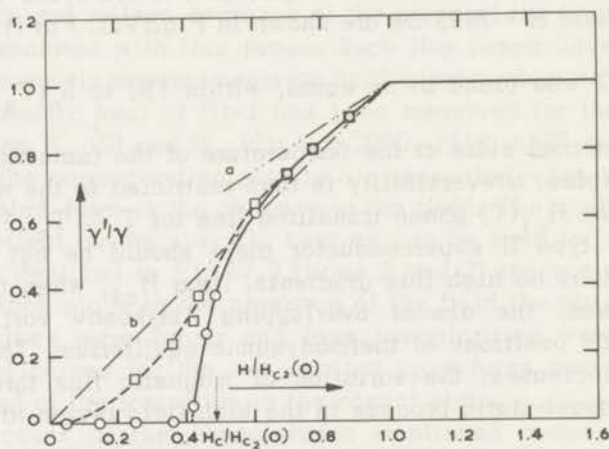


Fig. IV.17 The field dependence of the coefficient  $\gamma'$  of the linear term in the mixed state specific heat of Nb-3, plotted as  $\gamma'/\gamma$  versus  $H/H_{c2}(0)$ :

- O with sample cooled down in the absence of the field
- with sample cooled down in the presence of the field;
- line a : expected results according eq. (4-13)
- line b : expected results according eq.  $\gamma'/\gamma = H/H_{c2}(0)$ <sup>57,59</sup>.

the calculated value of the constant  $\alpha$  in eq.(2-56) (for the numerical values see Sections 4.2.7.1 (for  $\epsilon$ ) and 4.2.7.2 (for  $a$ )) is  $\alpha = 0.65$ , so that eq. (2-56) becomes

$$\frac{\gamma'}{\gamma} = 0.35 + 0.65 \frac{H}{H_{c2}(0)} \quad (4-13)$$

The field dependence of the coefficient  $\gamma'$  of the linear term in the mixed state specific heat according eq. (4-13) is represented in Fig.IV.17 by the straight line  $a$ . One can see that the field dependence of  $\gamma'$  do not quite follow what is expected on basis of the assumed assumption that the mixed state differential susceptibility  $\chi_m = (\partial M/\partial H)_T$  near  $H_{c2}$  was given by eq. (2-42).

The behaviour of the mixed state specific heat in the neighbourhood of the absolute zero for fields  $H > H_{c1}(0)$  contrasts flagrantly with the exponential variation of the specific heat with temperature in the Meissner region, where a field independent energy gap in the energy spectrum of the electrons sets a lower limit to the excitations above the Fermi surface. The existence of the linear term suggests, therefore, the depression of the energy gap in part of the specimen volume to such a low value that normal-like excitations can cross it, even in the neighbourhood of the absolute zero. Then, although the zero field gap may persist in the remaining part of the superconductive volume, it will be not anymore effective in determining the behaviour of the specific heat ("gapless" superconductivity).

According to Caroli et al.<sup>56)</sup> the energy spectrum of the electrons in the mixed state is allowed to include excitations of low energy in the cores of Abrikosov's vortices. The energy gap for these excitations is of the order  $\Delta_\omega^2/E_F$  where  $\Delta_\omega$  is the zero field gap and  $E_F$  is the Fermi energy. Because of the smallness of the energy gap in these regions they will behave in several respects like normal regions with a linear term in the specific heat. The empirical first evidence for the existence of such quasi-normal regions in the mixed state came from results on microwave surface resistance of a number of type II superconductors by Rosenblum and Cardona<sup>57)</sup>. From the results these authors had suggested that in the mixed state a fraction of the superconductive material, proportional to the applied field,  $H$ , behaves as being in the normal state, this implying a term in the specific heat, linear both in  $T$  and  $H$  which was in agreement with an earlier prediction of Gorter and Gorter et al., made on thermodynamic grounds (see the end of Section 2.4.2 and ref. 41,42), Chapter II). They had re-examined the specific heat results of Hake and Brammer<sup>58)</sup> on a V-Ta alloy and found it in accordance with their suggestion.

The field dependence of the linear term resulting from Rosenblum and Cardona assumption is in agreement with an approximate treatment due to Gorter<sup>59)</sup> for  $H \approx H_{c2}(0)$ , which yields  $\gamma'/\gamma = H/H_{c2}(0)$  and is represented by the straight line *b* in Fig.IV.17. Such a result was used in an earlier analysis<sup>59)</sup> of the data obtained on impure Nb(Nb-1). The actual field dependence of the linear term for  $H \approx H_{c2}(0)$  is not much different from that given by  $\gamma'/\gamma = H/H_{c2}(0)$ , to which eq. (2-56) is reduced for  $\alpha = 1$ .

For superconducting alloys Maki<sup>60)</sup> has calculated that in the field region just below  $H_{c2}$ , the specific heat can be expanded in powers of  $T$  due to the fact that the energy gap in the excitation spectrum vanishes in this region. According to this author there should, in qualitative features, not be much difference between the behaviour of the specific heat of pure and dirty type II superconductors. For Nb, the experimental results for fields  $H > H_{c1}(0)$  at the lowest temperatures, are of the form  $C_m = \gamma'T + BT^3$ . However, while according Maki<sup>60)</sup> the coefficient  $B$  should be field dependent, for all three Nb samples  $B$  was found to be practically field independent.

Marcus<sup>61)</sup> has studied the mixed state using a cellular approximation and derived also a linear term in the specific heat as the result of the change with temperature of the magnetic structure of Abrikosov's vortices. According Marcus' prediction<sup>61)</sup>  $\gamma'/\gamma$  should be somewhat larger than  $H/H_{c2}(0)$ , which is in agreement with experiment. For Nb-1 and Nb-2 the dependence of  $\gamma'/\gamma$  on  $H/H_{c2}(0)$  has a similar form to that found in Nb-3. The value of  $\alpha$  in (2-56) is 0.65 for Nb-1 and 0.70 for Nb-2.

For vanadium<sup>62)</sup> the field dependence of  $\gamma'/\gamma$  is rather similar to that found in Nb.

The calculated values of  $\gamma'/\gamma$  according to eq. (2-56) depend on the way according to which the extrapolation of the phase line  $H_{c2}(t)$  to  $t = 0$  is made, through the constant  $\alpha$ . Although the slope of the straight line corresponding to (2-56) could be somewhat reduced by fitting the experimental values ( $H_{c2}, t$ ) below  $t = 0.5$  by a parabolic relation  $H_{c2}(t) = H_{c2}(0)(1 - at^2)$ , still a difference of 7% remained at  $H/H_{c2}(0) = 0.7$  between the calculated and experimental values of  $\gamma'/\gamma$ .

The assumption made in the derivation of eq. (2-56) was that the slope of the magnetization curve versus the applied field is field independent near  $H_{c2}$ . If this does not hold ( $M(H)$  not varying strictly linearly near  $H_{c2}$ ),  $\gamma'/\gamma$  would not be linear as a function of  $H$  either. The resulting slight curvature of  $M(H)$  near  $H_{c2}$  brings the calculated values of  $\gamma'/\gamma$  nearer the experimental ones. Then the straight line corresponding to relation (2-56) should give the limiting slope at  $H = H_{c2}$ .



The magnetization data obtained with Nb-3 (see Fig.IV.12b) do not rule out this assumption and non-linearity of  $M(H)$  near  $H_{c2}$  might be connected with the small value of the GL parameter  $\kappa$  for high purity Nb ( $\kappa(\text{Nb-3}) = 0.893$ ), this implying a narrow field range for the mixed state. In Chapter V further evidence is presented in favour of non-linear magnetization near  $H_{c2}$ .

#### 4.2.7 The phase transition from the mixed to the normal state

In isothermal magnetic measurements on type II superconductors when the applied field reaches  $H_{c2}$ , the magnetization goes to zero with a finite discontinuity in the slope, this indicating a second-order transition in the Ehrenfest sense. In specific heat measurements such transition appears as a finite jump  $\Delta C(T_s) = C_m(T_s) - C_n(T_s)$  from the mixed state value  $C_m(T_s)$  to the normal state value  $C_n(T_s)$ , its magnitude  $\Delta C(T_s)$  being related to the change in the differential magnetic susceptibility  $(\partial M/\partial H)_T$  at  $H_{c2}$  by the Ehrenfest relation (2-47). The temperature  $T_s$  of the transition is reached when the constant applied field  $H$  equals  $H_{c2}$ . Actually, due to inhomogeneities of the sample and non-uniformity of the magnetic field, the transition is spread over a temperature interval  $\Delta T_s$ , which increases with the applied field and the impurity content of the specimen. For Nb-3 the transition in zero field was extremely sharp as already mentioned in Section 4.2.2.

For Nb-2 and Nb-3 in low fields,  $T_s$  could be determined directly from the heating curves being the temperature at which a break in slope occurred due to the discontinuous change of the specific heat. For higher fields, the transition at  $H_{c2}$  could hardly be directly obtained in that way in view of the decrease of  $\Delta C(T_s)$  and the increase of  $\Delta T_s$  with the field. In such cases  $T_s$  was taken at the middle of the temperature interval  $\Delta T_s$  in which the actual transition to the normal state took place as seen in the specific heat curves.

For Nb-2 and Nb-3, near  $T_c$ , the phase transition to the normal state could not be separated from the specific heat anomaly associated with the entrance into the mixed state as can be seen for Nb-3 in Fig.IV.2, for  $H = 194$  Oe. This is due to the proximity of the two phase transition lines  $H_{c1}(T)$  and  $H_{c2}(T)$ . In those cases the magnitude of  $C_m(T_s)$  required for calculating  $\Delta C(T_s)$  was derived from the analysis of the fore- and after-period lines, using the procedure described in Section 4.2.5.4. For all the other cases the magnitude of  $C_m(T_s)$  was determined by extrapolating the mixed state specific heat line  $C_m(T)$  to the middle of  $\Delta T_s$ .

#### 4.2.7.1 The temperature dependence of the specific heat jump at $H_{c2}$

The temperature dependence of  $\Delta C(T_s)$  is depicted in Fig. IV.18 as  $\Delta C(T_s)/T_s / \Delta C(T_c)/T_c$  versus  $t^2$  for Nb-1, Nb-2 and Nb-3. For the three samples the values depicted in this figure were determined by extrapolating to  $T_s$  the mixed state specific heat curves obtained when the magnetic field was established after the cooling of the sample. For Nb-1 the values determined from the curves obtained when the sample was cooled down in the presence of the field are somewhat lower<sup>63)</sup> (not shown). At the lower temperatures, corresponding to the "gapless" region, the magnitude of the specific heat jump has a similar behaviour for all samples, vanishing at the absolute zero and varying as a function of the temperature as  $T^3$ :  $\Delta C = \epsilon T^3$ . Close to  $T_c$  a markedly different behaviour appears. While for Nb-1,  $\Delta C(T_s)$  becomes less steep, for Nb-2 and Nb-3 the increase of  $\Delta C(T_s)$  with temperature becomes steeper. For Nb-2 and Nb-3  $\epsilon = 0.197 \text{ mJ} \cdot \text{mole}^{-1} \cdot \text{K}^{-4}$  while for Nb-1 the mean value  $\epsilon = 0.207 \text{ mJ} \cdot \text{mole}^{-1} \cdot \text{K}^{-4}$  was found.

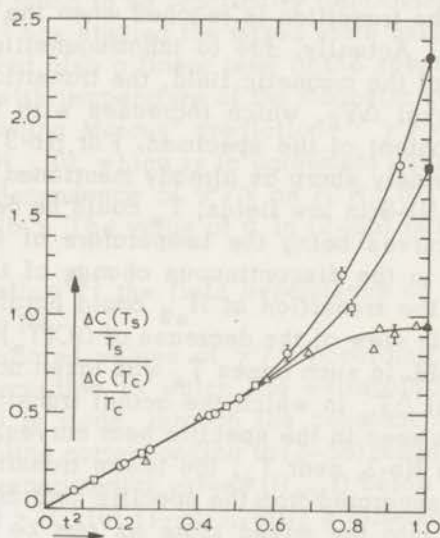


Fig. IV.18 The temperature dependence of the magnitude of the specific heat jump at the transition to the normal state compared to the jump in zero field.

- $\Delta$  and  $\hat{\Delta}$  experimental points for Nb-1
- $\square$  and  $\hat{\square}$  experimental points for Nb-2
- $\circ$  and  $\hat{\circ}$  experimental points for Nb-3.

The values for  $t \rightarrow 1$  were calculated by means of eq. (4-14) using the values of  $K$  given in Table V.

The fact that  $A = \lim_{T \rightarrow T_c} \Delta C(T_s)/T_s / \Delta C(T_c)/T_c \neq 1$ , is directly connected with the fundamental condition put forward by Maki:  $\lim_{T \rightarrow T_c} \kappa_1 = \lim_{T \rightarrow T_c} \kappa_2 = \kappa$  when  $T \rightarrow T_c$ . (see eq. (2-22) and (2-23) for the definitions of  $\kappa_1$  and  $\kappa_2$ ). In fact, using Rutgers' (2-37) and Ehrenfest's relations (2-47) and eq. (2-22) and (2-23) (with  $\beta = 1.16$ ) one gets

$$A = \lim_{T \rightarrow T_c} \frac{2\kappa_1^2}{1.16(2\kappa_2^2 - 1)} = \frac{2\kappa^2}{1.16(2\kappa^2 - 1)}. \quad (4-14)$$

The specific heat of type II superconductors in low fields near the transition to the normal state is thus a function of the GL parameter  $\kappa$  of the material. For  $\kappa = 1.91$  the specific heat jump  $\Delta C(T_s)$  varies continuously near  $T_c$ . For  $1/\sqrt{2} < \kappa < 1.91$ ,  $\Delta C(T_s)$  in low fields is larger than the jump in zero field  $\Delta C(T_c)$ , approaching infinity for  $\kappa \rightarrow 1/\sqrt{2}$ . For  $\kappa > 1.91$  the jump for low fields near  $T_c$  is smaller than in zero field. For type II superconductors with high  $\kappa$  values the ratio  $A$  is much less sensitive with respect to  $\kappa$  than in the case of materials with low  $\kappa$  values, the lowest value of  $A$  (for  $\kappa = \infty$ ) being 0.86. Marcus<sup>61)</sup> pointed out the explicit dependence of  $A$  on  $\kappa$ , although that could have already been inferred from earlier conclusions (Gorter<sup>64)</sup>). The different behaviour of  $\Delta C(T_s)$  near  $T_c$  for the three Nb samples is thus in agreement with that which one should expect from the respective  $\kappa$  values according to eq. (4-14). The transitions at  $H_{c2}$  for low fields and zero field are in reality quite different transitions. The former occur between the mixed and the normal state while the latter occur between the Meissner state and the normal state.

#### 4.2.7.2 The temperature dependence of $H_{c2}$

The upper threshold field  $H_{c2}$  is an equilibrium quantity well defined in specific heat measurements, at least on annealed samples. The uncertainty in the determination of  $H_{c2}$  increases with the transition width  $\Delta T_s$ . For the three samples  $H_{c2}$  was, near  $T_c$ , found to vary linearly with the temperature, with slopes  $(dH_{c2}/dT)_{T_c}$  given in Table V, those slopes increasing with the  $\kappa$  value of the sample. For temperatures not too close to  $T_c$  the experimental data  $(H_{c2}, t)$  was well represented by the empirical relation

$$H_{c2}(t) = H_{c2}(0) (1 + at^2 + bt^4 + ct^6). \quad (4-15)$$

The values of  $H_{c2}(0)$ ,  $a$ ,  $b$  and  $c$ , obtained by means of a computer are given in Table V for the three samples.

Table V

The values of  $H_{c2}(0)$  and coefficients  $a, b, c$  from relation (4-15),  $(dH_{c2}/dT)_{T_c}$  and  $\kappa$  for the three Nb samples.  $(dH_{c2}/dT)_{T_c}$  was obtained from a linear plot of the data near  $T_c$ .

sample	$\kappa$	$-(dH_{c2}/dT)_{T_c}$ (Oe. °K <sup>-1</sup> )	$H_{c2}(0)$ (Oe)	$a$	$b$	$c$
Nb-1	2.36	370	9087 ± 55	- 1.58	0.82	- 0.23
Nb-2	0.992	588	4450 ± 15	- 1.55	0.72	- 0.17
Nb-3	0.893	530	4116 ± 7	- 1.67	0.94	- 0.27

The values of  $\kappa$  were calculated by means of the relation

$$\kappa = \lim_{T \rightarrow T_c} \kappa_1 = \frac{(dH_{c2}/dT)_{T_c}}{\sqrt{2}(dH_c/dT)_{T_c}} \quad (4-16)$$

derived from eq. (2-22). The numerical values of  $(dH_c/dT)_{T_c}$  are given in Table III for the three samples (the values from column a) were used.

The linear character of  $H_{c2}(T)$  near  $T_c$  is in agreement with the results obtained by Ohtsuka and Takano<sup>65)</sup> on a high purity Nb single crystal (resistance ratio  $\Gamma = 1000$ ) for which they found  $(dH_{c2}/dT)_{T_c} = -531$  Oe. °K<sup>-1</sup> (due to uncertainties in  $(dH_c/dT)_{T_c}$  they gave for this sample  $\kappa = 0.92$  and  $0.84$ , the last value being more likely as will be shown in Section 4.2.8). The value  $H_{c2}(0) = 4116 \pm 7$  Oe for Nb-3 differs little from the reported values for Nb samples of somewhat higher purity namely  $H_{c2}(0) = 4035 \pm 8$  Oe (Ohtsuka and Takano<sup>65)</sup>) and  $H_{c2}(0) = 4040$  Oe (Finnemore et al.<sup>19)</sup>). Ohtsuka and Takano analysed their data for  $H_{c2}$  using, below  $t = 0.25$ , the expression  $H_{c2}(t) = H_{c2}(0)(1 - at^2)$ , with the result already mentioned for  $H_{c2}(0)$  and  $a = 1.49$ . Fitting the three highest experimental values of  $H_{c2}(t)$  (for  $0.28 < t < 0.44$ ) with the expression used by Ohtsuka and Takano

for  $t < 0.25$ , one gets for Nb-3  $\alpha = -1.47$  and  $H_{c2}(0) = 4070$  Oe. However, at the lowest temperatures, the absence in the expression for  $H_{c2}(t)$  of powers of  $T$  greater than the second, together with the well established fact that  $\Delta C = \epsilon T^3$  in the same region, would imply  $(\partial M / \partial T)_{T_s}$  (and therefore Maki's parameter  $\kappa_2$  defined by eq. (2-23)) to be temperature independent in that region, as shown in Section 2.4.2.

According to theory<sup>55a)</sup> in the limit of infinite mean free path of the electrons for  $t \ll 1$ ,  $H_{c2}(t)$  is given by  $H_{c2}(t) = H_{c2}(0) (1 - at^2)$  where  $a$  is temperature dependent and should have a logarithmic singularity as  $T \rightarrow 0$ . In real cases, the existence of a finite transport collision time might remove this singularity in the coefficient of the term in  $t^2$ , as has been predicted for concentrated alloys<sup>55)</sup>.

There are three ways in use to compare the temperature dependence of  $H_{c2}$  with theory, none of which has led, so far, to complete agreement in the case of pure type II superconductors. In the first one the relative variation of  $H_{c2}$  referred to  $H_{c2}(0)$  as a function of  $T$  is considered. In the second one  $H_{c2}$  is studied in comparison with the extrapolation to lower temperatures of the temperature dependence just below  $T_c$ . In the third the temperature dependence of  $H_{c2}/H_c$  is studied.

In Fig. IV.19 the data obtained with the three Nb samples for  $H_{c2}$  are compared with the results of Finnemore et al.<sup>19)</sup> obtained with a purer Nb sample and with two theoretical predictions, one a phenomenological one (Ginzburg's eq. (2-19)) while the other is derived from first principles (Gor'kov's, eq. (2-21)). Experimental and theoretical results are brought to common agreement at  $t = 1$  and  $t = 0$  by using reduced values:  $H_{c2}(t)/H_{c2}(0)$  in the plot. It can be concluded that the higher the purity of the sample, the more the results deviate from Gor'kov's prediction for the limit of infinite mean free path  $l$  of the electrons. Empirically, it is known that type II superconductors with low  $\kappa$  values have  $H_{c2}(t)$  closer to Ginzburg's expression (2-19) while high  $\kappa$  materials (concentrated alloys) have  $H_{c2}$  values in agreement with Gor'kov's prediction (eq. (2-21)<sup>66)</sup>). The coincidence of results for Nb-1 and Nb-2 might be caused by too high a value of  $H_{c2}(0)$  for Nb-1, which has the highest uncertainty in  $H_{c2}(t)$ .

Another alternative way of comparing the experimental values of  $H_{c2}(t)$  with theoretical predictions is to be found in the use of a reduced quantity normalized at  $t = 1$  as given by eq. (2-24). In Fig. IV.20 the experimental values of  $h^*(t) = H_{c2}(t) / - (dH_{c2}/dt)_{t=1}$  for Nb-1, Nb-2 and Nb-3 are compared with the theoretical prediction of Helfand and Werthamer<sup>67)</sup>. For the less pure sample (Nb-1) was obtained a value  $h^*(0) = 0.765$ , already higher than the theoretical pre-

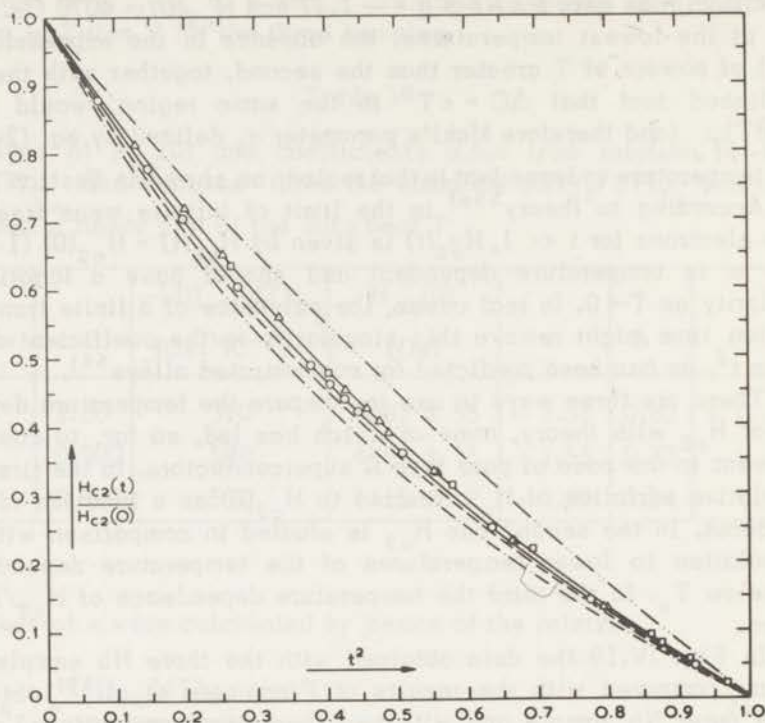


Fig. IV.19 The experimental values of  $H_{c2}$  for Nb-1 ( $\square$ ), Nb-2 ( $\Delta$ ) and Nb-3 ( $\circ$ ), compared with theory (Ginzburg's eq. (2-19), line --- and Gor'kov's eq. (2-21), line -·-·-). Values of  $H_{c2}$  for a purer Nb sample (Finnemore et al.<sup>19</sup>) (line - - -) are also given to confirm the observed dependence of  $H_{c2}$  on purity.

diction for the pure, clean limit ( $l = \infty$ ) ( $h^*(0) = 0.727$ ). For Nb-2,  $h^*(0) = 0.820$  and for Nb-3,  $h^*(0) = 0.836$ . Ohtsuka and Takano<sup>65</sup> reported a value  $h^*(0) = 0.823$  for their Nb sample, while Kim and Strnad<sup>68</sup> gave the value  $h^*(0) = 0.84$  for a Nb sample with a resistance ratio  $\Gamma = 1550$  and  $\kappa = 0.9$ .

The results qualitatively confirm the theoretical prediction regarding the decrease of  $h^*(t)$  with impurity concentration<sup>67</sup>) the effect, however, being larger than is predicted by theory. The 15% discrepancy between  $h^*(0)$  for high-purity Nb and the maximum theoretical prediction might be due to anisotropy of the Fermi-surface alone, since Werthamer and McMillan<sup>69</sup>) have shown that  $h^*(t)$  is practically insensitive to the strength of the electron-phonon interaction. In fact,

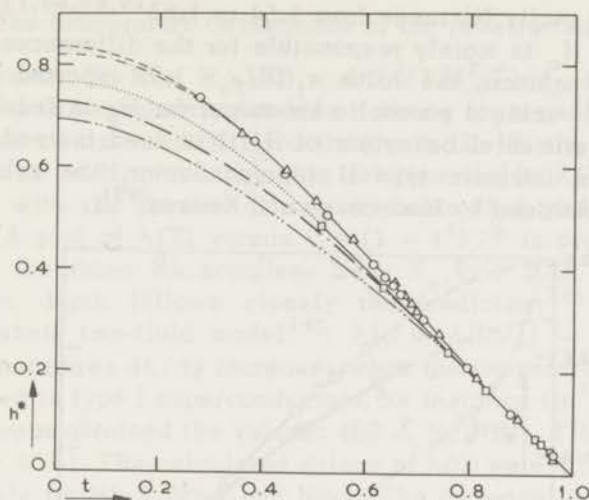


Fig. IV.20 Comparison between the experimental values of  $H_{c2}$  for Nb-1 ( $\square$ ), Nb-2 ( $\Delta$ ) and Nb-3 ( $\circ$ ) and the theoretical prediction for the pure line (—) and the dirty (---) limit, using the reduced quantity  $h^*$  defined in the text.

The lines fitting the experimental points (..... for Nb-1, --- for Nb-2 and --- for Nb-3) are extrapolated to  $t \rightarrow 0$  using the  $H_{c2}(t)$  values given by eq. (4-15) with the numerical coefficients from Table V.

the discrepancy also exists for  $V^{62}$  which is a weak coupling superconductor. Recently, Hohenberg and Werthamer<sup>70</sup> were able to prove qualitatively that, as regards to the role of the shape of the Fermi-surface, anisotropy enhances the theoretical values of  $h^*(t)$ , thus bringing them closer to the experimental results.

The most usual comparison of the experimental  $H_{c2}(t)$  and theory is made in terms of the parameter  $\kappa_1(t)$  relating  $H_{c2}(t)$  to  $H_c(t)$  (eq. 2-22). The experimental values of  $\kappa_1(t)/\kappa$  for the three Nb samples are compared in Fig. IV.21 with the theoretical prediction of Gor'kov (eq. (2-21)). Upon decreasing temperature  $\kappa_1$  rises more rapidly than theory predicts, reaching a maximum value of  $\kappa_1(0)/\kappa = 1.62$  for Nb-3 while theory gives for the clean limit  $\kappa_1(0)/\kappa = 1.25$  (Gor'kov (see eq. (2-21))) or 1.26 (Helfand and Werthamer<sup>67</sup>). For the dirty limit theory gives  $\kappa_1(0)/\kappa = 1.20$ . For Nb-2,  $\kappa_1(0)/\kappa = 1.58$  and for Nb-1  $\kappa_1(0)/\kappa = 1.46$ . The values of  $\kappa_1(0)/\kappa$  reported in the literature for

annealed high purity Nb range from 1.54 to 1.83<sup>19,65,68,71</sup>). Incorrect evaluation of  $H_c$  is mainly responsible for the differences among the results. For instance, the value  $\kappa_1(0)/\kappa = 1.73$  reported by Ohtsuka and Takano<sup>65</sup>) using a parabolic behaviour for  $H_c$  is reduced to 1.63 when the experimental behaviour of  $H_c(t)$  is used instead. For vanadium, also an intrinsic type II superconductor, the value 1.50 for  $\kappa_1(0)/\kappa$  was obtained by Radebaugh and Keesom<sup>62</sup>).

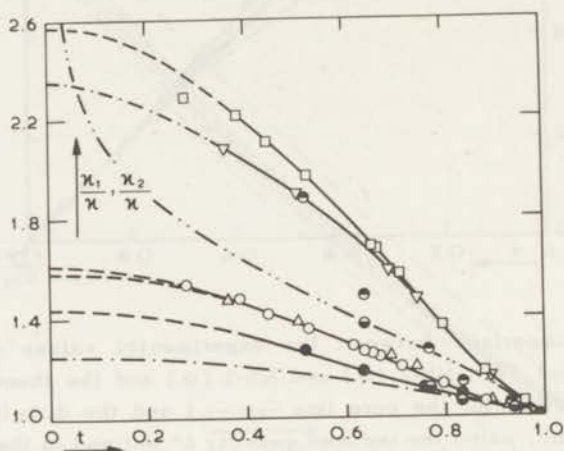


Fig. IV.21 The temperature dependence of the parameters  $K_1$  and  $K_2$  plotted as  $K_1/K$  and  $K_2/K$  versus  $t$ , for Nb-1, Nb-2 and Nb-3. The experimental values of  $K_1/K$  are compared with the Gor'kov prediction for the pure limit (line---). The experimental values of  $K_2/K$  are compared with Eilenberger's calculation for the pure limit (line-.-.-).

Nb-1: ●  $K_1/K$

●  $K_2/K$  with sample cooled down in the absence of the field

●  $K_2/K$  with sample cooled down in the presence of the field

Nb-2: △  $K_1/K$

▽  $K_2/K$

Nb-3: ○  $K_1/K$

□  $K_2/K$

The extrapolation to  $t \rightarrow 0$  of the lines fitting the experimental points was done according to the values of  $H_{c2}(t)$  given by eq. (4-15) with the numerical coefficients from Table V (for  $K_1/K$ ) and from the observed temperature dependence of the specific heat jump at  $H_{c2}(\Delta C = \epsilon T^3, \text{ for } T \ll T_c)$  and  $dH_{c2}/dT$  according eq. (4-15).



## 4.2.7.3 The temperature dependence of the penetration depth

Relation (2-18):  $H_{c2}(T) = 4\pi\lambda^2(T)H_c^2(T)/\phi_0$ , established on basis of the GL equations, provides a means for testing the GL theory in the limit of its validity. Substituting in (2-18) the experimentally found values of  $H_{c2}$  and  $H_c$ , this relation yields  $\lambda(T)$  that is then compared with the results of measurements that yield directly this quantity. A plot of  $\lambda(T)$  versus  $y = (1 - t^4)^{-1/2}$  is presented in Fig. IV.22 for the three Nb samples. Near  $T_c$  ( $y > 2.4$ ), the calculated penetration depth follows closely the prediction<sup>72)</sup> based on the Gorter-Casimir two-fluid model<sup>14)</sup>:  $\lambda(t) = \lambda(0)/(1 - t^4)^{1/2}$ , while at lower temperatures  $d\lambda/dy$  increases when the temperatures decreases, as observed in type I superconductors, for instance tin<sup>73)</sup>. For  $(d\lambda/dy)$ , near  $T_c$ , were obtained the values: 460 Å for Nb-3, 476 Å for Nb-2 and 775 Å for Nb-1. The calculated values of  $\lambda(0)$  were 409, 427 and 656 Å, respectively for Nb-3, Nb-2 and Nb-1. The increase of  $d\lambda/dy$  near  $T_c$

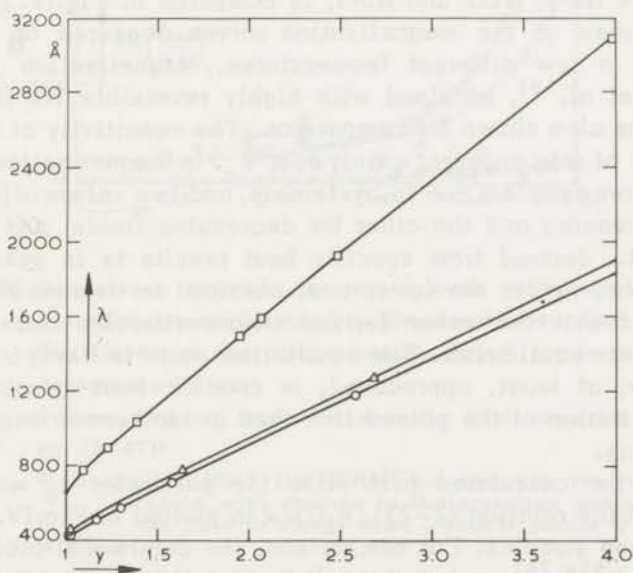


Fig. IV.22 The temperature dependence of the penetration depth  $\lambda$ , calculated by means of eq. (2-18) for Nb-1 ( $\square$ ), Nb-2 ( $\Delta$ ) and Nb-3 ( $\circ$ ) plotted as  $\lambda(t)$  versus  $y = (1 - t^4)^{-1/2}$ . The straight part of the curves (highest  $y$ ) were derived from the observed linearity of  $H_{c2}$  with respect to  $t$  near  $t = 1$ . The values of  $\lambda$  for  $t = 0$  correspond to the values of  $H_{c2}(0)$  given in Table V.

and  $\lambda(0)$  from the values for Nb-3 to the values for Nb-1 is in qualitative agreement with Pippard's non local theory<sup>74)</sup> which accounts for the dependence of  $\lambda$  on the mean free path of the electrons. The value  $(d\lambda/dy) = 460 \text{ \AA}$  for Nb-3, near  $T_c$ , is in good agreement with the value  $(d\lambda/dy) = 440 \pm 20 \text{ \AA}$ , also near  $T_c$ , reported by Maxfield and McLean<sup>75)</sup> from direct measurements of the penetration depth on a Nb sample with  $\Gamma = 115$  for which they estimated  $\lambda(0) = 470 \pm 50 \text{ \AA}$ .

Thus, as pointed out by Finnemore et al.<sup>19)</sup> and Ohtsuka and Takano<sup>65)</sup>, the temperature dependence of  $H_{c2}$  is reasonably well described by relation (2-18) derived from GL theory, when experimental values for  $H_c$  and  $\lambda$  are used.

#### 4.2.7.4 The mixed state differential magnetic susceptibility near $H_{c2}$

From the specific heat jump at  $T_s$ ,  $\Delta C(T_s)$ , the mixed state differential magnetic susceptibility near  $H_{c2}$ :  $\chi_m = (\partial M/\partial H)_T$  may be derived by means of the Ehrenfest relation (2-47).  $(\partial M/\partial H)_T$  thus obtained, for Nb-1, Nb-2 and Nb-3, is compared in Fig.IV.23 with the limiting slopes of the magnetization curves measured on the same samples at a few different temperatures. Magnetization results of Finnemore et al.<sup>19)</sup>, obtained with highly reversible Nb ( $\Gamma = 1600$ ,  $\kappa = 0.78$ ), are also shown for comparison. The sensitivity of  $(\partial M/\partial H)_T$  to the value of  $\kappa$  is apparent mainly near  $T_c$ . In magnetization measurements the three samples, due to hysteresis, had two values of  $(\partial M/\partial H)_T$ , one for increasing and the other for decreasing fields, and the value of  $(\partial M/\partial H)_T$  derived from specific heat results is in general found between them, nearer the lower one, obtained in decreasing field. It is presumed that the value derived calorimetrically corresponds to thermodynamic equilibrium. The equilibrium state is likely to be better achieved or, at least, approached, in specific heat measurement by thermal excitation of the pinned flux than in isothermal magnetization measurements.

From the calculated  $(\partial M/\partial H)_T$  the parameter  $\kappa_2$  was derived by means of the relation (2-23).  $\kappa_2(t)/\kappa$  is plotted in Fig.IV.21 versus  $t$  for the three samples. For comparison, the theoretical prediction for the pure limit<sup>55a,76)</sup> is also given. It is seen that in the whole temperature range, for each sample  $\kappa_2(t) > \kappa_1(t)$ . This is in qualitative agreement with Maki and Tsuzuki's<sup>55a)</sup> and Eilenberger's<sup>76)</sup> prediction for the pure clean limit. However, the experimental values are systematically higher than the theoretical line except for  $T = 0^\circ\text{K}$ . A similar result was observed with V<sup>62)</sup>. In the ideal case of infinite mean free path of the electrons a logarithmic singularity was predicted<sup>55a,76)</sup>, for

$\kappa_2(0)$ . Eilenberger<sup>76)</sup> has calculated that slight impurity concentration should bring  $\kappa_2(0)$  to a finite value. The condition:  $\lim \kappa_1 = \lim \kappa_2 = \kappa$  for  $T \rightarrow T_c$  is clearly obeyed by the three samples.  $\kappa_2(t)/\kappa$ , like  $\kappa_1(t)/\kappa$  increases monotonically from Nb-1 to Nb-3. For dirty type II superconductors, reasonable agreement was found between experiment<sup>71,77)</sup> and theoretical results<sup>78)</sup>, in particular,  $\kappa_2$  was found to be not much different from  $\kappa_1$  in the measured temperature range  $t \approx 1$ .

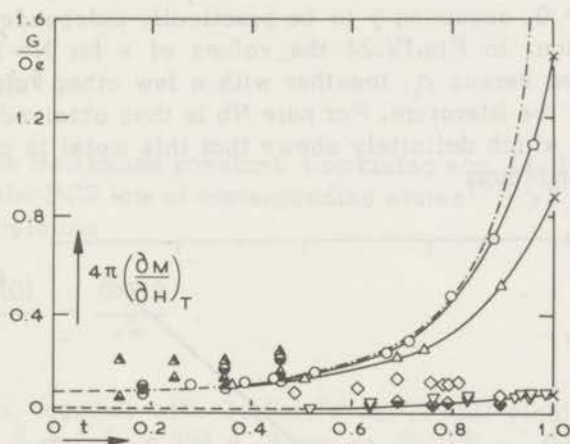


Fig. IV.23 Comparison between the mixed state differential magnetic susceptibility calculated from the specific heat jump at  $H_{c2}$  and the slopes of the magnetization curves for increasing and decreasing fields.

Values derived from the specific heat jump by means of eq. (2-47):

▽ Nb-1 (For Nb-1 the difference between the values obtained with cooling in the presence and absence of the field is hardly seen - double points ▽).

△ Nb-2

○ Nb-3

× Calculated values using for  $\lim_{T \rightarrow T_c} \Delta C(T)$  the values according to Fig. IV.18.

Slopes of the magnetization curves:

Nb-1    ◇ increasing H            ◆ decreasing H

Nb-2    ▲ increasing H            ▴ decreasing H

Nb-3    ● increasing H            ○ decreasing H

--- From Finnemore et al.<sup>19)</sup>.

#### 4.2.8 The calculation of $\kappa_o$ , $\lambda_L(0)$ , $\xi_o$ and $v_F$ for pure Nb

By means of Gor'kov - Goodman relation (2-25):  $\kappa = \kappa_o + f(\gamma, \rho_o)$ , where  $\kappa_o$  is the GL parameter of the pure material and  $f(\gamma, \rho_o)$  is a term dependent upon the residual resistivity of the impure material,  $\rho_o$ , and the coefficient  $\gamma$  of the normal state electronic specific heat,  $\kappa_o$  can be calculated from known values of  $\kappa$ ,  $\rho_o$  and  $\gamma$ . In the present case  $\rho_o$  is not accurately known for the three Nb samples. Defining  $\rho_r = \rho_o / (\rho_{273} - \rho_o) = 1 / (\Gamma - 1)$  where  $\rho_{273}$  is the room temperature resistivity of the specimen,  $\rho_o$  its residual resistivity and  $\Gamma$  the resistance ratio, a linear plot of  $\kappa$  versus  $\rho_r$  yields, by extrapolation,  $\kappa_o$  for  $\rho_r = \rho_o = 0$ , assuming  $\gamma$  to be practically independent of impurity concentration. In Fig. IV.24 the values of  $\kappa$  for Nb-1, Nb-2 and Nb-3 are plotted versus  $\rho_r$ , together with a few other values ( $\kappa, \rho_r$ ) for Nb found in the literature. For pure Nb is thus obtained  $\kappa_o = 0.83 \pm \pm 0.01 > 1/\sqrt{2}$ , which definitely shows that this metal is an intrinsic type II superconductor.

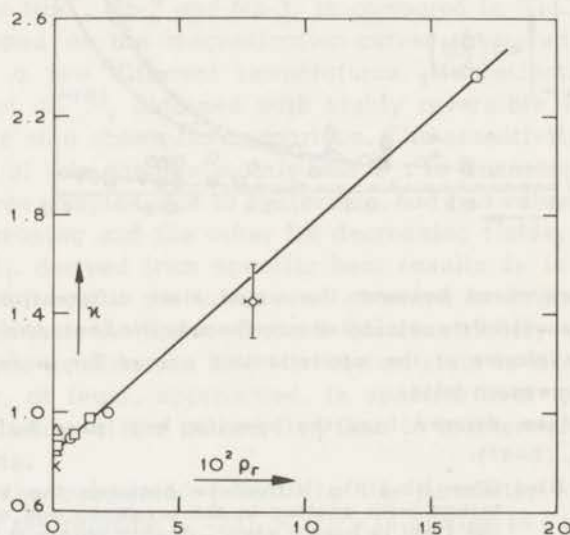


Fig. IV.24 Plot of  $\kappa$  versus  $\rho_r = \rho_o / (\rho_{273} - \rho_o)$  for a few Nb samples:

- present work
- McConville and Serin<sup>71)</sup>
- × Finnemore<sup>19)</sup>
- △ Ohtsuka and Takano<sup>65)</sup>
- ◇ Hecht and Halloran<sup>80)</sup>

The straight line corresponds to the Gor'kov-Goodman expression (2-25) assuming  $\gamma$  to be independent of impurity concentration.

The London penetration depth at the absolute zero  $\lambda_L(0)$ , in terms of microscopic characteristics of the metal, is given by (see reference 34) p. 224)

$$\lambda_L^2(0) = \frac{3 c^2}{8\pi N(0) v_F^2 e^2}, \quad (4-16)$$

where  $v_F$  is the Fermi velocity,  $e$  the electron charge and  $N(0)$  the density of states at the Fermi surface for one spin direction.  $N(0)$  is related to the coefficient  $\gamma$  of the normal state electronic specific heat by<sup>79)</sup>

$$\gamma = \frac{2}{3} \pi^2 N(0) k^2, \quad (4-17)$$

where  $k$  is the Boltzmann constant. Combining eqs. (4-16), (4-17) and (2-17) with the BCS law of corresponding states<sup>13)</sup>:  $\gamma T_c^2 = 0.17 H_c^2(0)$ , we have the relation

$$\frac{\xi_0 \lambda_L(0) H_c(0)}{\phi_0} = \frac{0.219}{\sqrt{\pi}}. \quad (4-18)$$

This relation, together with Gor'kov's eq. (2-12) yields for pure Nb  $\lambda_L(0) = 331 \text{ \AA}$  and  $\xi_0 = 384 \text{ \AA}$ . From eq. (2-17)  $v_F$  for pure Nb was calculated as  $v_F = 2.6 \times 10^7 \text{ cm/sec}$ , using for  $T_c$  the value obtained for Nb-3.

## References

1. See for instance Keesom, P.H. and Pearlman, N., *Handbuch der Physik*, vol. XIV, ed. S. Flügge, (Springer, Berlin, 1956) p. 286.
2. Leupold, H.A. and Boorse, H.A., *Phys.Rev.* **134** (1964) A 1322.
3. Van der Hoeven Jr., B.J.C. and Keesom, P.H., *Phys.Rev.* **134** (1964) A 1320.
4. Heiniger, F., Bucher, E. and Muller, J., *Phys.Cond.Matter* **5** (1966) 243.
5. Heiniger, F., unpublished; quoted in ref. 4.
6. Shen, L.Y.L., Senozan, N.M. and Phillips, N.E., *Phys.Rev.Letters* **14** (1965) 1025.
7. Alers, G.A. and Waldorf, D.L., *Phys.Rev.Letters* **6** (1961) 677.
8. Weber, R., *Phys.Rev.* **133** (1964) A 1487.

9. Carrol, K.J., *J.Appl.Phys.* **36** (1965) 3689.
10. Radebaugh, R. and Keesom, P.H., *Phys.Rev.* **149** (1966) 209.
11. Pippard, A.B., *Proc.Roy.Soc. (London) A* **203** (1950) 210.
12. De Sorbo, W., *Phys.Rev.* **132** (1963) 107.
13. Bardeen, J., Cooper, L.N. and Schrieffer, J.R., *Phys.Rev.* **108** (1957) 1175.
14. Gorter, C.J. and Casimir, H.B.G., *Phys.Z.* **35** (1934) 963; *Z.techn. Phys.* **15** (1934) 539.
15. See for instance, Bardeen, J. and Schrieffer, J.R., *Progress in Low Temperature Physics*, vol. 3, ed. C.J. Gorter, North Holland Publ.Co., Amsterdam, 1961.
16. Goodman, B.B., Hillairet, J., Veyssié, J.J. and Weil, L., *Comptes Rendus Acad.Sci.* **250** (1960) 542.
17. Melik-Barkhudarov, T.K., *Fiz.Tverdogo Tela* **7** (1965) 1368; *Soviet Phys.Solid State* **7** (1965) 1103.
18. Geilikman, B.T. and Krezin, V.Z., *JETP Pis'ma* **3** (1966) 48.
19. Finnemore, D.K., Stromberg, T.F. and Swenson, C.A., *Phys.Rev.* **149** (1966) 231.
20. Decker, D.L., Mapother, D.E. and Shaw, R.W., *Phys.Rev.* **112** (1958) 1888.
21. See for instance, Swihart, J.C., *I.B.M. J.Res. Develop.* **6** (1962) 14.
22. Kok, J.A., *Commun.Kamerlingh Onnes Lab., Leiden, Suppl. No.77a; Physica* **1** (1934) 1103.
23. Goodman, B.B., *Comptes Rendus Acad.Sci.* **246** (1958) 3031.
- 23a. Anderson, P.W., *J.Phys.Chem.Sol.* **11** (1959) 26.
24. Sherrill, M.D. and Edwards, H.H., *Phys.Rev.* **6** (1961) 460.
25. Townsend, P. and Sutton, J., *Phys.Rev.* **128** (1962) 591.
26. Dobbs, E.R. and Perz, J.M., *Rev.mod.Phys.* **36** (1964) 257.
27. Finnemore, D.K. and Mapother, D.E., *Phys.Rev.* **140** (1965) A 507.
28. Sheahen, T.P., *Phys.Rev.* **149** (1966) 370.
29. Toxen, A.M., *Phys.Rev.Letters* **15** (1965) 462.
30. Wada, Y., *Phys.Rev.* **135** (1964) A 1481.
31. Swihart, J.C., Scalapino, D.J. and Wada, Y., *Phys.Rev.Letters* **14** (1965) 106.
32. Ehrenfest, P., *Kon.Nederl.Akad.Wet., Amsterdam* **36** (1933) 153.
33. Goodman, B.B., *Phys.Letters* **1** (1962) 215.
34. De Gennes, P.G., *Superconductivity of Metals and Alloys*, ed. D. Pines, W.A. Benjamin, Inc., New York (1966) p. 54.
35. Marcus, P.M., *X Int.Conf. on Low Temp.Physics, Moscow, 1966, to be published.*
36. Kramer, L., *Phys.Letters* **23** (1966) 619.
37. Gorter, C.J., *Suppl. No. 124c, Comm.Kamerlingh Onnes Lab., Leiden; Physica* **34** (1967) 220.

38. Goodman, B.B., *Phys.Letters* **12** (1964) 6.
39. Serin, B., *Phys.Letters* **16** (1965) 112.
40. Van Laer, P.H., Thesis, University of Leiden, 1938, p. 49.
41. Dew-Hughes, D., *Mater.Sci.Eng.* **1** (1966) 2.
42. Goedemoed, S.H., Thesis, University of Leiden, 1967.
43. Anderson, P.W., *Phys.Rev.Letters* **9** (1962) 309.
44. Bean, C.P. and Livingston, J.D., *Phys.Rev.Letters* **12** (1964) 14.
- 44a. Goedemoed, S.H., van der Giessen, A., De Klerk, D. and Gorter, C.J. *Phys.Letters* **3** (1963) 250.
- 44b. Goedemoed, S.H., private communication.
45. Van Kolmeschate, C., private communication.
46. Kleiner, W.H., Roth, L.M. and Autler, S.H., *Phys.Rev.* **133** (1964) A 1226.
47. Matricon, J., *Phys.Letters* **9** (1964) 289; *Proc.IX Int.Conf. on Low Temp.Phys*, Columbus, Ohio, eds. J.G. Daunt, et al. (New York, Plenum Press) p. 544.
48. Matricon, J. and Saint-James, D., *Phys.Letters* **24A** (1967) 241.
49. Renard, J.C., and Rocher, Y.A., *Phys.Letters* **24A** (1967) 509.
50. Abrikosov, A.A., *J.exptl.theoret.Phys. (U.S.S.R.)* **32** (1957) 1442; *Soviet Phys. JETP* **5** (1957) 1174.
51. Harden, J.L. and Arp. V., *Cryogenics* **3** (1963) 105.
52. Silcox, J. and Rollins, R.W., *Rev.mod.Phys.* **36** (1964) 52.
53. Evetts, J.E., Champbell, A.M. and Dew-Hughes, D., *Phil.Mag.* **10** (1964) 339.
54. Goedemoed, S.H., Van Kolmeschate, C., Metselaar, J.W. and De Klerk, D., *Comm.Leiden, Suppl. No. 342b; Physica* **31** (1965) 573.
55. Maki, K., *Physics* **1** (1964) 21 and 127.
- 55a. Maki, K. and Tsuzuki, T., *Phys.Rev.* **139** (1965) A 868.
56. Caroli, C., De Gennes, P.G. and Matricon, J., *Phys.Letters* **9** (1964) 307.
57. Rosenblum, B. and Cardona, M., *Phys.Rev.Letters* **12** (1964) 657.
58. Hake, R.R. and Brammer, W.G., *Phys.Rev.* **133** (1964) A 719.
59. Ferreira da Silva, J., Scheffer, J., Van Duijkeren, N.W.J. and Dokoupil, Z., *Phys.Letters* **12** (1964) 166.
60. Maki, K., *Phys.Rev.* **139** (1965) A 702.
61. Marcus, P.M., *Conf. on Phys. of Type II superc.*, Cleveland, 1964 (unpublished); *Proc. IX Int.Conf.Low Temp.Phys.*, Columbus, Ohio, 1964 (Plenum Press, Inc., New York, 1965) 550.
62. Radebaugh, R. and Keesom, P.H., *Phys.Rev.* **149** (1966) 217.
63. Ferreira da Silva, J., Van Duijkeren, N.W.J. and Dokoupil, Z., *Phys.Letters* **20** (1966) 448; *Comm.No.348b, Kamerlingh Onnes Lab., Leiden; Physica* **32** (1966) 1253.
64. Gorter, C.J., *Rev.mod.Phys.* **36** (1964) 27.

65. Ohtsuka, T. and Takano, N., preprint, to be published in J.Phys. Soc.Japan.
66. Jones, C.K., Hulm, J.K. and Chandrasekhar, B.S., Rev.mod.Phys. **36** (1964) 74.
67. Helfand, E. and Werthamer, N.R., Phys.Rev. **147** (1966) 288.
68. Kim, Y.B. and Strnad, A.R., Quantum Fluids, Proceedings of the Sussex University Symposium ed. D.F. Brewer (North Holland, Amsterdam, 1966) p. 68.
69. Werthamer, N.R. and McMillan, W.L., Phys.Rev. **158** (1967) 415.
70. Hohenberg, P.C. and Werthamer, N.R., Phys.Rev. **153** (1967) 493.
71. McConville, T. and Serin, B., Phys.Rev. **140** (1965) A 1169.
72. Shoenberg, D., Superconductivity (Cambridge University Press, New York, 1965) p. 197.
73. Schawlow, A.L. and Devlin, G.E., Phys.Rev. **113** (1959) 120.
74. Pippard, A.B., Proc.Roy.Soc. A **216** (1953) 547.
75. Maxfield, B.W. and MacLean, W.L., Phys.Rev. **139** (1965) A 1515.
76. Eilenberger, G., Phys.Rev. **153** (1967) 584.
77. Bon Mardion, G., Goodman, B.B. and Lacaze, A., J.Phys.Chem. Sol. **26** (1965) 1143.
78. Caroli, C., Cyrot, M. and De Gennes, P.G., Solid State Commun. **4** (1966) 17.
79. Lynton, E.A., Superconductivity, ed. B.L. Worsnop (Methuen, London, 1962) p. 125.
80. Hecht, R. and Halloran, J.J., RCA Tech.Rep. AFML-TR-65-169, G.D. Cody et al., 1965, p. 10.



## Chapter V

THE MAGNETOCALORIC EFFECT IN TYPE II  
SUPERCONDUCTORS

## 5.1 Introduction

Since in a Meissner region the magnetization  $M$  at constant magnetic field, is temperature independent, the isothermal magnetization of a superconductor in such a region is an isentropic process:  $(\partial S/\partial H)_T = (\partial M/\partial T)_H = 0$ . Thus, for a type I superconductor with zero demagnetizing coefficient, the entropy difference  $\Delta S(T) = S_n(T) - S_s(T)$ , between the normal and the superconducting (Meissner) state remains unchanged under isothermal magnetization in the whole range of fields up to  $H_c(T)$ , the thermodynamic critical field, at which  $\Delta S(T)$  (and  $\Delta M = M_n - M_s$ ) abruptly vanishes in a first order transition. In specific heat measurements at constant field, such a transition is an isothermal process with latent heat  $L$  such that  $L = T_s [S_n(T_s) - S_s(T_s)]$  where  $T_s$  is the transition temperature. Under adiabatic magnetization, cooling is to be expected only when the field reaches  $H_c$ .

On the contrary, in the intermediate state of a type I superconductor or in the mixed state of a type II superconductor, the continuous variation of the magnetization from the perfect diamagnetism (in the Meissner state) to the normal state value (zero), implies the existence of a magnetocaloric effect:  $(\partial S/\partial H)_T \neq 0$ , since then  $(\partial M/\partial T)_H \neq 0$ . The cooling possibilities by adiabatic magnetization of type I superconductors have been studied in detail<sup>1,2,3</sup>. For a type II superconductor between  $H_{c1}$  and  $H_{c2}$  the entropy increases monotonically with the applied field,  $H$ , since  $(\partial M/\partial T)_H$  is found positive in the whole range of the mixed state. Thus, if the process is reversible, cooling is to be expected in the whole range of the mixed state when the specimen is adiabatically magnetized, while isothermal magnetization will require a flow of heat from the cryogenic bath to the sample, given by  $T(\partial S/\partial H)_T$  per unit change of the external field. Both processes are illustrated in Fig.V.1. The entropy change  $S_B - S_A$  is produced when the superconductor is isothermally magnetized from state  $A'$  to state  $B'$  in the phase diagram. Upon increasing, in adiabatic conditions, the external field from state  $A'$ , the superconductor undergoes an isentropic process, cooling down to the final temperature corresponding to point  $C$  in the entropy diagram and point  $C'$  in the phase diagram. The rate of cooling produced by the increase of the external field in

adiabatic conditions is related to the entropy variation upon isothermal magnetization by

$$\left(\frac{\partial T}{\partial H}\right)_S = -\frac{T}{C} \left(\frac{\partial S}{\partial H}\right)_T \quad (5-1)$$

where  $C$  refers, as always in this thesis, to constant field. The rate of entropy variation with the applied field in the mixed state at constant temperature, is connected with the rate at which the magnetic flux penetrates the specimen.

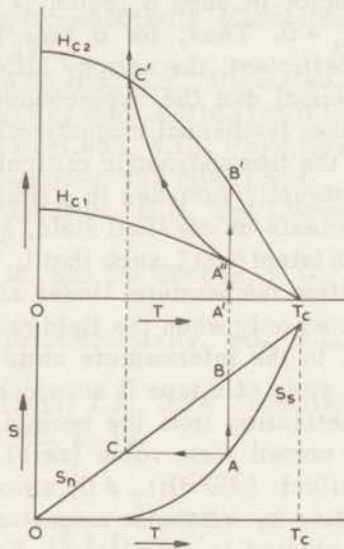


Fig. V.1 Illustration of an adiabatic and an isothermal magnetization process for a reversible type II superconductor.  $(H,T)$  and  $(S,T)$  are respectively the phase and the entropy diagrams. The path  $A'A''B'$  corresponds to an entropy increase of  $S_B - S_A$ . The path  $A'A''C'$  corresponds to an isentropic process.

The magnetocaloric effect is easily masked by irreversible effects caused by flux pinning. Sample Nb-1 did not show the effect at all. Increase of the field always led to an increase of temperature. The effect was, however, clearly observed in samples Nb-2 and Nb-3. For Nb-3 an experiment was performed in which the study of the magnetocaloric effect was combined with the measurement of the specific heat as a function of the magnetic field, while the temperature was kept constant within narrow limits:  $T = (4.22 \pm 0.02)^\circ\text{K}$ .

## 5.2 Analysis of the magnetocaloric effect near $H_{c2}$

For calculating the rate of entropy variation upon the change of the magnetic field a knowledge of the magnetization  $M$  in the mixed state is required. The theoretical prediction for the magnetization given by eq. (2-23) or its equivalent eq. (2-42) applies only near  $H_{c2}$ , so that the calculation of  $(\partial S/\partial H)_T$  will be restricted to the range of applied fields  $H_{c2} - H \ll H_{c2}$ . It will be shown, however, that such a predicted linearity of  $M$  versus  $H$  near  $H_{c2}$  yields a value for  $(\partial S/\partial H)_T$  which is in conflict with the experimental results.

In Chapter II, Section 2.4.2 an expression (eq. 2-45) was derived for the entropy in the mixed state near  $H_{c2}$ , under the sole assumption of the validity of eq. (2-23). Upon isothermal magnetization the rate of variation of entropy with the applied field,  $H$ , for  $H_{c2} - H \ll H_{c2}$  is, assuming  $\chi_m = (\partial M/\partial H)_T$  to be field independent near  $H_{c2}$ , given by

$$\left(\frac{\partial S_m}{\partial H}\right)_T = -\chi_m \frac{dH_{c2}}{dT} + (H - H_{c2}) \frac{d\chi_m}{dT}. \quad (5-2)$$

To keep the process isothermal, heat has to be exchanged between sample and bath at a rate

$$\frac{dQ}{dH} = T \left(\frac{\partial S_m}{\partial H}\right)_T = -T\chi_m \frac{dH_{c2}}{dT} + T(H - H_{c2}) \frac{d\chi_m}{dT}. \quad (5-3)$$

At the transition to the normal state ( $T = T_s$ ,  $H = H_{c2}(T_s)$ ) the quantity  $dQ/dH$  drops suddenly to zero, the magnitude of the jump being  $dQ/dH = -T\chi_m(dH_{c2}/dT)$ . The sharp disappearance of the magnetocaloric effect at  $H_{c2}$  may be used for determining this phase transition line<sup>4</sup>).

It follows from (5-3) that  $d^2Q/dH^2 = T(d\chi_m/dT)$ . Since  $\chi_m = (\partial M/\partial H)_T$ ,  $d\chi_m/dT > 0$ , as is seen in Fig. IV.23. Thus, it follows from the assumption (eq. (2-23) or its equivalent eq. (2-42)) that the rate at which the sample absorbs heat from the bath is expected to increase near  $H_{c2}$  when the type II superconductor is isothermally magnetized.

## 5.3 Experimental procedure

The procedure is illustrated in Fig. V.2.

The experiment proceeded as follows: with the temperature of the <sup>4</sup>He bath stabilized in the neighbourhood of the boiling point, the

specific heat of the sample was measured in the presence of the magnetic field, using temperature increments not exceeding  $0.04^\circ\text{K}$ . In low fields, after each specific heat point was taken, the field was raised in steps and the sample brought back to the initial temperature by means of the thermomechanical switch. Thereupon a new heat pulse was supplied and the whole cycle repeated until the first indication of the magnetocaloric effect appeared. Thereafter the sample temperature was returned to the initial value by the very cooling produced by the increase of the field. The time rate of increase of the magnetic field was  $6 - 7 \text{ Oe/sec}$ .

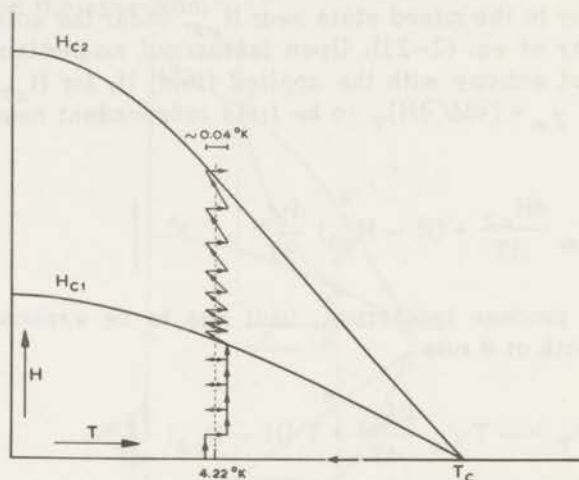


Fig. V.2 Illustration of the procedure used for measuring the specific heat of Nb-3 directly as a function of the external field at  $T = 4.22 \pm 0.02^\circ\text{K}$ . In the mixed state, the increments produced in the sample temperature by the externally supplied heat were compensated by the cooling produced in the subsequent rise of the external field. In the Meissner state the temperature of the sample was reduced to the initial value by closing the thermomechanical switch.

#### 5.4 Results and discussion

The rate at which the thermally insulated sample cooled upon increase of the external field is depicted in Fig.V.3 as  $(\partial T/\partial H)_S$  versus the applied field, corrected from the influence of the calorimeter plus addenda. The specific heat results are shown in Fig.V.4 as  $C/T$  versus the applied field,  $H$ , together with the magnetization curve obtained on the same sample for the same temperature,  $T = 4.22^\circ\text{K}$ , increasing the field. The specific results thus obtained are in agree-

ment with those derived from Fig.IV.2 at the same temperature, as also shown in Fig.V.4.

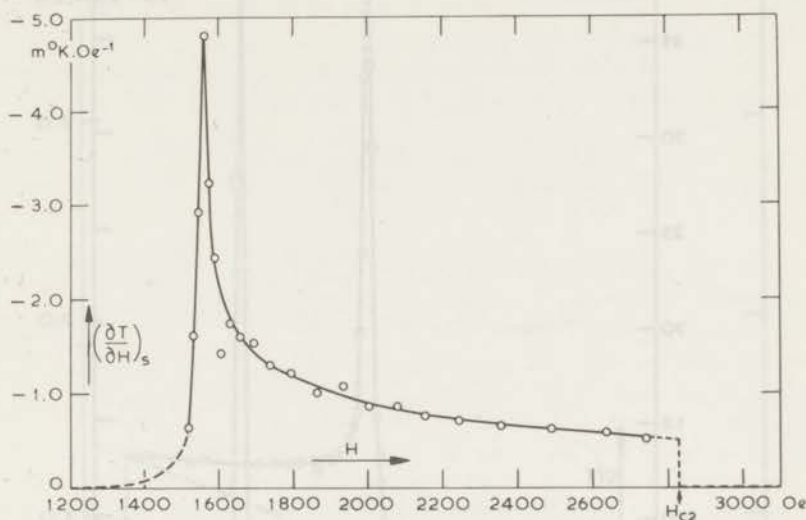


Fig. V.3 The field dependence of the rate  $(\partial T/\partial H)_s$  at which the thermally insulated sample (Nb-3) cooled down upon increase of the external field. The effect was studied with the sample temperature kept at  $T = 4.22^\circ\text{K}$  within  $0.02^\circ\text{K}$ .

From Fig.V.4 it is confirmed that, 1) the specific heat is field-independent in the region of complete diamagnetism, 2) the specific heat displays a strong anomaly at the field region where the magnetization has its greatest variation and, 3) the transition to the normal state has the same character (second order) in both magnetic and calorimetric measurements. The specific heat jump at  $H_{c2}$  (in agreement with the values of  $\Delta C(T_s)$  derived from Fig.IV.2 and plotted in Fig.IV.18) yields, through the Ehrenfest relation (2-47), a somewhat lower value of  $(\partial M/\partial H)_T$  than that corresponding to the actual magnetization curve at the same temperature ( $t = 0.455$ ) for increasing fields, on account of magnetic hysteresis, as can be seen in Fig.IV.23.

The rate  $dQ/dH$  at which heat had to be supplied to the sample in order to compensate the adiabatic cooling produced by the increase  $dH$  of the external field, is given by (5-1) as  $dQ/dH = -C(dT/dH)$ .  $dQ/dH$  is plotted against the applied field  $H$  in Fig.V.5. The straight line  $a$  represents the slope at  $H_{c2}$  to be expected on basis of linear magnetization. An interesting result is that, with the exclusion of the field region near  $H_{c1}$  (where demagnetizing effects anticipate the end

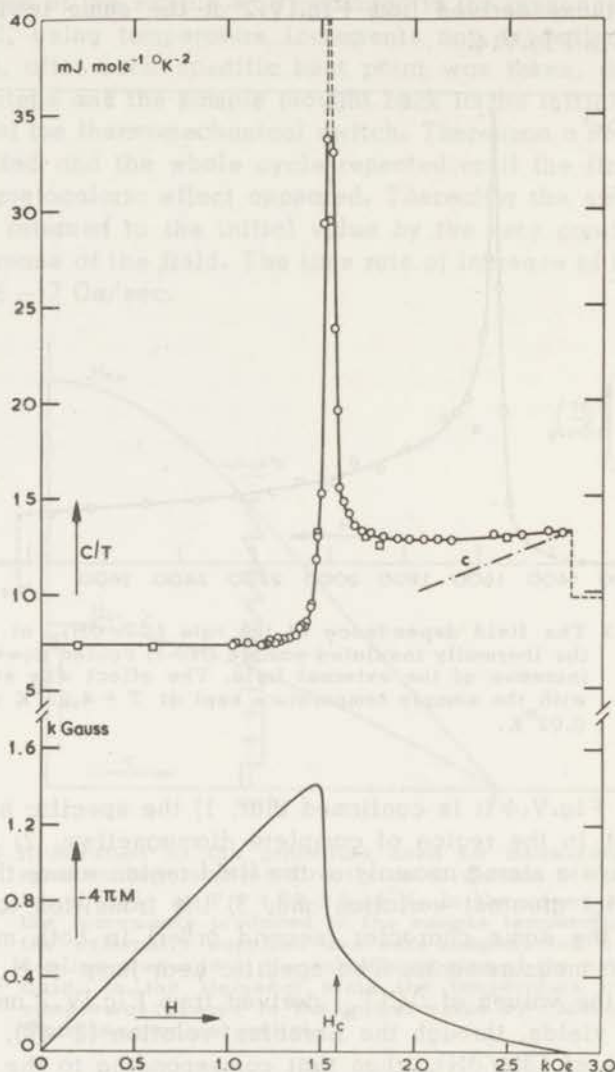


Fig. V.4 The field dependence of the specific heat and the magnetization of Nb-3 (both for increasing field) at  $T = 4.22 \text{ } ^\circ\text{K}$ . The magnetization was measured independently by Van Kolmeschate (ref. 45, in Chapter IV).  
 ○ experimental points  
 □ points derived from Fig. IV.2  
 line c: slope of the curve  $C/T$  versus  $H$  near  $H_{c2}$  to be expected on basis of linear mixed state magnetization near  $H_{c2}$  according eq. (2-42).

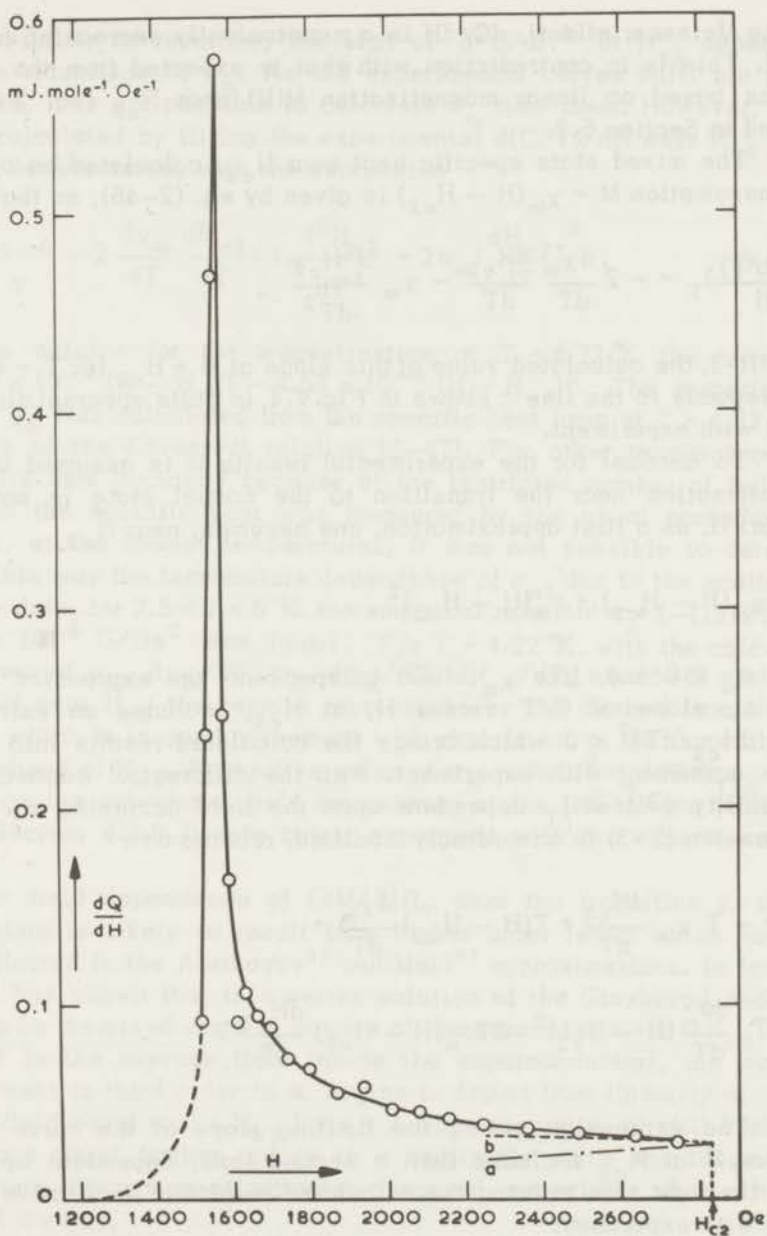


Fig. V.5 The field dependence of the rate  $dQ/dH$  at which heat has to be supplied to the sample (Nb-3) to keep the magnetization process isothermal at  $T = 4.22 \pm 0.02^\circ\text{K}$ . See text for symbols a and b.

of the Meissner effect),  $dQ/dH$  is a monotonically decreasing function of  $H$ . This is in contradiction with what is expected from the calculations based on linear magnetization  $M(H)$  near  $H_{c2}$  (eq. 2-42) as stated in Section 5.2.

The mixed state specific heat near  $H_{c2}$ , calculated on basis of the assumption  $M = \chi_m(H - H_{c2})$  is given by eq. (2-46), so that

$$\left(\frac{\partial(C/T)}{\partial H}\right)_T = -2 \frac{d\chi_m}{dT} \frac{dH_{c2}}{dT} - \chi_m \frac{d^2H_{c2}}{dT^2} \quad (5-4)$$

For Nb-3, the calculated value of this slope at  $H = H_{c2}$  for  $T = 4.22^\circ\text{K}$  corresponds to the line  $c$  shown in Fig.V.4, in quite apparent disagreement with experiment.

To account for the experimental results it is assumed that the magnetization near the transition to the normal state is not quite linear. If, as a first approximation, one assumes, near  $H_{c2}$

$$M = \chi_m(H - H_{c2}) + \sigma_m(H - H_{c2})^2, \quad (5-5)$$

with  $\sigma_m < 0$  and, like  $\chi_m$ , field independent, the expression for the limiting slope of  $C/T$  versus  $H$ , at  $H_{c2}$ , includes an extra term  $2\sigma_m(dH_{c2}/dT)^2 < 0$  which brings the calculated results into qualitative agreement with experiment. With the differential magnetic susceptibility  $(\partial M/\partial H)_T$  dependent upon the field according eq. (5-5), expression (5-3) is accordingly modified, reading now

$$\begin{aligned} \frac{dQ}{dH} = & -T \chi_m \frac{dH_{c2}}{dT} + T(H - H_{c2}) \frac{d\chi_m}{dT} + \\ & + T \frac{d\sigma_m}{dT} (H - H_{c2})^2 - 2T\sigma_m (H - H_{c2}) \frac{dH_{c2}}{dT}. \end{aligned} \quad (5-6)$$

The expression giving the limiting slope of the curve  $dQ/dH$  versus  $H$  at  $H_{c2}$  includes then a second term, dependent upon  $\sigma_m$ , with the right sign to bring the calculated results in qualitative agreement with experiment

$$\frac{d^2Q}{dH^2} = T \frac{d\chi_m}{dT} - 2T\sigma_m \frac{dH_{c2}}{dT} \quad (5-7)$$



The possibility of reversing the sign of  $d^2Q/dH^2$  at  $H_{c2}$  depends upon the magnitude of  $\sigma_m$ . As the experimental curves  $M(H)$  are not reversible, it is not possible to calculate  $\sigma_m$  from them. However,  $\sigma_m$  can be calculated by fitting the experimental  $d(C/T)/dH$  near  $H_{c2}$ , at different temperatures, with the expression

$$\left(\frac{\partial(C/T)}{\partial H}\right)_T = -2 \frac{d\chi_m}{dT} \frac{dH_{c2}}{dT} - \chi_m \frac{d^2H_{c2}}{dT^2} + 2\sigma_m \left(\frac{dH_{c2}}{dT}\right)^2. \quad (5-8)$$

One thus obtains for the magnetization at  $T = 4.22^\circ\text{K}$  the result:  $M = 1.15 \times 10^{-4} (H - H_{c2}) - 4.53 \times 10^{-6} (H - H_{c2})^2$ . The numerical value of  $\chi_m$  was calculated from the specific heat jump at  $T = 4.22^\circ\text{K}$  by means of the Ehrenfest relation (2-47). For other temperatures, the results lack accuracy because of the restricted number of fields for which the specific heat was measured by the usual procedure. Although, at the lowest temperatures, it was not possible to determine in this way the temperature dependence of  $\sigma_m$ , due to the scattering of the data, for  $2.5 < T < 5^\circ\text{K}$ , the empirical relation:  $\sigma = (-1.512T + 1.84) \times 10^{-6} \text{ G/Oe}^2$  was found. For  $T = 4.22^\circ\text{K}$ , with the calculated values of  $\chi_m$ ,  $d\chi_m/dT$ ,  $\sigma_m$ ,  $d\sigma_m/dT$ ,  $dH_{c2}/dT$ , eq. (5-6) yields for  $dQ/dH$  near  $H_{c2}$  the results represented by the dashed line *b* in Fig.V.5, which is in good agreement with experiment in the immediate neighbourhood of  $H_{c2}$ . A negative value of  $\sigma_m$  with  $(d^2\sigma_m/dT^2)_{T=0} = 0$  also brings the calculated field dependence of the linear term (Chapter IV, Section 4.2.6.3) into better agreement with the experimental data.

The field dependence of  $(\partial M/\partial H)_T$  near the transition to the normal state is likely to result from higher order terms which have been neglected in the Abrikosov<sup>5)</sup> and Maki<sup>6)</sup> approximations. In fact, Lasher<sup>7)</sup> has shown that in a series solution of the Ginzburg-Landau equations for the mixed state in powers of the parameter  $\alpha = (B - H_{c2})/B$  (where  $B$  is the average field inside the superconductor), the magnetic moment to third order in  $\alpha$ , begins to depart from linearity at an external field equal to  $0.4 H_{c2}$  for  $\kappa = 2$ . The inclusion of still higher order terms might further reduce to a negligible value the range of fields where linear magnetization is observed, especially when  $\kappa$  has too small a value.

The field dependence of the magnetic differential susceptibility near  $H_{c2}$  is of difficult direct observation in measurements of the magnetic moment, since the departure from linearity is very small as can be seen in Fig.V.6. However, the effect should be quite apparent in measurements that yield directly the magnetic differential susceptibility.

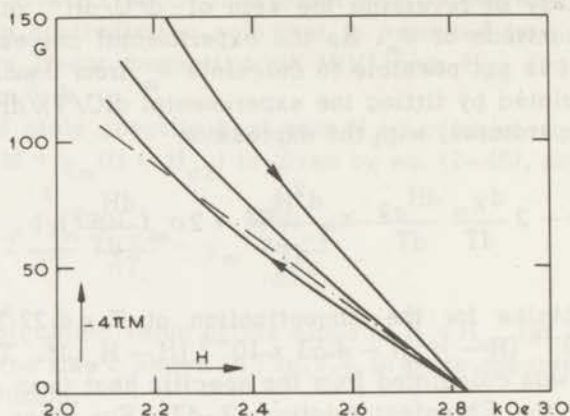


Fig. V.6 The magnetization  $M$  of Nb-3 near  $H_{c2}$  at  $T = 4.22^\circ\text{K}$ , plotted as  $-4\pi M$  versus the applied field.

- line  $\longrightarrow$ , obtained for increasing field  
 line  $\longleftarrow$ , obtained for decreasing field (from Fig. IV.12b)  
 line  $-\cdot-\cdot-$ , derived from the specific heat jump at the same temperature by means of the Ehrenfest relation (eq. (2-47) and assuming linear dependence of  $M$  on  $H$  near  $H_{c2}$  according eq. ((2-42)).  
 line  $\text{---}$ , calculated from the specific results assuming  $M = \chi_m(H - H_{c2}) + \sigma_m(H - H_{c2})^2$  with  $\chi_m$  and  $\sigma_m$  field independent.

## References

1. Mendelssohn, K. and Moore, J.R., *Nature* **133** (1934) 413 and **135** (1935) 826.
2. Keesom, W.H. and Kok, J.A., *Physica* **1** (1934) 595.
3. Yaqub, M., *Cryogenics* **1** (1960) 101.
4. Ohtsuka, T., *Phys. Letters* **17** (1965) 194; Ohtsuka, T. and Takano, N., preprint to be published in *J. Phys. Soc. Japan*.
5. Abrikosov, A.A., *J. exptl. theoret. Phys. (U.S.S.R.)* **32** (1957) 1442; *Soviet Phys. JETP* **5** (1957) 1174.
6. Maki, K., *Physics* **1** (1964) 21 and 127; Maki, K. and Tsuzuki, T., *Phys. Rev.* **139** (1965) A 868.
7. Lasher, G., *Phys. Rev.* **140** (1965) A 523.

## Chapter VI

## CONCLUDING REMARKS

It was shown on basis of results derived from measurements of the specific heat in the presence of a constant magnetic field (ranging from zero to 9.4 kOe, in the temperature interval  $1 \lesssim T \lesssim 10^\circ\text{K}$ ) that niobium is an intrinsic type II superconductor with electron-phonon coupling of intermediate strength. The energy gap at the absolute zero  $2\Delta(0)$ , the temperature dependence of the thermodynamic critical field,  $H_c$ , and the relative magnitude of the specific heat jump in zero field compared with the electronic normal state specific heat at  $T_c$ ,  $\gamma T_c$ , were found to deviate from the values predicted by the BCS theory, in agreement with a correlation scheme that is known to exist between these quantities and the strength of the electron-phonon interaction (see Fig.IV.8 for  $H_c$ ).

The values of the Debye characteristic temperature  $\Theta$  derived from the normal state data at the lower temperatures are in agreement with the results derived from the elastic constants for samples of similar quality when the normal state data is properly analysed (Section 4.2.1, Table I and Figs.IV.4,5,6).

The transition at  $H_{c2}$  was found to have always the character of a second order transition in the Ehrenfest sense and it was extremely sharp for the purest (lowest  $\kappa$ ) specimen (Nb-3) in zero field.

In the less pure (highest  $\kappa$ ) specimen (Nb-1) the transition at  $H_{c1}$  was obscured by the effects of hysteresis while for the annealed ones (Nb-2 and Nb-3) a pronounced anomaly in the specific heat appeared associated with this transition. On account of demagnetizing effects and irreversibility (most apparent in this region) it is difficult to assert unambiguously the order of the transition. Irreversible effects were observed in the three samples. For the less pure sample (Nb-1) these effects were present in the whole mixed state region. For the high-purity, annealed samples (Nb-2 and Nb-3) the effects of irreversibility appeared concentrated in the mixed state region close to the lower phase transition line  $H_{c1}(T)$  for  $T \ll T_c$ .

For  $H > H_{c1}(0)$  it was found that the mixed state specific heat contains, already at the lowest temperatures, a linear term ( $\gamma'T$ ) of which the coefficient  $\gamma'$  increases with the applied field (Fig.IV.17). But the observed field dependence of  $\gamma'$  is not in agreement with what should be expected from a field independent mixed state differential magnetic susceptibility near  $H_{c2}$   $(\partial M/\partial H)_T$  (Abrikosov, Maki). The

combined study of the magnetocaloric effect and the specific heat as a function of the magnetic field, at a given temperature, further confirms the disagreement between the experimental results and those to be expected on basis of field independent  $(\partial M/\partial H)_T$  near  $H_{c2}$  (Figs. V.4,5).

The magnitude of the mixed state specific heat jump  $\Delta C$  to the normal state was found to vary with temperature and to vanish at the absolute zero as  $T^3$  for  $T \ll T_c$ ; near  $T_c$ ,  $\Delta C$  depends markedly upon the  $\kappa$  value of the sample (Fig.IV.18) with a discontinuity at  $T_c$ , for the three samples, as expected (Section 4.2.7.1).

Although niobium exhibits the qualitative features of type II superconductivity as given by Abrikosov's vortex model, it deviates, in several respects from this and its later extensions. In particular, the temperature dependence of the lower ( $H_{c1}$ ) and the higher ( $H_{c2}$ ) critical fields for  $T \ll T_c$  is not accounted for by any present theory or model, the experimental values being higher than those predicted by theory (Figs.IV.16 for  $H_{c1}(t)$  and IV.20 for  $H_{c2}(t)$ ). Anisotropy of the Fermi-surface may account for the discrepancy in the case of  $H_{c2}(t)$ .

The parameters  $\kappa_1$  and  $\kappa_2$  introduced by Maki in connection with, respectively, the ratio  $H_{c2}/H_c$  and the mixed state magnetic susceptibility at  $H_{c2}$ , were found to follow the theoretical prediction  $\kappa_2(t) > \kappa_1(t)$  for  $t \neq 1$ , the requirement  $\kappa_2(1) = \kappa_1(1) = \kappa$  being fulfilled (Fig.IV.21). But their temperature dependence was found to be larger than is predicted by the theory (Fig.IV.21). The theoretical prediction that  $\kappa_1$  increases with the purity of the sample was experimentally confirmed. The temperature dependence of the penetration depth  $\lambda$  deduced from eq. (2-18) (Fig.IV.22) by using the empirical values of  $H_{c2}$  and  $H_c$  was found to be in agreement with the values obtained from a measurement that yields directly this quantity. This confirms the validity of the GL equations (from which eq. (2-18) was deduced) near the second order upper phase transition line.

When the magnetization curve shows hysteresis, the mixed state magnetic susceptibility at  $H_{c2}$  derived from the specific heat jump  $\Delta C$  by means of the Ehrenfest relation (2-47) is in better agreement with the slope of the magnetization curve corresponding to decreasing field (Fig.IV.23). It is presumed that the value of  $(\partial M/\partial H)_T$  at  $H_{c2}$  derived calorimetrically corresponds to reversibility since, for Nb-3, the values thus derived are in excellent agreement (for  $T \ll T_c$ ) with the slopes of the magnetization curves (at the same temperature) of a highly reversible niobium sample with a  $\kappa$  value of the same order of magnitude (Fig.IV.23). This is equivalent to stating that in cases of hysteresis, the magnetization curve for decreasing field, near  $H_{c2}$ ,

is nearer the reversible one than that for increasing field.

In an attempt to account for the observed field dependence of the mixed state specific heat and the magnetocaloric effect it is suggested that the magnetization near  $H_{c2}$  should include powers of  $(H - H_{c2})$  higher than the first. The expected order of magnitude of the coefficient of the term in  $(H - H_{c2})^2$  was calculated from the results. The resultant magnetization curve lies between the experimental ones for increasing and decreasing field, but still nearer to that obtained in decreasing field (Fig.V.6). It is, therefore, concluded that the Abrikosov result yielding linear magnetization near  $H_{c2}$  is only a first order approximation, the validity of which is probably restricted to type II superconductors with not-too-low values of the GL parameter  $\kappa$ .

## SAMENVATTING

Van drie niobium preparaten, die in zuiverheid verschillen, werden in het temperatuurgebied van 1 tot 10°K de soortelijke warmten gemeten in magneetvelden tot en met 9,4 kOe. Uit de resultaten bleek, dat niobium een intrinsieke supergeleider van de tweede soort is met een middelmatige electron-phonon koppeling. De energiespleet bij het absolute nulpunt ( $2\Delta(0)$ ), de temperatuurafhankelijkheid van het thermodynamische kritische veld ( $H_c$ ) en de verhouding van de sprong in de soortelijke warmte ( $\Delta C$ ) tot de waarde van de soortelijke warmte van de electronen in de normale toestand bij het sprongpunt  $T_c$ , bleken van de waarden afgeleid uit de BCS theorie te verschillen volgens een bekende correlatie tussen deze grootheden en de sterkte van de electron-phonon wisselwerking (zie Fig.IV.8 voor  $H_c$ ).

Voor  $H > H_{c1}(0)$  werd gevonden, dat de soortelijke warmte in de mengtoestand reeds bij de laagste temperaturen een lineaire term  $\gamma'T$  bevat, waarvan de coëfficiënt  $\gamma'$  toeneemt met het veld (Fig.IV.17). Op grond van een thermodynamische beschouwing was deze lineaire term door Gorter voorspeld. Deze term duidt er op, dat (voor  $H > H_{c1}$ ) de supergeleider gebieden bevat, die zich overeenkomstig de normale toestand gedragen (dit zouden kernen zijn van de wervels, voortvloeiend uit het Abrikosov model, waar de electronen lage energie toestanden innemen). De waargenomen veldafhankelijkheid van  $\gamma'$  is echter niet in overeenstemming met de differentiële magnetische susceptibiliteit ( $\partial M/\partial H$ )<sub>T</sub> bij  $H_{c2}$  volgend uit de theorie (Abrikosov, Maki), die voorspelt, dat ( $\partial M/\partial H$ )<sub>T</sub> bij  $H_{c2}$  voor de mengtoestand onafhankelijk van het veld is. De gecombineerde bestudering van het magnetocalorische effect en de soortelijke warmte als functie van het magnetische veld (bij een bepaalde temperatuur), bevestigt het ontbreken van overeenstemming tussen de experimentele resultaten en die, welke men op grond van een van het veld onafhankelijke ( $\partial M/\partial H$ )<sub>T</sub> bij  $H_{c2}$  zou verwachten.

De grootte van de sprong in de soortelijke warmte  $\Delta C$  bij overgang van de mengtoestand naar de normale toestand bleek voor  $T \ll T_c$  volgens  $T^3$  te verlopen, bovendien zou deze sprong bij  $T = 0$  verdwijnen. Bij  $T_c$  hangt  $\Delta C$  duidelijk af van de  $\kappa$ -waarde van het preparaat, zoals voor de drie preparaten wordt verwacht (paragraaf 4.2.7.1); de krommen van  $\Delta C$  tegen  $T^3$  vertonen bij  $T_c$  een discontinuïteit (Fig.IV.18).

De door Maki geïntroduceerde parameters  $\kappa_1$  en  $\kappa_2$ , die in verband staan met respectievelijk de verhouding  $H_{c2}/H_c$  en de magne-

tische susceptibiliteit bij  $H_{c2}$  in de mengtoestand, bleken te voldoen zowel aan de theoretische voorspelling, dat  $\kappa_2(t) > \kappa_1(t)$  voor  $t \neq 1$  is, als aan de voorwaarde, dat  $\kappa_2(1) = \kappa_1(1) = \kappa$  (Fig.IV.21). Uit de metingen volgde echter dat deze parameters sterker van de temperatuur afhankelijk zijn, dan theoretisch was voorspeld (Fig.IV.21). De verwachte toename van  $\kappa_1$  met de graad van zuiverheid van het preparaat werd experimenteel bevestigd.

Als er hysteresis optreedt, is de magnetische susceptibiliteit van de mengtoestand bij  $H_{c2}$ , zoals deze is afgeleid van de sprong in soortelijke warmte  $\Delta C$  met behulp van de Ehrenfest relatie (2-47), in betere overeenstemming met de helling van de magnetisatiekromme bij afnemend veld. Aangenomen is, dat de waarde van  $(\partial M / \partial H)_T$  bij  $H_{c2}$ , aldus afgeleid, beantwoordt aan die voor het reversibele geval en wel omdat voor  $T \ll T_c$  de voor het zuiverste niobium preparaat afgeleide waarden in volledige overeenstemming zijn met de hellingen van de magnetisatie krommen van een zich in hoge mate reversibel gedragend niobium preparaat met een  $\kappa$ -waarde van dezelfde orde van grootte (Fig.IV.23).

Bij een poging rekening te houden met de waargenomen veldafhankelijkheid van de soortelijke warmte in de mengtoestand en het magnetocalorische effect, wordt er voorgesteld de magnetisatie bij  $H_{c2}$  niet alleen door een lineaire term in  $(H - H_{c2})$ , maar bovendien door hogere machten in  $(H - H_{c2})$  weer te geven; de coëfficiënt van de tweede macht is in orde van grootte bepaald uit de resultaten. Hieruit zou volgen dat de resultaten van Abrikosov, die een lineaire magnetisatie bij  $H_{c2}$  geven, slechts een benadering van de eerste-orde zijn, waarvan de geldigheid waarschijnlijk is beperkt tot supergeleiders van de tweede soort met een niet te kleine GL parameter  $\kappa$ .

## SUMÁRIO

Com base em resultados derivados de medidas do calor específico em campo magnético constante (desde zero até 9,4 kOe, no intervalo de temperatura 1 – 10 °K) de três amostras de nióbio de diferente grau de pureza, mostrou-se que este metal é um supercondutor intrínseco de segunda espécie, no qual a interacção fónão – electrão tem uma intensidade de valor intermédio. Desvios em relação às predições da teoria de Bardeen - Cooper - Schrieffer (BCS) foram encontrados para as grandezas que dependem sensivelmente da intensidade da interacção (largura da banda interdita no espectro energético dos electrões a 0 °K,  $2\Delta(0)$ , variação do campo crítico termodinâmico,  $H_{c1}$ , em função da temperatura (Fig.IV.8) e o valor  $\Delta C(T_c)/\gamma T_c$  da descontinuidade que o calor específico em campo nulo apresenta na transição para o estado normal, referido ao calor específico electrónico no estado normal à mesma temperatura).

Para valores do campo magnético,  $H$ , acima do primeiro campo crítico a 0 °K,  $H_{c1}(0)$ , o calor específico no estado misto contém, já nas imediações do zero absoluto, um termo linear,  $\gamma'T$ , cujo coeficiente,  $\gamma'$ , aumenta com a intensidade do campo aplicado (Fig.IV.17). A existência de semelhante termo havia sido predita por Gorter em bases termodinâmicas. O aparecimento deste termo linear implica a existência no supercondutor, para  $H > H_{c1}(0)$ , de regiões com um comportamento análogo ao estado normal (os núcleos dos vórtices de Abrikosov, onde o espectro energético dos electrões comporta excitações de baixa energia).

Todavia, a variação de  $\gamma'$  com o campo magnético aplicado não pode ser cabalmente explicada com base nos resultados preditos pelo modelo de Abrikosov (generalizado por Maki), segundo o qual a susceptibilidade magnética diferencial  $(\partial M/\partial H)_T$  no estado misto nas imediações do segundo campo crítico,  $H_{c2}$ , é independente do campo magnético. O estudo paralelo do calor específico e do efeito magneto-calórico em função do campo magnético a uma determinada temperatura, confirma o desacôrdo entre experiência e teoria.

A grandeza da descontinuidade  $\Delta C$  que o calor específico apresenta na transição para o estado normal varia proporcionalmente com  $T^3$ , para  $T \ll T_c$ , ( $T_c$  sendo a temperatura da transição em campo nulo). Para  $T \approx T_c$ ,  $\Delta C$  depende, efectivamente, de um modo notório, do valor do parâmetro de Ginzburg - Landau ( $\kappa$ ), o comportamento das três amostras concordando, neste aspecto, com a previsão (Secção 4.2.7.1) (Fig.IV.18).



Os parâmetros  $\kappa_1$  e  $\kappa_2$  introduzidos por Maki para caracterizar a variação com a temperatura de, respectivamente,  $H_{c2}/H_c$  e  $(\partial M/\partial H)_T$  nas imediações de  $H_{c2}$ , verificam o resultado teórico  $\kappa_2(t) > \kappa_1(t)$  para  $t = T/T_c \neq 1$  e satisfazem à condição  $\kappa_1(1) = \kappa_2(1) = \kappa$ . (Fig.IV.21). Todavia, a variação destes parâmetros com a temperatura é bastante mais acentuada do que prevê a teoria (Fig.IV.21). A predição teórica segundo a qual  $\kappa_1$  aumenta com o grau de pureza foi confirmada experimentalmente.

Quando se manifesta histerese no comportamento magnético da amostra, o valor da susceptibilidade magnética diferencial no estado misto junto do segundo campo crítico, deduzida dos resultados calorimétricos ( $\Delta C$ ) por intermédio da relação de Ehrenfest (2-47), concorda melhor com a curva de magnetização obtida em campo magnético decrescente. Presume-se que os valores de  $(\partial M/\partial H)_T$ , para  $H \approx H_{c2}$ , assim derivados, correspondem a estados de equilíbrio pois, no caso da amostra Nb-3 (a mais pura), excelente concordância foi verificada, para  $T \ll T_c$ , com resultados magnéticos obtidos com um espécimen de nióbio altamente reversível e com um valor de  $\kappa$  da mesma ordem de grandeza (Fig.IV.23).

Para explicar a observada variação do calor específico no estado misto e do efeito magneto-calórico com o campo magnético, admitiu-se que a susceptibilidade magnética diferencial no estado misto junto de  $H_{c2}$  depende do campo magnético (linearmente, em primeira aproximação). Em conformidade, a expressão da magnetização em função do campo aplicado  $H$  deve incluir, além do habitual termo linear,  $H - H_{c2}$ , outros de expoente mais elevado. A ordem de grandeza do coeficiente do termo quadrático foi calculada a partir dos resultados. Conclue-se, conseqüentemente, que o resultado do modelo de Abrikosov (magnetização linear junto de  $H_{c2}$ ) representa uma aproximação de primeira ordem, provavelmente válida apenas para supercondutores de segunda espécie com valores do parâmetro  $\kappa$  não muito pequeno.

Teneinde te voldoen aan de wens van de Faculteit der Wiskunde en Natuurwetenschappen volgt hier een kort overzicht van mijn studie.

In 1949, na het afleggen van het eindexamen aan het Liceu Nacional de D. Manuel II te Porto, Portugal, ben ik mijn studie in de electrotechniek aan de Faculdade de Ciências da Universidade do Porto begonnen, die ik daarna heb voortgezet aan de Faculdade de Engenharia van dezelfde universiteit. Van 1955 tot 1958 heb ik mijn studie onderbroken om de militaire dienstplicht te vervullen. Hierna heb ik het ingenieursdiploma in 1959 verkregen. Van 1959 tot 1962 assisteerde ik in het Laboratório de Física da Faculdade de Ciências da Universidade do Porto. In 1961-'62 gaf ik een cursus algemene natuurkunde aan studenten in de wiskunde. Een vrijstelling van deze onderwijstaak werd mogelijk gemaakt door het Instituto de Alta Cultura, Lisboa, en door de welwillendheid van Prof. Dr. C.A. Coutinho Braga, Prof. Dr. J.M.R. Moreira de Araújo en Prof. Dr. A.A. Pires de Carvalho van het Laboratório de Física do Porto. Prof. Dr. C.J. Gorter, bood mij op verzoek van Prof. Dr. J.M.R. Moreira de Araújo een plaats op het Kamerlingh Onnes Laboratorium aan. Eind 1962 begon ik op het Kamerlingh Onnes Laboratorium met het onderzoek voor mijn promotie, waarvan de laatste meting eind 1966 geschiedde. Gedurende deze periode genoot ik financiële steun van de Fundação Calouste Gulbenkian, Lisboa. Op grond van mijn studie in Portugal, het verrichte onderzoek op het Kamerlingh Onnes Laboratorium en een tentamen quantummechanica bij Prof. Dr. J.A.M. Cox, legde ik in 1966 het doctoraal examen experimentele natuurkunde af aan de Rijksuniversiteit te Leiden. Gedurende de eerste helft van 1967 heb ik een cursus experimentele natuurkunde gegeven aan studenten in de natuurkunde op het Laboratório de Física, Porto. Teruggekomen in Leiden voor de samenstelling van het proefschrift kreeg ik financiële hulp van Nederlandse zijde.

Een gedeelte van de resultaten van het onderzoek is reeds gepubliceerd:

Ferreira da Silva, J., Scheffer, J., van Duykeren, N.W.J. and Dokoupil, Z., *Phys. Letters* **12** (1964) 166.

Ferreira da Silva, J., van Duykeren, N.W.J. and Dokoupil, Z., *Phys. Letters* **20** (1966) 448.

Ferreira da Silva, J., van Duykeren, N.W.J. and Dokoupil, Z., *Comm. No 348b Kamerlingh Onnes Lab., Leiden; Physica* **32** (1966) 1253.

Ferreira da Silva, J. and Dokoupil, Z., *Proceedings of the XIIth Int. Congress of Refrigeration, Madrid, 1967.*

Ferreira da Silva, J., Burgemeister, E.A. and Dokoupil, Z., *Phys. Letters* **25A** (1967) 354.

Veel medewerking bij de metingen en berekeningen heb ik onder-  
vonden van de Heren Drs. J. Scheffer, Drs. N.W.J. van Duykeren en  
E.A. Burgemeister. Veel waardering heb ik voor de hulp, die ik kreeg  
van de Heren H. Kuipers en B. Kret, van de glasinstrumentmakerij,  
de Heren J. de Vink, E.S. Prins en H.R.A. Nater, van de ontwikke-  
lingswerkplaatsen, de Heren L. Neuteboom en J. Turenhout, van de  
cryogene afdeling, de Heer W.F. Tegelaar, van de tekenkamer en Mejuf-  
vrouw S.M.J. Ginjaar, van de administratie en andere leden van de  
technische en administratieve staf van het laboratorium.

Door bemiddeling van Dr. G.J. van den Berg werden de zuivere  
niobium preparaten verkregen van Dr. W. De Sorbo van General Electric  
Laboratory te Schenectady, N.Y. De weerstandsmetingen werden ver-  
richt door de werkgroep Mt IV van F.O.M.-T.N.O. Prof. Dr. J. Volger  
van het Natuurkundig Laboratorium van Philips te Eindhoven voldeed  
aan het verzoek een spectrochemische analyse van de preparaten te  
laten maken. Andere analyses werden gedaan door Dr. Ir. J.T. Tiedema  
van de N.V. Hollandse Metallurgische Industrie Billiton te Arnhem.  
De Heer L.J.A. van Bentveld van het Centraal Reken Instituut te  
Leiden heeft de programmering verzorgd voor de digitale rekenmachin-  
es, de X-1 en de IBM 360. De Engelse tekst werd gecorrigeerd gedeel-  
telijk door Dr. F.R. McCourt en gedeeltelijk door de Heer en Mevrouw  
P.J. Worsley.

Van der Meer, J., Schaffner, J., van Duijven, H.W.J., and Dehaene, J., *Phys. Letters* **12** (1964) 106.  
 Van der Meer, J., van Duijven, H.W.J., and Dehaene, J., *Phys. Letters* **10** (1963) 462.  
 Van der Meer, J., van Duijven, H.W.J., and Dehaene, J., *Compt. Rend. Acad. Sci. Paris, Ser. B* (1963) 223.  
 Van der Meer, J., and Dehaene, J., *Proceedings of the XIIth Int. Congress of Theoretical Physics, Madrid, 1962*.  
 Van der Meer, J., Gijssels, E.A., and Dehaene, J., *Phys. Letters* **35A** (1961) 334.

Een gedeelte van de resultaten van het onderzoek te zien op het

Panzer de Silva, J., Schaffner, J., van Duijven, H.W.J., and Dehaene, J., *Phys. Letters* **12** (1964) 106.

Panzer de Silva, J., van Duijven, H.W.J., and Dehaene, J., *Phys. Letters* **10** (1963) 462.

Panzer de Silva, J., van Duijven, H.W.J., and Dehaene, J., *Compt. Rend. Acad. Sci. Paris, Ser. B* (1963) 223.

Panzer de Silva, J., and Dehaene, J., *Proceedings of the XIIth Int. Congress of Theoretical Physics, Madrid, 1962*.

Panzer de Silva, J., Gijssels, E.A., and Dehaene, J., *Phys. Letters* **35A** (1961) 334.

## STELLINGEN

### I

Als in de soortelijke warmte grote anomalieën voorkomen, zoals dit bij supergeleiders van de tweede soort bij de fasenovergangen  $H_{c1}(t)$  en  $H_{c2}(t)$  gebeurt, mag de registratie van de opwarmingscurven in geen geval buiten beschouwing worden gelaten.

### II

Het argument, dat door Radebaugh en Keesom wordt gegeven voor de produktie van "irreversible internal heating" bij  $H_{c1}(t)$ , is ongegrond.

R. Radebaugh and P.H. Keesom,  
*Phys.Rev.* **149** (1966) 217.

### III

De dissipatieve processen veroorzaakt door de beweging van Abrikosov's wervels in de gemengde toestand van een supergeleider van de tweede soort behoeven niet noodzakelijkerwijs de resultaten van metingen der soortelijke warmte te beïnvloeden.

H. van Beelen, Proefschrift, Leiden, 1967,  
Stelling II.

### IV

De door Finnemore e.a. uit de magnetisatie van zeer zuiver niobium berekende sprong in de soortelijke warmte bij  $T_c$  verschilt 6% van de experimenteel gevonden waarde. Dit wordt veroorzaakt door het gebruik van een te grote waarde van  $(dH_c/dT)_{T_c}$ , waardoor ook wordt verklaard, dat zij een te kleine  $\kappa$  waarde berekenen.

D.K. Finnemore, T.F. Stromberg and C.A. Swenson,  
*Phys.Rev.* **149** (1966) 231.

### V

Door van het magnetocalorische effect gebruik te maken in een zuiver preparaat, dat een supergeleider van de tweede soort is, zou het mogelijk zijn de soortelijke warmte te meten in de omgeving van  $H_{c2}$  bij temperaturen lager dan gewoonlijk bereikt met een  $^4\text{He}$ -bad.

Dit proefschrift, paragraaf 5.1, Fig. V.1.

### VI

De bewering van Skinner e.a. dat overeenstemming bestaat tussen  $\kappa_1(t)$  en de fenomenologische uitdrukking van Ginzburg en tussen  $\kappa_2(t)$  en de voorspelling van Maki-Tsuzuki voor drie één-kristallen van niobium is ongegrond.

L.C. Skinner, II, R.M. Rose and J. Wulff,  
*J.Appl.Physics* **37** (1966) 2191.

## VII

Het meten van de differentiële magnetische susceptibiliteit bij  $H_{c2}$  in de gemengde toestand van supergeleiders van de tweede soort, die een kleine  $\kappa$  waarde hebben en zich zeer reversibel gedragen, is gewenst.

## VIII

De door Null voorgestelde thermodynamische "consistency test" voor fasenevenwicht tussen een z.g. van Laer vloeistof (L) en een regulier vaste-stof mengsel (S) van een binair systeem behoeft niet in alle gevallen een éénduidig uitsluitsel te geven bij de beoordeling van experimenteel gevonden (L+S) fasendiagrammen.

H.R. Null, A.I.Ch.E. Journal **11** (1965) 780.

## IX

De argumenten, op grond waarvan de Adviserende Commissie voor Thermometrie de waarde 20,280 °K heeft aanbevolen voor het kookpunt van waterstof, zijn niet overtuigend.

Verslag van de Vergaderingen van het Comité Consultatif de Thermométrie van het Bureau International des Poids et Mesures in Washington en Ottawa (september, 1967).

## X

Voor temperaturen beneden een honderdste graad Kelvin heeft de anisotropie van de gamma-straling van radioactieve kernen, die opgenomen zijn in een metallische ferromagneet, als thermometer voordelen boven andere mogelijkheden, bijvoorbeeld de susceptibiliteit van een paramagnetisch zout.

## XI

De bewering van Mumford: "Only a minute span of experience is really open to private verification and adequate experimental proof: the rest must be taken on faith in the integrity of authority, in science no less than in theology", is aanvechtbaar.

Lewis Mumford, *The Condition of Man*, Mercury Books, London, 1963, p. 195.

## XII

De beknopte manier, waarop H.G. Wells de ontdekkingen, die door Portugezen in de vijftiende en zestiende eeuw werden gedaan, behandelt, doet geen recht aan hun uitzonderlijke ondernemingszin en aan de gevolgen dezer ontdekkingen.

H.G. Wells, *The Outline of History*, Cassell and Company, Ltd, London, 1951.

Stellingen behorende bij het proefschrift van J. Ferreira da Silva.

